Cardiovascular and Neuropathic Complications Associated with Impaired Glucose Tolerance and Type 1 Diabetes of Extreme Duration

A thesis submitted to the University of Manchester for the degree of Doctor of Philosophy in Medicine

in the Faculty of Medical and Human Sciences

2014

Dr Omar Asghar

School of Medicine

Institute of Human Development,

Centre for Endocrinology and Diabetes

Contents

Figures

Tables

The University of Manchester

November 2014

Candidate: Omar Asghar

Degree: Doctor of Philosophy

Thesis Title: Cardiovascular and Neuropathic Complications Associated with Impaired Glucose Tolerance and Type 1 Diabetes of Extreme Duration

Abstract

In this project, we have studied two pathophysiologically distinct and opposite groups, using advanced non-invasive imaging techniques to establish whether such individuals exhibit microvascular complications and to what extent.

Impaired glucose tolerance (IGT) is a clinically silent, altered state of glycemia and a precursor to type 2 diabetes. The presence of IGT is associated with an adverse cardiovascular risk which may be attributable to the early development of microvascular complications, although the risk factors and exact time of onset are unknown. Detailed and robust cardiac studies in IGT cohorts are lacking however recent advances in non-invasive cardiac imaging allow us to detect early and sub-clinical alterations in cardiac structure and function. Using gold standard imaging modalities and state of the art techniques, we have demonstrated that subjects with IGT exhibit a comparable cardiac phenotype to age matched healthy controls. These are the first studies to employ robust, detailed and reproducible methodologies in an IGT cohort and our findings challenge the existing data.

In addition to cardiovascular complications, there is also data to support the presence of small fibre neuropathy in subjects with IGT. The diagnosis of small fibre neuropathy often requires invasive skin biopsy. Corneal confocal microscopy (CCM) has emerged as a potential surrogate for skin biopsy in the detection of small fibre neuropathy across a variety of conditions however has yet to be validated in subjects with IGT. We have demonstrated the utility of CCM in detecting small fibre neuropathy in subjects with IGT.

Medalists represent a unique group of patients with an extreme duration of Type 1 diabetes and a variable degree of microvascular and macrovascular complications. As such they constitute a special phenotype, which merits further study, especially given the excess cardiovascular mortality in patients with Type 1 diabetes, even in those with good glycemic control. Detailed cardiac studies in medalist cohorts identifying the exact phenotype are lacking. Using gold standard imaging modalities and state of the art techniques, we were able to demonstrate that subjects with type 1 diabetes of extreme duration, remarkably exhibit normal cardiac structure and function.

Declaration

No portion of the work referred to in the thesis has been submitted in support of an application for another degree or qualification of this or any other university or other institute of learning.

Copyright Statement

i. The author of this thesis (including any appendices and / or schedules to this thesis) owns certain copyright or related rights in it (the "Copyright") and he has given The University of Manchester certain rights to use such Copyright, including for administrative purposes.

ii. Copies of this thesis, either in full or in extracts and whether in hard or electronic copy, may be made only in accordance with the Copyright, Designs and Patents Act 1988 (as amended) and regulations written under it or, where appropriate, in accordance with the licensing agreements which the University has from time to time. This page must form part of any such copies made.

iii. The ownership of certain copyright, patents, designs, trademarks and other intellectual property (the "Intellectual Property") and any reproductions of copyright works in this thesis, which may be described in this thesis, may not be owned by the author and may be owned by third parties. Such Intellectual Property and Reproductions cannot and must not be made available for use without the prior written permission of the owner(s) of the relevant Intellectual Property and / or Reproductions.

iv. Further information on the conditions under which disclosure, publication and commercialisation of this thesis, the Copyright and any Intellectual Property and / or Reproductions described in it may take place is available in the University IP Policy (see http://www.campus.manchester.ac.uk/medialibrary/policies/intellectual-property.pdf), in any relevant Thesis restriction declarations deposited in the University Library, The University Library's regulations (see http://www.manchester.ac.uk/library/aboutus/regulations) and in the University's policy on presentation of Theses.

Contribution

For the cardiac arm of this study, Omar Asghar (OA) made a significant contribution to study concept and design alongside Prof Rayaz Malik, Prof Simon Ray and Drs Matthias Schmitt and Parthiban Arumugam. OA was solely responsible for ethics approval, funding applications, patient recruitment and induction to the study and all administrative duties. CMR imaging was carried out in conjunction with the CMR unit at the North West Cardiac Centre, Wythenshawe. MR protocols and sequences were devised by Dr Matthias Schmitt and supervised by Dr Chris Miller and OA. MIBG imaging was carried out by the technical staff at the Department of Nuclear Medicine, Central Manchester NHS Foundation Trust under the supervision and guidance of Dr Parthiban Arumugam and Ian Armstrong. Autonomic function testing was carried out by OA. CMR data analysis was performed by OA with the assistance and supervision of Dr Chris Miller. MIBG image processing was carried out by Ian Armstrong and analysis was carried out by OA under the guidance of Dr Parthiban Arumugam.

For the neuropathy study OA recruited subjects with IGT and consented subjects, performed peripheral neuropathy assessments and undertook skin biopsies in the majority of subjects in the included studies. OA also performed intra-epidermal nerve fibre analysis for all IGT subjects under the supervision of Dr Maria Jeziorska. Other contributors were as follows: Dr Andrew Marshall (neurophysiology), Drs Ioannis Petropoulos and Mitra Tavakoli (CCM), Dr Hassan Fadavi (neuropathy assessments), Dr Maria Jeziorska, Simon Forman, Louisa Nelson, Aisha Meskiri, and Wendy Jones (skin biopsy processing), Georgios Ponirakis (recruitment and administration), staff at the Wellcome Trust Clinical Research Facility (patient blood and urine sample

collections and anthropometric measurements), the directorate of Laboratory Medicine, Central Manchester University Hospitals (blood sampling).

OA was the sole author of all the chapters in this thesis with the exception of chapter 9, which was jointly authored with Dr Ioannis Petropoulos.

Alternative Thesis Format

The author has been granted permission by his supervisor Professor Rayaz Malik, to submit this PhD thesis in alternative format approved under the regulations of the University of Manchester (Faculty of Medical and Human Sciences), including sections which are in a format suitable for submission for publication or dissemination.

The following chapters are either published, pending publication or will be submitted for publication in due course:

Chapter 3 – Submitted to the Journal of Nuclear Cardiology.

Chapter 4 – Accepted for publication by the Journal of Nuclear Cardiology 2014.

Chapter 5 – Submitted to Diabetes Care.

Chapter 6 – To be submitted for publication.

Chapter 7 – To be submitted for publication.

Chapter 8 – Published in Diabetes Care 2014 (Diabetes Care. 2014 Sep;37(9):2643-6. doi: 10.2337/dc14-0279. Epub 2014 Jun 26)

“Read! In the name of your Lord who created;

Created man from a clinging clot.

Read! Your Lord is the Most Generous,

Who taught by the pen.

Taught man what he did not know….”

Al-Quran s96:1-5

Dedication

I dedicate this work to my mother Khalda and my children Adam, Ibraheem and Zaara: You are my source of love, strength, inspiration and hope on this earth.

Acknowledgements

Having reached the point of completion despite the most difficult and testing circumstances in my life, I pause to contemplate on the eve of my thesis submission date. As a result of great pain, sacrifice and struggle in my personal life; I never thought I would see the day when this work would reach completion. It is nothing short of a miracle that I have been able to achieve this and I take no credit for it. I remain greatly indebted to those who helped and supported me (see below) however I feel immense pride at having shown the courage and determination to see this PhD project come to fruition despite the obstacles and I am grateful to Allah (SWT) for everything.

I am fortunate and blessed to be surrounded by amazing family, friends and professional colleagues. To mention each individual by name would likely double the length of this thesis and I apologise to those not mentioned by name.

To my supervisor, friend and confidant Rayaz Malik; to you I am forever indebted and eternally grateful. You are the sole reason I am where I am today and you have been an unrelenting pillar of support, friendship and guidance. You have shown great faith, patience and perseverance with me when perhaps others might have not. To say that this work would not have been possible without you cannot be overstated and you must take all the credit. You leaving Manchester has been a great loss but you deserve everything good and more. I thank you.

To my boss, friend and mentor Bernard Clarke; without your personal assistance, particularly lately, this thesis would never have been completed in time and I am truly grateful. PhD aside, you have been a great role model and a mentor to me and you have been instrumental in my career development to date. You have also shown great faith in me and been a great listener and I always feel better having talked to you. Thank you.

To my mother and role model Khalda; as the last and most challenging of your six children, I have learned so much from you. Through difficult and testing times, you made great sacrifices in order to privately educate me and it was your dream for me to become a doctor. You always encouraged me to excel academically and strive for great achievements; advice that has never been lost on me and I hope you now feel proud of my achievements which serve as a testament to your dedication and sacrifice as a mother. Your faith, strength of character, wisdom and selflessness are truly inspirational and have shaped me to be the person I am today. May Allah protect you, continue to bless you and give prosperity.

To my angel Zaara, I did this for you. When you fell from the heavens into Daddy's arms in May 2009, I started this PhD and five and a half years later, I have completed it. For me, this PhD is symbolic of the struggle for you and your brothers over the last 2 years. The love I have for you is beyond description and one day I hope you will read this as a reminder. You (and "the bruvvers") are the beacon of light which shines within me and gives me the strength to continue to strive for you. You are already showing all the promise of being a true Asghar with your brilliant work at school and long may it continue. May Allah (SWT) protect you all.

To my lieutenants, Adam and Ibraheem: I have always stressed the importance of striving hard and achieving to the best of your ability in life. That fire should never stop burning and should continue to drive you to aim to be the best at everything you apply yourself to. I hope that in me, you have an example of just that and a role model for everything in life. You two have supported me through this PhD and I wish I could attach your names to it!

I am indebted to Dr Uazman Alam for his assistance with chapter 9 and statistics but mostly his friendship during and beyond the PhD. The same can be said for Dr Ioannis Petropoulos.

To my best friend J, thank you for everything; you have a heart of gold and are a true friend to me. To Dawood, Ateeq and Omar; you have been more like guardian angels than friends to me and I remain truly indebted.

I must also thank my brother Jamal and my eldest sister Aysha for their unrelenting support.

Omar Asghar

28th November 2014.

1 Introduction

1.1 Background

Diabetes Mellitus (DM) is defined as a metabolic disorder of multiple aetiology characterised by chronic hyperglycaemia with disturbances of carbohydrate, fat and protein metabolism resulting from defects in insulin secretion, insulin action, or both (1). It is associated with long term multi-systemic complications and accounts for considerable morbidity, mortality and burden on healthcare resources.

Two major subtypes of diabetes exist, categorised according to their pathophysiological and aetiological mechanisms; type 1 (T1DM), which accounts for 5-10% of all cases of diabetes, presents early and has an autoimmune basis whereby autoantibody-mediated destruction of the pancreatic beta cells occurs resulting in insulin deficiency (2). This condition has a strong HLA association in addition to environmental and genetic factors. Individuals with T1DM are dependent on lifelong insulin replacement therapy. In contrast, type 2 diabetes (T2DM) accounts for the majority of diabetes cases. The condition is characterised by hyperglycaemia secondary to insulin resistance which occurs in the context of abdominal obesity and is related to the metabolic syndrome. Excessive visceral fat and centripetal obesity give rise to insulin resistance and hyperglycaemia in the presence of either normal or elevated insulin production. In contrast to T1DM, the pathophysiological basis of T2DM is multifactorial and associated with genetic, environmental, lifestyle factors as well as ethnicity. Treatment of hyperglycaemia is with a combination of lifestyle interventions, hypoglycaemic and insulin sensitizing drugs and when these measures fail, insulin (2).

Individuals may exhibit abnormal glucose metabolism without fulfilling the diagnostic criteria for diabetes and such individuals have either impaired fasting glucose (IFG), impaired

glucose tolerance (IGT) or both. Often termed ‘pre-diabetes’, these potentially reversible conditions are associated with a high risk of progression to T2DM (1). Pre-diabetes is a clinically silent entity and IFG is often an incidental finding however IGT is diagnosed with an oral glucose tolerance test (OGTT).

It is estimated that over 300 million individuals worldwide have pre-diabetes with this figure predicted to rise to over 400 million by 2025 (3). Several studies have reported the prevalence of pre-diabetes however the findings have been inconsistent due to differences in study populations and diagnostic criteria, suggesting that prevalence may be population specific. In the Framingham study, the prevalence of isolated IFG and IGT were 20% and 5% with the combination of the two present in 6%. Pooled data from 13 European and 10 Asian studies in the DECODE and DECODA studies, indicated an increased prevalence of IFG in males which plateaued in middle age and increased thereafter, up to 8 times higher in the age range 50 to 70 (4,5). IGT however, was more prevalent in females in the under 70 age group and there was limited overlap observed between IFG and IGT which may have been due to population specific metabolic and anthropomorphic differences.

1.2 The Risk of Progression from Pre-Diabetes to T2DM

Pre-diabetes is associated with a high risk of progression to T2DM. The risks of T2DM and CVD are related to blood glucose in a continuous fashion (6). In addition, there appears to be considerable variability between glycaemic indices in their ability to predict diabetes (7). Several studies have reported the risk of progression from pre-diabetes to diabetes however these studies have been inconsistent with regard to the populations studied, definitions of IFG and IGT as well as the statistical methods employed in determining such risk.

In a recent systematic review and meta-analysis of 35 studies with follow up ranging between one and seventeen years, the calculated annualised risk of developing T2DM varied for IGT (1.8-16.8%), IFG (1.6-34%) and the combination of IGT and IFG (10-15%) (8). In a study of multi-ethnic Mauritian nationals followed up for 11 years, 45.9% of individuals with IGT at baseline progressed to DM, 23.6% reverted to normal glucose tolerance, 26.4% remained glucose intolerant and 4.1% converted to IFG (9). More recently, data from a Finnish prospective study indicated similar rates of T2DM incidence across all categories of dysglycaemia (37.8% IFG, 37.1% IGT and 37.5% IH) over ten years (10). IGT was the commonest precursor to T2DM (40.6%), followed by elevated HbA1c (32.8%) and IFG (21.9%) and factors associated with progression to T2DM were FPG, 2hG, HbA1c and BMI. In the ADDITION study, in which over 1000 subjects with either IFG, IGT, or both, the progression rates for developing T2DM over the three year duration of the study were 11.8, 11.8 and 28% per hundred patient years respectively (11). Progression to T2DM was strongly associated with BMI and triglycerides in the IFG group and hypertension in the IGT group. Weight loss of 1 Kg per year was associated with a 20% risk reduction for the development of T2DM. In addition to glycaemia, other risk factors associated with the development of

T2DM in pre-diabetic individuals include systolic hypertension, elevated triglycerides and low HDL cholesterol (12). Prediction tools such as the Finnish Diabetes Risk Score (FINDRISC), have incorporated such risk factors and are able to accurately predict the 10-year risk for developing T2DM (13).

1.3 Pre-Diabetes and Cardiovascular Risk

Hyperglycaemia is associated with elevated CV mortality on a global scale (6). Gabir et al first described an association between glycaemic status and the risks of microvascular disease and cardiovascular-renal mortality in diabetic and pre-diabetic Pima Indians, findings which subsequently formed the basis of the current diagnostic glycaemic thresholds for T2DM (14).

The CV risk associated with pre-diabetes has since been reported in several meta-analyses. In a meta-analysis of 20 studies totaling over 12 years follow up, Coutinho et al reported an increased risk of CVD according to fasting and 2 hour glucose levels accordingly compared with controls (RR 1.33 and 1.58 for FPG 6.1 and 2HG 7.8 mmol/l respectively) (15). Similarly, in a meta-analysis of 38 studies, IGT was associated with a 27% increased risk of CVD, which remained elevated (19%) after adjustment for non-glycaemic CV risk factors (16). More recently, CV outcomes in the Framingham offspring cohort were compared using the WHO and ADA definitions for IFG (17). In females, both definitions of IFG were predictive of CHD however only the WHO definition was predictive of CVD whereas neither definition was able to predict CVD in men. In a recent systematic review, pre-diabetes was associated with a modestly elevated risk of CVD which was greater with IFG (RR 1.12-1.37) than IGT (RR 0.97 to 1.30) (18). Recently published results from the multinational prospective Epi-DREAM study indicated a relationship between glycaemia and CV

morbidity and mortality whereby for every 1 mmol/l increment in FPG, there was a 17% increased risk of CV events or death (95% CI 1.13-1.22) (19).

Other large population based studies have provided conflicting findings. In a recent study of over 650,000 Korean men followed over 8.8 years, there was no association between IFG and myocardial infarction or haemorrhagic stroke, but there was a linear relationship between ischaemic stroke and IFG (20). Furthermore, there was no association between IFG and CV morbidity and mortality at 15 years in the WOSCOP study cohort, although FPG predicted the onset of DM (21).

Recent studies suggest HbA1c may be a better predictor of CV outcomes compared to glycaemic indices. In the ADDITION study, HbA1c was predictive of all-cause mortality across all groups (NGT, IFG, IGT, T2DM) and was more predictive of high CV risk than questionnaires and glucose indices (22,23).

1.4 Cardiovascular Complications Associated with IGT

1.4.1 Cardiac autonomic neuropathy

Cardiac autonomic neuropathy (CAN) is the commonest manifestation of diabetic autonomic neuropathy (DAN), often present at diagnosis and is a strong independent risk factor for CV morbidity and mortality (24-26). This risk may be attributable to features of advanced CAN including sudden cardiac death (SCD), cardiac arrhythmias, silent myocardial ischaemia (SMI) and lack of hypoglycaemia awareness. It is now apparent that CAN is a common factor in several cardiac conditions and thus may be an important aetiological factor in the pathogenesis of a distinct cardiomyopathy specific to diabetes, characterised by metabolic derangement, neurohumoral activation and microvascular inflammation leading to structural and functional cardiac remodeling (27).

In addition to the risk of arrhythmia, CAN in diabetic subjects is also associated with diminished coronary artery flow reserve, altered myocardial blood flow and diastolic dysfunction (28). In a study of subjects with T1DM, CAN was associated with impaired vasodilator response of coronary resistance vessels to increased sympathetic stimulation (29). More recently, Sacre et al reported associations between CAN, regional impairment of left ventricular diastolic function and corresponding areas of dysinnervation on MIBG scintigraphy in subjects with T2DM, emphasising the potential role of cardiac neuropathy in the pathogenesis of heart failure (30). Although the exact role of glycaemia in the progression of CAN is not fully understood, several large clinical trials have demonstrated the beneficial effects of glycaemic control and multifactorial cardiovascular intervention on delaying the onset of CAN (31-34).

In contrast to the extensive work on CAN in diabetes, relatively few studies have been performed in pre-diabetic cohorts. An association between fasting glucose, insulin and cardiac autonomic abnormalities was first observed in healthy subjects (35). These studies were followed by cohort studies in which IGT was associated with CAN (36). In a study of a cohort from the Cardiovascular Health Study, increased resting heart rate and reduced heart rate variability (HRV), the earliest detectable manifestation of CAN, were associated with IFG and MetS (37).

The QT interval is affected by disturbances in autonomic function (38,39). Prolongation of the QT interval is present in diabetic patients and associated with a risk of cardiac arrhythmia and sudden cardiac death (SCD) (40-42). In the EURODIAB IDDM complication study, the reported prevalence of QT prolongation was 16% and was independently associated with age, HbA1c, blood pressure, CHD and nephropathy. In addition, the presence of CAN was associated with a higher QT in males (43). Hypoglycaemia has been associated with an increased mortality risk which may be attributable to the pro-arrhythmic effects of hypoglycaemia on the QT interval (44), however in the ACCORD trial, there were fewer arrhythmia related deaths both during intensive treatment and following termination of this arm if the study (45). Several studies in pre-diabetic cohorts have reported associations between glycaemia, insulin resistance and the QT interval (46-48). Fiorentini et al reported an association between indices of HRV and QT prolongation in subjects with IFG and IGT, but not in normoglycaemic subjects with insulin resistance (49). In the NHANES III survey, QT prolongation was present in 22%, 29.9% and 42.2% of subjects with normal glucose tolerance, IFG and diabetes respectively which in addition to conventional cardiovascular risk factors, was independently associated with c-peptide and insulin levels (50).

1.4.2 Coronary Microvascular Disease

Myocardial blood flow is regulated by the coronary microvasculature and is influenced by several factors including endothelial function, local metabolic factors and sympathetic tone (29,51). Studies using positron emission tomography (PET) have allowed the detailed study of adverse effects of DM on myocardial blood flow (28,52,53). Coronary microvascular dysfunction is also a feature of pre-diabetes and insulin resistance (54). Prior et al studied coronary microvascular function in Mexican American subjects with dysglycaemia ranging from isolated insulin resistance to IGT and T2DM (55). Endothelial dysfunction was present in all groups and worsened progressively across the spectrum of glucose dysmetabolism, whereas total vasodilatory capacity was reduced only in the T2DM group with no difference observed between the other groups.

1.4.3 Cardiac Structural and Functional Alterations

Data on cardiac structure and function in IGT are limited. Several population-based echocardiographic studies have reported increased left ventricular mass (LVM) in subjects with IGT. In the Framingham Heart Study, LVM and wall thickness (LVWT) increased with worsening glucose tolerance and were more pronounced in female participants free of CVD (56). Similarly, in the Hoorn study, LVM was associated with glycemic status only in females with IGT (57). The Strong Heart Study (SHS) also reported increased LVM and LVWT in American Indians with IGT (58). Although, LVM index (LVMI) was found to be abnormal in subjects with normal glucose tolerance, this was accounted for by obesity and hypertension, particularly in Afro-Caribbean's (59). In the Multi Ethnic Study of Atherosclerosis (MESA) and the Framingham Offspring cohort study, assessment by cardiac

magnetic resonance (CMR) imaging showed an association between LVM and glycaemic indices in subjects with impaired fasting glucose (IFG) and DM (60,61).

Diastolic dysfunction is one of the earliest detectable cardiac functional abnormalities and is characterized by a reduction in longitudinal and radial myocardial deformation and an increase in LV torsion (62). Echocardiographic techniques such as tissue Doppler imaging (TDI) and speckle tracking (STE) allow for the accurate tracking of myocardial tissue displacement and the measurement of velocity, strain and torsion (62). Indeed long axis function has been show to be reduced both at rest and during exercise in diabetic subjects without evidence of ischemic heart disease (63,64). Furthermore, studies using STE in diabetic subjects have reported impaired longitudinal but preserved radial and circumferential contraction in asymptomatic males with T2DM free of CVD (65). Asymptomatic patients with T2DM have demonstrated significant reductions in circumferential, radial and longitudinal function, compared with age-matched controls (66). Sacre et al reported an association between CAN and regional impairment of left ventricular diastolic function on CMR, which corresponded with areas of dysinnervation on MIBG scintigraphy in subjects with T2DM (30). To date, studies in IGT cohorts have been limited by relatively insensitive measures of diastolic dysfunction (67-69). A comprehensive CMR assessment showed differences in LV mass and torsion angle as well as myocardial perfusion reserve in patients with T2DM, but not in those with pre-diabetes (70). Furthermore, in young adults [mean age 31.8(6.6) years] with a short duration of T2DM [4.7(4.0) years], CMR has shown preserved cardiac volumes and function and normal circumferential strain and myocardial perfusion reserve with no evidence of myocardial fibrosis when compared to BMI matched controls (71).

Although extensively studied in animal models of DM, the need for endomyocardial biopsy has limited the study of myocardial fibrosis in man (72). Fischer et al demonstrated interstitial fibrosis in myocardial biopsy, but did not differentiate subjects with IGT from those with diabetes (73). Integrated back scatter assessment has been used to show myocardial fibrosis in subjects with T2DM and metabolic syndrome (74-76). T1 mapping has been utilised to demonstrate fibrosis associated with impaired systolic and diastolic function and biomarkers of fibrosis in patients with type 1 and 2 diabetes (77-79). Quantitative assessment of myocardial extracellular volume (ECV), a surrogate of myocardial fibrosis, shows much promise and has been recently validated in man (80-82). In the only such study published to date, diabetic subjects showed ECV expansion (83).

1.5 Peripheral Neuropathy in IGT

Neuropathy is a frequent complication of diabetes affecting peripheral (sensory and motor) and autonomic nerves equally and is a significant cause of morbidity and mortality (84). The prevalence varies vastly according to the criteria and methods used to define its presence; consequently reported values range anywhere between 10 and 90% (85). DN predisposes to foot ulceration which if severe, can give rise to gangrene and amputation which significantly impact on quality of life and healthcare costs. More recently a history of neuropathy, poor glycaemic control and aspirin use were the only baseline factors which predicted increased mortality in the intensive versus standard glycaemia arms of the ACCORD trial (86).

Several observational studies in patients with idiopathic peripheral neuropathy have found a high prevalence of IGT compared to healthy age-matched controls, suggesting that this may represent the earliest stage of hyperglycaemic nerve injury (87,88). This argument is

reinforced by the fact that histological and clinical findings in such subjects mimic those found in early DPN, features compatible with a predominantly small fibre neuropathy (89-91). The Impaired Glucose Tolerance Neuropathy (IGTN) Study was a 3-year study of 71 subjects with IGT and neuropathy which involved an annual neuropathic assessment including QST and skin biopsy. Sural sensory amplitude was normal in 36% and peroneal motor conduction velocity was normal in 61%. Cold detection was impaired in 64% whilst vibration perception threshold (VPT) was abnormal in 56% of subjects. QSART, a sensitive measure of sudomotor (i.e., sweat) nerve function, was abnormal in 61%. Intraepidermal nerve fibre density (IENFD) was reduced in 83% with the remainder demonstrating morphologically abnormal epidermal nerve fibres (92). Lifestyle intervention in these subjects with IGT showed an improvement in IENFD after 1 year of intervention and this was associated with an improvement in symptoms. Two population-based studies have investigated the prevalence of neuropathy in IGT. The San Luis Valley and MONICA/KORA studies found the prevalence of neuropathy in subjects with IGT to be 11-13% compared with 4-8% in healthy controls. The dominant clinical features in subjects with IGT neuropathy are pain, diminished response to thermal stimuli (93) and autonomic dysfunction, all of which occur secondary to small myelinated Aδ and unmyelinated C fibre injury (87,90). Chronic hyperglycaemia has been proposed as the major aetiological factor in DPN neuropathy and studies in both animals and humans have shown that transient hyperglycaemia increases spontaneous discharge from small diameter nociceptive afferent C fibres and is associated with increased neuropathic pain (94,95). More recent studies however, have suggested that factors other than hyperglycaemia may be involved in the pathophysiology of neuropathy in IGT (96). Elevated triglycerides and cholesterol, features of the metabolic syndrome, have been shown, in three separate studies, to be related to the presence of neuropathy (97,98).

Small fibre neuropathy is often undetectable with standard neuropathy tests and has, up until recently, required skin biopsy and IENFD analysis for diagnosis.

1.6 Subjects with Type 1 Diabetes of Extreme Duration

The rising worldwide prevalence of diabetes and subsequent complications poses a significant public health issue (99). Previous studies have identified risk factors in those with Type 1 diabetes which include glycaemic control, hypertension, duration of diabetes and hyperlipidaemia (100,101). However, glycaemic control in the latter years of those with long duration Type 1 diabetes may be unrelated to complications (102). A significant proportion of those with Type 1 diabetes continue to survive into the 4th and 5th decades of the disease (102,103). In a study of 400 UK patients with more than 50 years Type 1 diabetes, over 60% were found to have no evidence of micro or macroalbuminuria and after adjusting for age, gender, HbA1c, disease duration and presence of macrovascular disease, only hypertriglyceridemia (104) and adiponectin levels (105) were associated with albuminuria. Persistence and function of insulin-producing beta cells in the medallist group has previously been associated with protection from complications (106) and even on a background of risk factors such as dyslipidaemia a significant proportion will remain free of severe complications (107).

Those with over fifty years duration of Type 1 Diabetes are a unique group of patients who have previously shown protection from microvascular complications (102,107,108) although nephropathy has been previously found at similar rates in one UK study (109). A previous study of self reported complications in the U.S. suggested that greater than 40% of patients remain free from multiple complications (107). This is also mirrored by a Danish study from

the Steno Memorial Hospital were ~25% of patients who had Type 1 diabetes for more than 40 years had no major complications (110). The UK Golden Year study has characterised nephropathy (108) whilst the Joslin 50 year Medalist study assessed retinopathy, nephropathy, neuropathy and cardiovascular disease (102). However, the methods of assessment of neuropathy and cardiovascular disease were crude thus underestimating their true prevalence in the medallist cohort. To date there have been no studies which have accurately phenotyped neuropathy or cardiovascular disease in those with extreme duration of type 1 diabetes.

1.7 The Principles of Clinical Assessment of Neuropathy

Although early DPN can be clinically silent, the predominant symptom is pain which is associated with considerable morbidity in the diabetic patient. Painful neuropathy occurs with damage to small myelinated (Aδ) and unmyelinated (C) nerve fibres but can also occur with larger myelinated (Aβ) fibre involvement (111). Neuropathic pain may also present with allodynia, hyperalgesia, hyperpathia, paraesthesia or dysaesthesia (111). In addition to pain, subjects may describe other symptoms such as numbness, tightness or coldness (112). Signs of autonomic neuropathy may include orthostatic hypotension, abnormal sweating, dry eyes and/or mouth, and erectile dysfunction to name a few (113). The classification of peripheral nerves and their relative sensory modalities are summarised in tables 1-1 and 1-2.

Type	**Diameter (mm)**	**Conduction velocity (m/s)**	**Function**
Aα	10-18	90	A-Motor
A γ	4-8	30	Efferents to muscle
Aδ	2-6	30	Fast pain fibres
C	1-2	<1	Slow pain fibres, temperature, post-ganglionic autonomic fibres

Table 1-1 Peripheral nerves and their properties

	Functional Class	Normal Function	Symptoms and Signs of Dysfunction	Diagnostic Test
Small Fibre	Sensory	Pain and temperature sensation	Loss of pain and thermal sensation, spontaneous and stimulus evoked pain	QST for heat and cold, skin biopsy with IENFD
	Autonomic	Sweating, bowel, bladder and sexual function, vasomotor and heart rate control	Abnormal sweating, incontinence, constipation, gastroparesis, orthostatic hypotension	QSART, HRV, orthostatic BP and HR
Large Fibre	Sensory	Proprioception, touch and pressure sensation	Loss of touch sensation, sensory ataxia, spontaneous and stimulus evoked pain	QST for vibration, NCS
	Motor	Muscle movement	weakness	NCS and electromyography

Table 1-2 Classification of nerves according to size and function

1.7.1 Neuropathic Symptom Questionnaires

Several validated questionnaires exist for the assessment of neuropathic symptoms. The Michigan Neuropathy Screening Instrument (MNSI) (114), The Neuropathy Symptom Score (NSS) (115) and the modified NSS (116) have all been validated in previous studies.

The Neuropathy Symptom Profile (NSP) is a more detailed questionnaire spanning 34 categories and evaluates general neuropathic symptoms but is not specific for DPN. In the Rochester Diabetic Neuropathy Study, the authors concluded that in combination with neurological clinical assessment, NSP or NSS was a valid means of assessing neuropathy. Shorter questionnaires such as The Diabetic Neuropathy Symptom (DNS) score are reproducible and easy to perform screening tools in DPN (117).

The McGill pain questionnaire is another useful diagnostic tool which locates, categorises and characterises pain symptoms and has been used effectively in previous studies (118).

The neuropathy disability score (NDS) is a screening tool based on the presence of a number of clinical signs of neuropathy. Three sensory modalities are tested for; pin-prick, temperature (hot/cold) and vibration are tested for in addition to the Achilles tendon reflex and a total score out of ten is derived. Several studies have shown that NDS is a reliable screening tool for signs of neuropathy (119,120) and independently predicts the development of neuropathy and risk of diabetic foot ulceration (121).

1.7.2 Quantitative Sensory Testing

Quantitative sensory testing (QST) is a well established methodology for the quantitative assessment of sensory neuropathy. Vibration perception thresholds (VPT) are tested for using a bioesthesiometer and thermal sensitivity and thresholds are obtained using the TSA system (MEDOC) (93). These techniques are easily performed, well tolerated and provide sensitive, accurate and reproducible results. The tests are limited however by their subjectivity. Patient motivation, attention and expectation bias can affect the results (122) whilst room temperature, inter-stimulus intervals, gender, age and lifestyle may also affect outcomes (123). Standardisation of the procedure and an appropriate test environment can overcome these limitations thus providing highly sensitive and reproducible results (112).

Vibration Perception Threshold (VPT) testing

Previous studies in subjects with DPN have demonstrated VPT to be a robust and reproducible test of vibration perception (124). Furthermore, VPT alone can identify patients at risk of limb or foot ulceration (125-127).

Thermal threshold Testing

Thermal testing consists of graded and standardised warm and cold stimuli delivered through a thermode attached to the foot. Thermal testing is able to quantify warm and cold thresholds, temperature induced pain and temporal summation(111). Studies in subjects with DPN have demonstrated the clinical applicability of thermal thresholds testing (128,129). One such study showed that temperature sensitivity is selectively affected when compared with VPT, suggesting that small nerve fibres (SNF) may be more vulnerable and the first to be involved in symptomatic DPN (130).

1.7.3 Nerve Electrophysiology

Nerve conduction studies (NCS) allow for a functional measure of both sensory and motor nerves and are widely used in the diagnosis and quantification of neuropathy and DPN. Commonly, conduction velocity, amplitude and latency are measured, providing an overall assessment of neuromuscular transmission. Nerves commonly tested are the peroneal (motor) and sural (sensory) nerves. The Toronto consensus on diabetic neuropathy recommends the use of NCS in combination with other tests to diagnose and characterise neuropathy (131). NCS are non-invasive, objective and highly sensitive but are limited by their inability to test small fibre function. In a 10-year follow-up study of newly diagnosed patients with Type 2

diabetes, defects in conduction velocity, sensory and motor amplitudes were reported in 16.7% and 41.9% at 5 years at 10 years respectively (132). Nerve conduction abnormalities correlate significantly with morphologic features and QST in small fibre neuropathy (91). Sural nerve myelinated fibre density has been shown to correlate with summated peripheral nerve amplitudes and clinical deficits (133).

1.7.4 Autonomic function testing

Several methods exist for the functional assessment of the autonomic nervous system. The most commonly used tests in the context of DPN include the heart rate variability in response to deep breathing test and the Valsalva maneouver (134). Other tests include the quantitative sudomotor axon reflex test (QSART), thermoregulatory sweat testing, adrenergic autonomic testing (112), sympathetic skin response (135) and the recent sudomotor assessment Neuropad® test (136).

Several studies in subjects with neuropathy have found abnormalities in HRV as an indicator of autonomic dysfunction (113,137,138). In a study in type 1 diabetics, a composite score of autonomic function was derived from the Valsalva manoeuvre and HRV in response to deep breathing and standing. Abnormal scores were found in 16.6% of subjects.

Neuropad® sudomotor function test

Cholinergic sympathetic function can be evaluated through a variety of available tests such as QSART, sympathetic skin response and thermoregulatory sweat testing (112). The Neuropad®, a new commercially available device, has been utilised for the diagnosis of peripheral autonomic dysfunction (136). The Neuropad is placed on the plantar aspect of the

foot for 10 min and observed for a change in colour from blue to pink depending on the degree of sweat production by the skin. The rate of change has been related to the severity of neuropathy. In a study of 102 type 2 diabetic patients, sensitivity of Neuropad was reported to be 94.4% and specificity 69.7% (139,140) in another study of 123 patients with type 2 DM found sudomotor dysfunction in 95% of the patients with neuropathy, regardless of SNF involvement with a sensitivity and specificity of 95% and 69.8% respectively. When sensitivity and specificity were recalculated for those with small fibre neuropathy they were found to be 99% and 78% respectively. Finally, Neuropad demonstrated similar diagnostic capability in detecting small fibre neuropathy to other clinical examinations. Agreement, inter- and intra-observer reproducibility were also excellent in a separate study (139).

1.7.5 Corneal Confocal Microscopy (CCM)

First developed for ophthalmic use in the 1990's, CCM allows for the non-invasive visualisation of the cellular structure of the cornea with a high degree of spatial resolution and magnification. Although conventionally used for the diagnosis of various corneal epithelial disorders, CCM has proven useful in delineating the neural anatomy of the cornea with a high degree of accuracy. Using CCM, it is possible to measure nerve fibre length (NFL), density (NFD), branch density (NBD) and tortuosity (NFT). Such quantitative and qualitative analysis of the corneal nerves using CCM has demonstrated its potential use as a clinical screening tool for neuropathy in several diseases. Studies in subjects with dry eyes have also found a correlation between a reduction in NFD and decreased corneal sensitivity (141). Furthermore, NFT may represent degeneration and regeneration of corneal nerves (142). Other studies have been performed in healthy subjects in order to quantify the corneal nerves however the results have been inconsistent due to differences in the equipment and

analytical methods used (94,95,143). Nevertheless, grading scales and algorithms have previously been published for the quantitative and qualitative analysis of corneal nerves (144) and the search for a robust and reproducible methodology remains the subject of ongoing research. Some studies in healthy subjects have found an association between aging and decreased corneal nerve density however other studies have not confirmed these findings, indicating the need for further research.

We have previously demonstrated the ability of CCM to detect early neuropathy in diabetic patients (145,146). We were able to demonstrate a reduction in NFL, NFT, NFD and NBD in diabetic subjects with peripheral neuropathy compared with healthy controls. Furthermore, the degree of reduction correlated with the severity of neuropathy (assessed using standard neuropathy tests) and corneal sensitivity was also reduced in a similar fashion. We have also demonstrated an improvement in corneal nerve morphology with improvements in glycaemic control (147). In addition to standard neuropathy tests, we compared CCM with skin biopsy for the qualitative and quantitative assessment of small fibre pathology in diabetic subjects. IENFD correlated with CNFD and IENFBD correlated with CNFBD but IENFL did not correlate with CNFL. Nevertheless, CCM quantifies small fibre damage rapidly and non-invasively and detects earlier stages of nerve damage compared to IENF pathology. We have also performed studies in subjects with ISFN and IGT (148). These individuals were found to have abnormalities in electrophysiology and quantitative sensory testing. They also demonstrated markedly abnormal corneal nerve morphology with a significant reduction in NFD, NBD and NFL compared to healthy controls, however there was no difference between those with and without IGT. We have also demonstrated corneal nerve regeneration

following simultaneous kidney and pancreas transplantation as well as following improvements in HbA1c (149).

1.8 References

1. Alberti K, Zimmet P, Consultation W. Definition, diagnosis and classification of diabetes mellitus and its complications. Part 1: diagnosis and classification of diabetes mellitus. Provisional report of a WHO consultation. Diabetic Medicine. 1998;15(7):539–53.

2. Wass JAH, Stewart PM, Amiel SA, and Davies MC. Oxford Textbook of Endocrinology and Diabetes. Oxford University Press.

3. Definition, diagnosis and classification of diabetes mellitus and intermediate hyperglycaemia. WHO consultation 2006.

4. Qiao Q, Hu G, Tuomilehto J, Nakagami T, Balkau B, Borch-Johnsen K, et al. Age- and sex-specific prevalence of diabetes and impaired glucose regulation in 11 Asian cohorts. Diabetes Care. 2003 Jun;26(6):1770–80.

5. DECODE Study Group. Age- and sex-specific prevalences of diabetes and impaired glucose regulation in 13 European cohorts. Diabetes Care. 2003 Jan;26(1):61–9.

6. Danaei G, Lawes C, vander Hoorn S, Murray C, Ezzati M. Global and regional mortality from ischaemic heart disease and stroke attributable to higher-than-optimum blood glucose concentration: comparative risk assessment. The Lancet. 2006;368(9548):1651–9.

7. Soulimane S, Simon D, Shaw JE, Zimmet PZ, Vol S, Vistisen D, et al. Comparing incident diabetes as defined by fasting plasma glucose or by HbA(1c). The AusDiab, Inter99 and DESIR studies. Diabet Med. 2011 Nov;28(11):1311–8.

8. Gerstein H, Santaguida P, Raina P, Morrison K, Balion C, Hunt D, et al. Annual incidence and relative risk of diabetes in people with various categories of dysglycemia: a systematic overview and meta-analysis of prospective studies. Diabetes research and clinical practice. 2007;78(3):305–12.

9. Söderberg S, Zimmet P, Tuomilehto J, de Courten M, Dowse GK, Chitson P, et al. High incidence of type 2 diabetes and increasing conversion rates from impaired fasting glucose and impaired glucose tolerance to diabetes in Mauritius. J Intern Med. 2004 Jul;256(1):37–47.

10. Cederberg H, Saukkonen T, Laakso M, Jokelainen J, Harkonen P, Timonen M, et al. Postchallenge Glucose, A1C, and Fasting Glucose as Predictors of Type 2 Diabetes and Cardiovascular Disease: A 10-year prospective cohort study. Diabetes Care. 2010 Aug 30;33(9):2077–83.

11. Rasmussen SS, Glümer C, Sandbaek A, Lauritzen T, Borch-Johnsen K. Determinants of progression from impaired fasting glucose and impaired glucose tolerance to diabetes in a high-risk screened population: 3 year follow-up in the ADDITION study, Denmark. Diabetologia. 2008 Feb;51(2):249–57.

12. Haffner SM, Stern MP, Hazuda HP, Mitchell BD, Patterson JK. Cardiovascular risk factors in confirmed prediabetic individuals. Does the clock for coronary heart disease start ticking before the onset of clinical diabetes? JAMA. 1990 Jun 6;263(21):2893–8.

13. Lindström J, Tuomilehto J. The diabetes risk score: a practical tool to predict type 2 diabetes risk. Diabetes Care. 2003 Mar;26(3):725–31.

14. Gabir MM, Hanson RL, Dabelea D, Imperatore G, Roumain J, Bennett PH, et al. Plasma glucose and prediction of microvascular disease and mortality: evaluation of 1997 American Diabetes Association and 1999 World Health Organization criteria for diagnosis of diabetes. Diabetes Care. 2000 Aug;23(8):1113–8.

15. Coutinho M, Gerstein HC, Wang Y, Yusuf S. The relationship between glucose and incident cardiovascular events. A metaregression analysis of published data from 20 studies of 95,783 individuals followed for 12.4 years. Diabetes Care. 1999 Feb;22(2):233–40.

16. Levitan EB, Song Y, Ford ES, Liu S. Is Nondiabetic Hyperglycemia a Risk Factor for Cardiovascular Disease?: A Meta-analysis of Prospective Studies. Archives of internal medicine. American Medical Association; 2004 Oct 25;164(19):2147–55.

17. Levitzky Y, Pencina M, D'Agostino R, Meigs J, Murabito J, Vasan R, et al. Impact of Impaired Fasting Glucose on Cardiovascular Disease: The Framingham Heart Study. Journal of the American College of Cardiology. 2008;51(3):264–70.

18. Ford ES, Zhao G, Li C. Pre-Diabetes and the Risk for Cardiovascular Disease. JAC. 2031 Feb 13;55(13):1310–7.

19. Anand SS, Dagenais GR, Mohan V, Diaz R, Probstfield J, FREEMAN R, et al. Glucose levels are associated with cardiovascular disease and death in an international cohort of normal glycaemic and dysglycaemic men and women: the EpiDREAM cohort study. Eur J Prev Cardiol. 2012 Aug;19(4):755–64.

20. Sung J, Song Y-M, Ebrahim S, Lawlor DA. Fasting blood glucose and the risk of stroke and myocardial infarction. Circulation. 2009 Feb 17;119(6):812–9.

21. Preiss D, Welsh P, Murray HM, Shepherd J, Packard C, Macfarlane P, et al. Fasting plasma glucose in non-diabetic participants and the risk for incident cardiovascular events, diabetes, and mortality: results from WOSCOPS 15-year follow-up. European Heart Journal. 2010 May 2;31(10):1230–6.

22. Skriver MV, Borch-Johnsen K, Lauritzen T, Sandbaek A. HbA1c as predictor of all-cause mortality in individuals at high risk of diabetes with normal glucose tolerance, identified by screening: a follow-up study of the Anglo-Danish-Dutch Study of Intensive Treatment in People with Screen-Detected Diabetes in Primary Care (ADDITION), Denmark. Diabetologia. 2010 Nov;53(11):2328–33.

23. Lauritzen T, Sandbaek A, Skriver MV, Borch-Johnsen K. HbA1c and cardiovascular risk score identify people who may benefit from preventive interventions: a 7 year follow-up of a high-risk screening programme for diabetes in primary care (ADDITION), Denmark. Diabetologia. 2011 Jun;54(6):1318–26.

24. Gerritsen J, Dekker JM, TenVoorde BJ, Kostense PJ, Heine RJ, Bouter LM, et al. Impaired autonomic function is associated with increased mortality, especially in subjects with diabetes, hypertension, or a history of cardiovascular disease: the Hoorn Study. Diabetes Care. 2001 Oct;24(10):1793–8.

25. Valensi P, Sachs RN, Harfouche B, Lormeau B, Paries J, Cosson E, et al. Predictive value of cardiac autonomic neuropathy in diabetic patients with or without silent myocardial ischemia. Diabetes Care. 2001 Feb;24(2):339–43.

26. Vinik AI, Ziegler D. Diabetic Cardiovascular Autonomic Neuropathy. Circulation. 2007 Jan 8;115(3):387–97.

27. Asghar O, Al-Sunni A, Khavandi K, Khavandi A, Withers S, Greenstein A, et al. Diabetic cardiomyopathy. Clinical Science. 2009 May;116(10):741–60.

28. Pop-Busui R, Kirkwood I, Schmid H, Marinescu V, Schroeder J, Larkin D, et al. Sympathetic dysfunction in type 1 diabetes. Journal of the American College of Cardiology. 2004 Dec;44(12):2368–74.

29. Di Carli MF, Bianco-Batlles D, Landa ME, Kazmers A, Groehn H, Muzik O, et al. Effects of autonomic neuropathy on coronary blood flow in patients with diabetes mellitus. Circulation. 1999 Aug 24;100(8):813–9.

30. Sacre JW, Franjic B, Jellis CL, Jenkins C, Coombes JS, Marwick TH. Association of cardiac autonomic neuropathy with subclinical myocardial dysfunction in type 2 diabetes. JACC Cardiovasc Imaging. 2010 Dec;3(12):1207–15.

31. The effect of intensive diabetes therapy on measures of autonomic nervous system function in the Diabetes Control and Complications Trial (DCCT). Diabetologia. 1998 Apr;41(4):416–23.

32. Reichard P, Jensen-Urstad K, Ericsson M, Jensen-Urstad M, Lindblad LE. Autonomic neuropathy--a complication less pronounced in patients with Type 1 diabetes mellitus who have lower blood glucose levels. Diabetic Medicine. 2000 Dec;17(12):860–6.

33. Ziegler D, Weise F, Langen KJ, Piolot R, Boy C, Hübinger A, et al. Effect of glycaemic control on myocardial sympathetic innervation assessed by [123I]metaiodobenzylguanidine scintigraphy: a 4-year prospective study in IDDM patients. Diabetologia. 1998 Apr;41(4):443–51.

34. Gaede P, Vedel P, Larsen N, Jensen GVH, Parving H-H, Pedersen O. Multifactorial intervention and cardiovascular disease in patients with type 2 diabetes. N Engl J Med. 2003 Jan 30;348(5):383–93.

35. Watkins LL, Surwit RS, Grossman P, Sherwood A. Is there a glycemic threshold for impaired autonomic control? Diabetes Care. 2000 Jun;23(6):826–30.

36. Putz Z, Tabak AG, Toth N, Istenes I, Nemeth N, Gandhi RA, et al. Noninvasive Evaluation of Neural Impairment in Subjects With Impaired Glucose Tolerance. Diabetes Care. 2009 Jan 1;32(1):181–3.

37. Stein PK, Barzilay JI, Domitrovich PP, Chaves PM, Gottdiener JS, Heckbert SR, et al. The relationship of heart rate and heart rate variability to non-diabetic fasting glucose levels and the metabolic syndrome: the Cardiovascular Health Study. Diabetic Medicine. 2007 Aug;24(8):855–63.

38. Diedrich A, Jordan J, Shannon JR, Robertson D, Biaggioni I. Modulation of QT interval during autonomic nervous system blockade in humans. Circulation. 2002 Oct 22;106(17):2238–43.

39. Lo SS, Mathias CJ, Sutton MS. QT interval and dispersion in primary autonomic failure. Heart. 1996 May;75(5):498–501.

40. Langen KJ, Ziegler D, Weise F, Piolot R, Boy C, Hübinger A, et al. Evaluation of QT interval length, QT dispersion and myocardial m-iodobenzylguanidine uptake in insulin-dependent diabetic patients with and without autonomic neuropathy. Clin Sci. 1997 Oct;93(4):325–33.

41. Stevens MJ, Raffel DM, Allman KC, Dayanikli F, Ficaro E, Sandford T, et al. Cardiac sympathetic dysinnervation in diabetes: implications for enhanced cardiovascular risk. Circulation. 1998 Sep 8;98(10):961–8.

42. Veglio M, Sivieri R, Chinaglia A, Scaglione L, Cavallo-Perin P. QT interval prolongation and mortality in type 1 diabetic patients: a 5-year cohort prospective study. Neuropathy Study Group of the Italian Society of the Study of Diabetes, Piemonte Affiliate. Diabetes Care. 2000 Sep;23(9):1381–3.

43. Veglio M, Borra M, Stevens LK, Fuller JH, Perin PC. The relation between QTc interval prolongation and diabetic complications. The EURODIAB IDDM Complication Study Group. Diabetologia. 1999 Jan;42(1):68–75.

44. Nordin C. The case for hypoglycaemia as a proarrhythmic event: basic and clinical evidence. Diabetologia. 2010 Aug;53(8):1552–61.

45. ACCORD Study Group, Gerstein HC, Miller ME, Genuth S, Ismail-Beigi F, Buse JB, et al. Long-term effects of intensive glucose lowering on cardiovascular outcomes. N Engl J Med. 2011 Mar 3;364(9):818–28.

46. Dekker J, Crow R, Folsom A, Hannan P. Low heart rate variability in a 2-minute rhythm strip predicts risk of coronary heart disease and mortality from several causes: the ARIC Study. Circulation. 2000 Jan 1.

47. Shin H-S, Lee W-Y, Kim S-W, Jung C-H, Rhee E-J, Kim B-J, et al. Sex difference in the relationship between insulin resistance and corrected QT interval in non-diabetic subjects. Circ J. 2005 Apr;69(4):409–13.

48. van Noord C, Sturkenboom MCJM, Straus SMJM, Hofman A, Kors JA, Witteman JCM, et al. Serum glucose and insulin are associated with QTc and RR intervals in nondiabetic elderly. Eur J Endocrinol. 2010 Feb;162(2):241–8.

49. Fiorentini A, Perciaccante A, Valente R, Paris A, Serra P, Tubani L. The correlation among QTc interval, hyperglycaemia and the impaired autonomic activity. Auton Neurosci. 2010 Apr 19;154(1-2):94–8.

50. Brown DW, Giles WH, Greenlund KJ, Valdez R, Croft JB. Impaired fasting glucose, diabetes mellitus, and cardiovascular disease risk factors are associated with prolonged QTc duration. Results from the Third National Health and Nutrition Examination Survey. J Cardiovasc Risk. 2001 Aug;8(4):227–33.

51. Muller JM, Davis MJ, Chilian WM. Integrated regulation of pressure and flow in the coronary microcirculation. Cardiovascular research. 1996 Oct;32(4):668–78.

52. Di Carli MF, Janisse J, Grunberger G, Ager J. Role of chronic hyperglycemia in the pathogenesis of coronary microvascular dysfunction in diabetes. Journal of the American College of Cardiology. 2003 Apr;41(8):1387–93.

53. Hattori N, Rihl J, Bengel F, Nekolla S. Cardiac autonomic dysinnervation and myocardial blood flow in long-term Type 1 diabetic patients. Diabetic …. 2003.

54. Schelbert HR. Coronary Circulatory Function Abnormalities in Insulin Resistance. JAC. American College of Cardiology Foundation; 2009 Feb 3;53(5):S3–S8.

55. Prior JO. Coronary Circulatory Dysfunction in Insulin Resistance, Impaired Glucose Tolerance, and Type 2 Diabetes Mellitus. Circulation. 2005 May 10;111(18):2291–8.

56. Rutter MK. Impact of Glucose Intolerance and Insulin Resistance on Cardiac Structure and Function: Sex-Related Differences in the Framingham Heart Study. Circulation. 2003 Jan 28;107(3):448–54.

57. Henry R, Kamp O, Kostense P, Spijkerman A, Dekker J, van Eijck R, et al. Left ventricular mass increases with deteriorating glucose tolerance, especially in women: independence of increased arterial stiffness or decreased flow-mediated dilation. Diabetes Care. 2004;27(2):522.

58. Ilercil A. Relationship of impaired glucose tolerance to left ventricular structure and function: The Strong Heart Study. American Heart Journal. 2001 Jun 1;141(6):992–8.

59. Chaturvedi N. A comparison of left ventricular abnormalities associated with glucose intolerance in African Caribbeans and Europeans in the UK. Heart. 2001 Jun 1;85(6):643–8.

60. Bertoni A, Goff D, D Agostino R, Liu K, Hundley W, Lima J, et al. Diabetic Cardiomyopathy and Subclinical Cardiovascular Disease. Diabetes Care. 2006;29(3):588.

61. Velagaleti RS, Gona P, Chuang ML, Salton CJ, Fox CS, Blease SJ, et al. Relations of Insulin Resistance and Glycemic Abnormalities to Cardiovascular Magnetic Resonance Measures of Cardiac Structure and Function: The Framingham Heart Study. Circulation: Cardiovascular Imaging. 2010 May 1;3(3):257–63.

62. Oh JK, Park SJ, Nagueh SF. Established and Novel Clinical Applications of Diastolic Function Assessment by Echocardiography. Circulation: Cardiovascular Imaging. 2011 Jul 19;4(4):444–55.

63. Ha J-W, Lee H-C, Kang E-S, Ahn C-M, Kim J-M, Ahn J-A, et al. Abnormal left ventricular longitudinal functional reserve in patients with diabetes mellitus: implication for detecting subclinical myocardial dysfunction using exercise tissue Doppler echocardiography. Heart. 2007 Dec;93(12):1571–6.

64. Fang Z, Najos-Valencia O, Leano R, Marwick T. Patients with early diabetic heart disease demonstrate a normal myocardial response to dobutamine* 1. Journal of the American College of Cardiology. 2003;42(3):446–53.

65. Ng ACT, Delgado V, Bertini M, Meer RWVD, Rijzewijk LJ, Shanks M, et al. Findings from Left Ventricular Strain and Strain Rate Imaging in Asymptomatic Patients With Type 2 Diabetes Mellitus. AJC. 2009 Jan 11;104(10):1398–401.

66. Nakai H, Takeuchi M, Nishikage T, Lang RM, Otsuji Y. Subclinical left ventricular dysfunction in asymptomatic diabetic patients assessed by two-dimensional speckle tracking echocardiography: correlation with diabetic duration. European Journal of Echocardiography. 2009 Dec 1;10(8):926–32.

67. Okura H, Inoue H, Tomon M, Nishiyama S, Yoshikawa T, Yoshida K, et al. Impaired glucose tolerance as a determinant of early deterioration of left ventricular diastolic function in middle-aged healthy subjects. The American Journal of Cardiology. 2000;85(6):790.

68. Fujita M, Asanuma H, Kim J, Liao Y, Hirata A, Tsukamoto O, et al. Impaired glucose tolerance: a possible contributor to left ventricular hypertrophy and diastolic dysfunction. International Journal of Cardiology. 2007 May 16;118(1):76–80.

69. Shimabukuro M, Higa N, Asahi T, Yamakawa K, Oshiro Y, Higa M, et al. Impaired glucose tolerance, but not impaired fasting glucose, underlies left ventricular diastolic dysfunction. Diabetes Care. 2011 Mar;34(3):686–90.

70. Larghat AM, Swoboda PP, Biglands JD, Kearney MT, Greenwood JP, Plein S. The microvascular effects of insulin resistance and diabetes on cardiac structure, function, and perfusion: a cardiovascular magnetic resonance study. European Heart Journal - Cardiovascular Imaging [Internet]. 2014 Aug 12.

71. Khan JN, Wilmot EG, Leggate M, Singh A, Yates T, Nimmo M, et al. Subclinical diastolic dysfunction in young adults with Type 2 diabetes mellitus: a multiparametric contrast-enhanced cardiovascular magnetic resonance pilot study assessing potential mechanisms. European Heart Journal - Cardiovascular Imaging. 2014 Oct 24;15(11):1263–9.

72. Asbun J, Villarreal F. The pathogenesis of myocardial fibrosis in the setting of diabetic cardiomyopathy. Journal of the American College of Cardiology. 2006;47(4):693–700.

73. Fischer VW, Fischer VW, Fischer VW, Fischer VW, Barner HB, Barner HB, et al. Pathomorphologic aspects of muscular tissue in diabetes mellitus. Human pathology [Internet]. 1984 Dec;15(12):1127–36.

74. Fang Z, Yuda S, Anderson V, Short L, Case C, Marwick T. Echocardiographic detection of early diabetic myocardial disease* 1. Journal of the American College of Cardiology. 2003;41(4):611–7.

75. Kosmala W, Przewlocka-Kosmala M, Szczepanik-Osadnik H, Mysiak A, O'Moore-Sullivan T, Marwick TH. A Randomized Study of the Beneficial Effects of Aldosterone Antagonism on LV Function, Structure, and Fibrosis Markers in Metabolic Syndrome. JCMG. Elsevier Inc; 2011 Dec 1;4(12):1239–49.

76. Marwick TH, Raman SV, Carrió I, Bax JJ. Recent Developments in Heart Failure Imaging. JCMG. 2011 Jan 14;3(4):429–39.

77. Ng ACT, Auger D, Delgado V, van Elderen SGC, Bertini M, Siebelink HM, et al. Association Between Diffuse Myocardial Fibrosis by Cardiac Magnetic Resonance Contrast-Enhanced T1 Mapping and Subclinical Myocardial Dysfunction in Diabetic Patients: A Pilot Study. Circulation: Cardiovascular Imaging. 2012 Jan 17;5(1):51–9.

78. Jellis C, Wright J, Kennedy D, Sacre J, Jenkins C, Haluska B, et al. Association of Imaging Markers of Myocardial Fibrosis with Metabolic and Functional Disturbances in Early Diabetic Cardiomyopathy. Circulation: Cardiovascular Imaging. 2011 Sep 23.

79. Messroghli DR, Radjenovic A, Kozerke S, Higgins DM, Sivananthan MU, Ridgway JP. Modified Look-Locker inversion recovery (MOLLI) for high-resolutionT1 mapping of the heart. Magn Reson Med. 2004;52(1):141–6.

80. Flett AS, Hayward MP, Ashworth MT, Hansen MS, Taylor AM, Elliott PM, et al. Equilibrium Contrast Cardiovascular Magnetic Resonance for the Measurement of Diffuse Myocardial Fibrosis: Preliminary Validation in Humans. Circulation. 2010 Jul 12;122(2):138–44.

81. Miller CA, Naish JH, Bishop P, Coutts G, Clark D, Zhao S, et al. Comprehensive Validation of Cardiovascular Magnetic Resonance Techniques for the Assessment of Myocardial Extracellular Volume. Circulation: Cardiovascular Imaging. 2013 May 21;6(3):373–83.

82. Aus dem Siepen F, Buss SJ, Messroghli D, Andre F, Lossnitzer D, Seitz S, et al. T1 mapping in dilated cardiomyopathy with cardiac magnetic resonance: quantification of diffuse myocardial fibrosis and comparison with endomyocardial biopsy. European Heart Journal - Cardiovascular Imaging. 2014 Sep 22.

83. Wong TC, Piehler KM, Kang IA, Kadakkal A, Kellman P, Schwartzman DS, et al. Myocardial extracellular volume fraction quantified by cardiovascular magnetic resonance is increased in diabetes and associated with mortality and incident heart failure admission. European Heart Journal. 2014 Mar;35(10):657–64.

84. Edwards JL, Vincent AM, Cheng HT, Feldman EL. Diabetic neuropathy: mechanisms to management. Pharmacology & therapeutics. 2008 Oct;120(1):1–34.

85. Dyck PJ, Kratz KM, Karnes JL, Litchy WJ, Klein R, Pach JM, et al. The prevalence by staged severity of various types of diabetic neuropathy, retinopathy, and nephropathy in a population-based cohort: the Rochester Diabetic Neuropathy Study. Neurology. 1993 Apr;43(4):817–24.

86. Calles-Escandón J, Lovato LC, Simons-Morton DG, Kendall DM, Pop-Busui R, Cohen RM, et al. Effect of intensive compared with standard glycemia treatment strategies on mortality by baseline subgroup characteristics: the Action to Control Cardiovascular Risk in Diabetes (ACCORD) trial. Diabetes Care. 2010 Apr;33(4):721–7.

87. Sumner CJ, Sheth S, Griffin JW, Cornblath DR, Polydefkis M. The spectrum of neuropathy in diabetes and impaired glucose tolerance. Neurology. 2003 Jan 14;60(1):108–11.

88. Novella SP, Inzucchi SE, Goldstein JM. The frequency of undiagnosed diabetes and impaired glucose tolerance in patients with idiopathic sensory neuropathy. Muscle Nerve. 2001 Sep;24(9):1229–31.

89. Singleton J, Smith A, Russell J, Feldman E. Microvascular complications of impaired glucose tolerance. Diabetes. 2003;52(12):2867.

90. Smith AG, Ramachandran P, Tripp S, Singleton JR. Epidermal nerve innervation in impaired glucose tolerance and diabetes-associated neuropathy. Neurology. 2001 Nov 13;57(9):1701–4.

91. Løseth S, Stålberg E, Jorde R, Mellgren SI. Early diabetic neuropathy: thermal thresholds and intraepidermal nerve fibre density in patients with normal nerve conduction studies. J Neurol. 2008 Aug;255(8):1197–202.

92. Smith AG, Russell J, Feldman EL, Goldstein J, Peltier A, Smith S, et al. Lifestyle intervention for pre-diabetic neuropathy. Diabetes Care. 2006 Jun;29(6):1294–9.

93. Boulton A, Malik RA, Arezzo JC. Diabetic somatic neuropathies. Diabetes Care. 2004.

94. Burchiel KJ, Russell LC, Lee RP, Sima AA. Spontaneous activity of primary afferent neurons in diabetic BB/Wistar rats. A possible mechanism of chronic diabetic neuropathic pain. Diabetes. 1985 Nov;34(11):1210–3.

95. Boulton A. What causes neuropathic pain? J Diabetes Complicat. 1992 Jan;6(1):58–63.

96. Green AQ, Krishnan S, Finucane FM, Rayman G. Altered C-fiber function as an indicator of early peripheral neuropathy in individuals with impaired glucose tolerance. Diabetes Care. 2010 Jan;33(1):174–6.

97. Hughes RAC, Umapathi T, Gray IA, Gregson NA, Noori M, Pannala AS, et al. A controlled investigation of the cause of chronic idiopathic axonal polyneuropathy. Brain. 2004 Aug;127(Pt 8):1723–30.

98. Smith AG, Rose K, Singleton JR. Idiopathic neuropathy patients are at high risk for metabolic syndrome. J Neurol Sci. 2008 Oct 15;273(1-2):25–8.

99. Whiting DR, Guariguata L, Weil C, Shaw J. IDF diabetes atlas: global estimates of the prevalence of diabetes for 2011 and 2030. Diabetes research and clinical practice. 2011 Dec;94(3):311–21.

100. Tesfaye S, Chaturvedi N, Eaton SEM, Ward JD, Manes C, Ionescu-Tirgoviste C, et al. Vascular risk factors and diabetic neuropathy. N Engl J Med. 2005 Jan 27;352(4):341–50.

101. The effect of intensive treatment of diabetes on the development and progression of long-term complications in insulin-dependent diabetes mellitus. The Diabetes Control and Complications Trial Research Group. New England Journal of Medicine. 1993 Sep 30;329(14):977–86.

102. Sun JK, Keenan HA, Cavallerano JD, Asztalos BF, Schaefer EJ, Sell DR, et al. Protection From Retinopathy and Other Complications in Patients With Type 1 Diabetes of Extreme Duration: The Joslin 50-Year Medalist Study. Diabetes Care. 2011 Mar 29;34(4):968–74.

103. Gale EAM. How to survive diabetes. Diabetologia. 2009 Feb 7;52(4):559–67.

104. Daousi C, Bain SC, Barnett AH, Gill GV. Hypertriglyceridaemia is associated with an increased likelihood of albuminuria in extreme duration (> 50 years) Type 1 diabetes. Diabet Med. 2008 Oct;25(10):1234–6.

105. Prior SL, Tang TS, Gill GV, Bain SC, Stephens JW. Adiponectin, total antioxidant status, and urine albumin excretion in the low-risk "Golden Years" type 1 diabetes mellitus cohort. Metab Clin Exp. 2011 Feb;60(2):173–9.

106. Keenan HA, Sun JK, Levine J, Doria A, Aiello LP, Eisenbarth G, et al. Residual insulin production and pancreatic ß-cell turnover after 50 years of diabetes: Joslin Medalist Study. Diabetes. 2010 Nov;59(11):2846–53.

107. Keenan HA, Costacou T, Sun JK, Doria A, Cavellerano J, Coney J, et al. Clinical factors associated with resistance to microvascular complications in diabetic patients of extreme disease duration: the 50-year medalist study. Diabetes Care. 2007 Aug;30(8):1995–7.

108. Bain SC, Gill GV, Dyer PH, Jones AF, Murphy M, Jones KE, et al. Characteristics of Type 1 diabetes of over 50 years duration (the Golden Years Cohort). Diabetic Medicine. 2003 Oct;20(10):808–11.

109. Gill GV, Daousi C, Barnett AH, Bain SC. Chronic kidney disease in long duration type 1 diabetes lasting more than 50 years. Curr Med Res Opin. 2009 Feb;25(2):395–400.

110. Borch-Johnsen K, Nissen H, Henriksen E, Kreiner S, Salling N, Deckert T, et al. The natural history of insulin-dependent diabetes mellitus in Denmark: 1. Long-term survival with and without late diabetic complications. Diabetic Medicine. 1987 May;4(3):201–10.

111. Freeman RL. Painful peripheral neuropathy: diagnosis and assessment. CONTINUUM: Lifelong Learning in Neurology. 2009.

112. Lacomis D. Small-fiber neuropathy. Muscle Nerve. 2002 Jul 29;26(2):173–88.

113. Novak V, Freimer ML, Kissel JT, Sahenk Z, Periquet IM, Nash SM, et al. Autonomic impairment in painful neuropathy. Neurology. 2001 Apr 10;56(7):861–8.

114. Feldman EL, Stevens MJ, Thomas PK, Brown MB, Canal N, Greene DA. A practical two-step quantitative clinical and electrophysiological assessment for the diagnosis and staging of diabetic neuropathy. Diabetes Care. 1994 Nov;17(11):1281–9.

115. Dyck PJ, Kratz KM, Lehman KA, Karnes JL, Melton LJ, O'Brien PC, et al. The Rochester Diabetic Neuropathy Study: design, criteria for types of neuropathy, selection bias, and reproducibility of neuropathic tests. Neurology. 1991 Jun;41(6):799–807.

116. Young MJ, Boulton AJ, MacLeod AF, Williams DR, Sonksen PH. A multicentre study of the prevalence of diabetic peripheral neuropathy in the United Kingdom hospital clinic population. Diabetologia. 1993 Feb;36(2):150–4.

117. Meijer JWG, Smit AJ, Sonderen EV, Groothoff JW, Eisma WH, Links TP. Symptom scoring systems to diagnose distal polyneuropathy in diabetes: the Diabetic Neuropathy Symptom score. Diabetic Medicine. 2002 Nov;19(11):962–5.

118. Masson EA, Hunt L, Gem JM, Boulton AJ. A novel approach to the diagnosis and assessment of symptomatic diabetic neuropathy. Pain. 1989 Jul;38(1):25–8.

119. Abbott CA, Carrington AL, Ashe H, Bath S, Every LC, Griffiths J, et al. The North-West Diabetes Foot Care Study: incidence of, and risk factors for, new diabetic foot ulceration in a community-based patient cohort. Diabetic Medicine. 2002 May;19(5):377–84.

120. Pham H, Armstrong DG, Harvey C, Harkless LB, Giurini JM, Veves A. Screening techniques to identify people at high risk for diabetic foot ulceration: a prospective multicenter trial. Diabetes Care. 2000 May;23(5):606–11.

121. Perkins BA, Orszag A, Ngo M, Ng E, New P, Bril V. Prediction of incident diabetic neuropathy using the monofilament examination: a 4-year prospective study. Diabetes Care. 2010 Jul;33(7):1549–54.

122. Dyck PJ, Dyck PJ, Kennedy WR, Kesserwani H, Melanson M, Ochoa J, et al. Limitations of quantitative sensory testing when patients are biased toward a bad outcome. Neurology. 1998 May;50(5):1213.

123. Hansson P, Backonja M, Bouhassira D. Usefulness and limitations of quantitative sensory testing: clinical and research application in neuropathic pain states. Pain. 2007 Jun;129(3):256–9.

124. Gelber DA, Pfeifer MA, Broadstone VL, Munster EW, Peterson M, Arezzo JC, et al. Components of variance for vibratory and thermal threshold testing in normal and diabetic subjects. J Diabetes Complicat. 1995 Jul;9(3):170–6.

125. Boulton AJ, Hardisty CA, Betts RP, Franks CI, Worth RC, Ward JD, et al. Dynamic foot pressure and other studies as diagnostic and management aids in diabetic neuropathy. Diabetes Care. 1983 Jan;6(1):26–33.

126. Boulton AJ, Kubrusly DB, Bowker JH, Gadia MT, Quintero L, Becker DM, et al. Impaired vibratory perception and diabetic foot ulceration. Diabetic Medicine. 1986 Jul;3(4):335–7.

127. Abbott CA, Vileikyte L, Williamson S, Carrington AL, Boulton AJ. Multicenter study of the incidence of and predictive risk factors for diabetic neuropathic foot ulceration. Diabetes Care. 1998 Jul;21(7):1071–5.

128. Navarro X, Kennedy WR. Evaluation of thermal and pain sensitivity in type I diabetic patients. J Neurol Neurosurg Psychiatr. 1991 Jan;54(1):60–4.

129. Pfeifer MA, Cook D, Brodsky J, Tice D, Reenan A, Swedine S, et al. Quantitative evaluation of cardiac parasympathetic activity in normal and diabetic man. Diabetes. 1982 Apr;31(4 Pt 1):339–45.

130. Guy RJ, Clark CA, Malcolm PN, Watkins PJ. Evaluation of thermal and vibration sensation in diabetic neuropathy. Diabetologia. 1985 Mar;28(3):131–7.

131. Dyck PJ, Albers JW, Andersen H, Arezzo JC, Biessels G-J, Bril V, et al. Diabetic polyneuropathies: update on research definition, diagnostic criteria and estimation of severity. Diabetes Metab Res Rev. 2011 Oct;27(7):620–8.

132. Partanen J, Niskanen L, Lehtinen J, Mervaala E, Siitonen O, Uusitupa M. Natural history of peripheral neuropathy in patients with non-insulin-dependent diabetes mellitus. New England Journal of Medicine. 1995 Jul 13;333(2):89–94.

133. Russell JW, Karnes JL, Dyck PJ. Sural nerve myelinated fiber density differences associated with meaningful changes in clinical and electrophysiologic measurements. J Neurol Sci. 1996 Feb;135(2):114–7.

134. Vinik AI, Maser RE, Mitchell BD, FREEMAN R. Diabetic Autonomic Neuropathy. Diabetes Care. 2003 May 1;26(5):1553–79.

135. Asahina M, Yamanaka Y, Akaogi Y, Kuwabara S, Koyama Y, Hattori T. Measurements of sweat response and skin vasomotor reflex for assessment of autonomic dysfunction in patients with diabetes. J Diabetes Complicat. 2008 Jul;22(4):278–83.

136. Papanas N, Papatheodorou K, Christakidis D, Papazoglou D, Giassakis G, Piperidou H, et al. Evaluation of a new indicator test for sudomotor function (Neuropad) in the diagnosis of peripheral neuropathy in type 2 diabetic patients. Exp Clin Endocrinol Diabetes. 2005 Apr;113(4):195–8.

137. Stewart JD, Low PA, Fealey RD. Distal small fiber neuropathy: results of tests of sweating and autonomic cardiovascular reflexes. Muscle Nerve. 1992 Jun;15(6):661–5.

138. Tobin K, Giuliani MJ, Lacomis D. Comparison of different modalities for detection of small fiber neuropathy. Clin Neurophysiol. 1999 Nov;110(11):1909–12.

139. Papanas N, Papatheodorou K, Papazoglou D, Christakidis D, Monastiriotis C, Maltezos E. Reproducibility of the new indicator test for sudomotor function (Neuropad) in patients with type 2 diabetes mellitus: short communication. Exp Clin Endocrinol Diabetes. 2005 Dec;113(10):577–81.

140. Papanas N, Giassakis G, Papatheodorou K, Papazoglou D, Monastiriotis C, Christakidis D, et al. Sensitivity and specificity of a new indicator test (Neuropad) for the diagnosis of peripheral neuropathy in type 2 diabetes patients: a comparison with clinical examination and nerve conduction study. J Diabetes Complicat. 2007 Nov;21(6):353–8.

141. Benítez-Del-Castillo JM, Acosta MC, Wassfi MA, Díaz-Valle D, Gegúndez JA, Fernandez C, et al. Relation between corneal innervation with confocal microscopy and corneal sensitivity with noncontact esthesiometry in patients with dry eye. Invest Ophthalmol Vis Sci. 2007 Jan;48(1):173–81.

142. Kallinikos P, Berhanu M, O'Donnell C, Boulton AJM, Efron N, Malik RA. Corneal nerve tortuosity in diabetic patients with neuropathy. Invest Ophthalmol Vis Sci. 2004 Feb;45(2):418–22.

143. Patel DV, McGhee CNJ. In vivo confocal microscopy of corneal stromal nerves in patients with peripheral neuropathy. Arch Neurol. 2009 Sep;66(9):1179–80–authorreply1180.

144. Scarpa F, Grisan E, Ruggeri A. Automatic recognition of corneal nerve structures in images from confocal microscopy. Invest Ophthalmol Vis Sci. 2008 Nov;49(11):4801–7.

145. Malik RA, Kallinikos P, Abbott CA, van Schie CHM, Morgan P, Efron N, et al. Corneal confocal microscopy: a non-invasive surrogate of nerve fibre damage and repair in diabetic patients. Diabetologia. 2003 May;46(5):683–8.

146. Rosenberg ME, Tervo TM, Immonen IJ, Müller LJ, Grönhagen-Riska C, Vesaluoma MH. Corneal structure and sensitivity in type 1 diabetes mellitus. Invest Ophthalmol Vis Sci. 2000 Sep;41(10):2915–21.

147. Iqbal A, Kallinikos PA, Efron N, Boulton AJ, Malik RA. Corneal nerve morphology: A surrogate marker for human diabetic neuropathy improves with improved glycaemic control. Centre for Health Research; Faculty of Health; Institute of Health and Biomedical Innovation. 2005.

148. Tavakoli M, Marshall A, Pitceathly R, Fadavi H, Gow D, Roberts ME, et al. Corneal confocal microscopy: a novel means to detect nerve fibre damage in idiopathic small fibre neuropathy. Exp Neurol. 2010 May;223(1):245–50.

149. Mehra S, Tavakoli M, Kallinikos PA, Efron N, Boulton AJM, Augustine T, et al. Corneal confocal microscopy detects early nerve regeneration after pancreas transplantation in patients with type 1 diabetes. Diabetes Care. 2007 Oct;30(10):2608–12.

2 Human Cardiac Innervation

2.1 Introduction

Regulation of cardiovascular reflexes, heart rate, myocardial function and coronary blood flow is carried out by the cardiac autonomic nervous system (ANS), which is divided into two functionally distinct branches; the sympathetic (SNS) and parasympathetic (PNS) nervous systems. The interaction between the PNS and SNS determines the cardiovascular response to any given physiological situation. The cardiac ANS is influenced by and interacts with neurones at several different levels of the human nervous system in a complex and integrated hierarchal system (figure 2-1) (1,2).

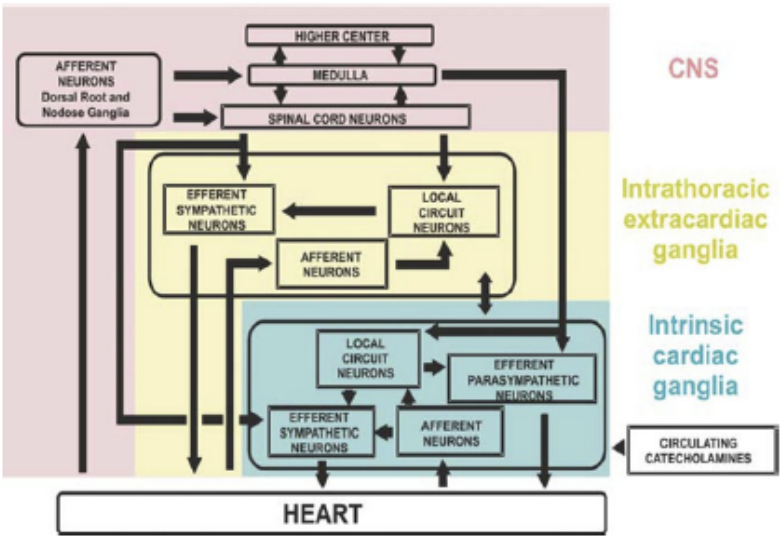

Figure 2-1 The hierarchy of cardiac neuronal control (from Armour JA. Heart Rhythm. 2010; 7(7): 994-6).

Under resting conditions, heart rate is predominantly under the control of the PNS. SNS stimulation however, stimulates noradrenaline (NA) release from cardiac sympathetic nerve terminals, which activates post-synaptic β–receptors, resulting in positive inotropic, chronotropic and dromotropic effects on the heart. Damage to these cardiac nerves termed cardiac autonomic neuropathy (CAN), can have detrimental mechanical and

electrophysiological effects on cardiac function, predisposing to arrhythmogenesis, impairment of coronary blood flow, diastolic and systolic dysfunction and an increased risk of sudden death (3-6). CAN has recently attracted renewed interest in relation to several cardiovascular disorders, in particular heart failure (HF), which is characterized by neuronal loss, SNS over-activation and reduced myocardial catecholamine levels, secondary to increased turnover, spillover and abnormalities of NA uptake (7-12). A detailed knowledge of the structure and function of the human cardiac nervous system is essential to our understanding of the pathophysiology of CAN. Imaging of the cardiac SNS is emerging as a sensitive and reproducible diagnostic tool for CAN and has demonstrated potential as a prognostic tool to guide therapeutic interventions (13-15).

2.2 Gross Anatomy of The Human Cardiac Nervous System

Study of autopsy hearts has allowed for the detailed description of the macro and micro-anatomy of human cardiac nerves. More recently, advances in immuno-histochemical techniques have facilitated the functional differentiation of cardiac nerves, thus enhancing our knowledge of cardiac autonomic control. The human heart is innervated by a vast network of both intrinsic and extrinsic, predominantly autonomic fibres, estimated to exceed 14,000 in number (16,17). The cardiac conduction system is innervated with the highest density of nerves, predominantly parasympathetic fibres, thus supporting the physiological findings of vagal dominance of control of the human heart under resting conditions (13,18). In contrast, the myocardium is predominantly innervated by sympathetic fibers in a heterogeneous pattern characterized by differences in nerve density between atria and ventricles, endocardium and epicardium, with significant intra-ventricular regional variations (19,20).

Thoracic cardiopulmonary nerves containing fibers originating from the vagus nerve (parasympathetic), cervical and stellate ganglia (sympathetic) unite to form two

cardiopulmonary plexuses at the base of the heart. These plexuses give rise to three nerves, which project onto the heart, following the course of the three main coronary arteries (figure 2-2 and 2-3). The left coronary cardiac nerve divides into branches that course along the circumflex and left anterior descending coronary arteries and the adjacent epicardium, whereas the left lateral cardiac nerve traverses the lateral wall of the left ventricle. The right coronary cardiac nerve projects along the course of the right coronary artery.

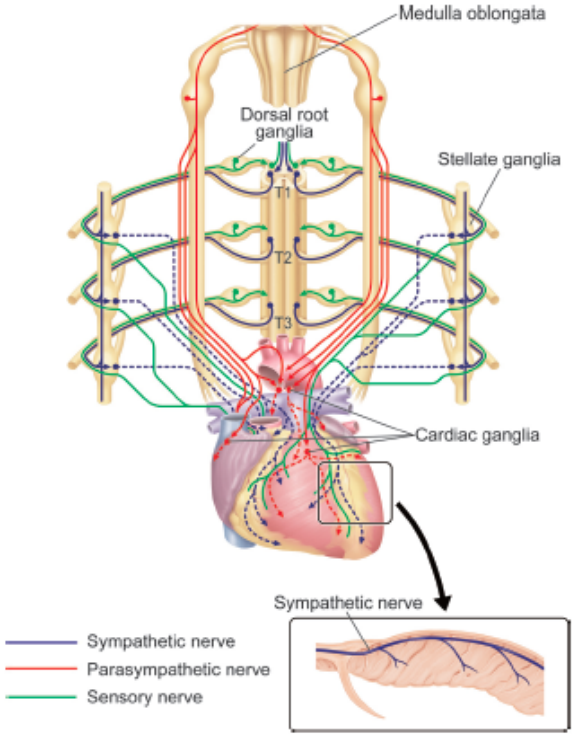

Figure 2-2 Schematic representation of the human cardiac ANS (from Kimura, K et al. Circ Res 2012; 110(2): 325–336).

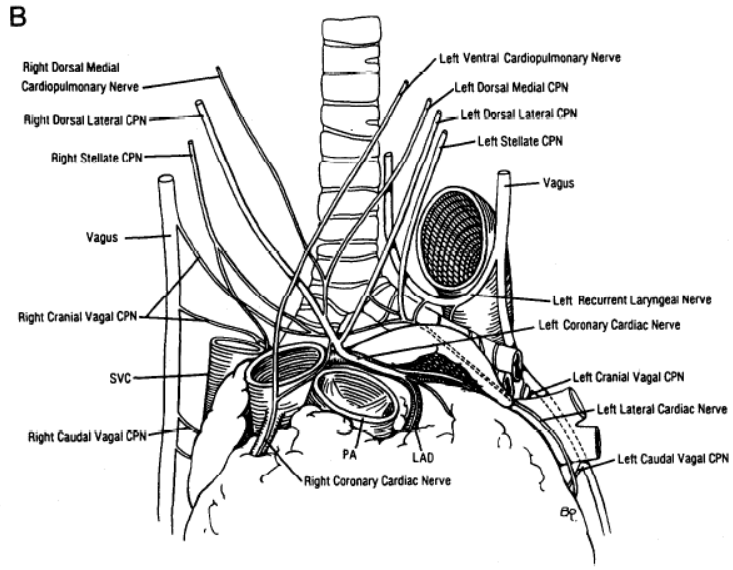

Figure 2-3 Diagrammatic representation of the thoracic cardiopulmonary nerves (from Janes, RD et al. AJC 1986; 57(4): 299–309).

In addition to extrinsic nerves, the heart also has an intrinsic nervous system consisting of ganglionated plexuses of interconnecting nerves in the atria and ventricles (17,21). The ventricular plexuses are typically found in fat surrounding the aortic root and at the origins of the right, left, posterior descending, right acute marginal and left obtuse marginal coronary arteries (figures 2-4 a and b). Sensory afferent nerves project to the upper thoracic dorsal horn via dorsal root ganglia and are primarily thinly myelinated A-fibers and unmyelinated C-fibers.

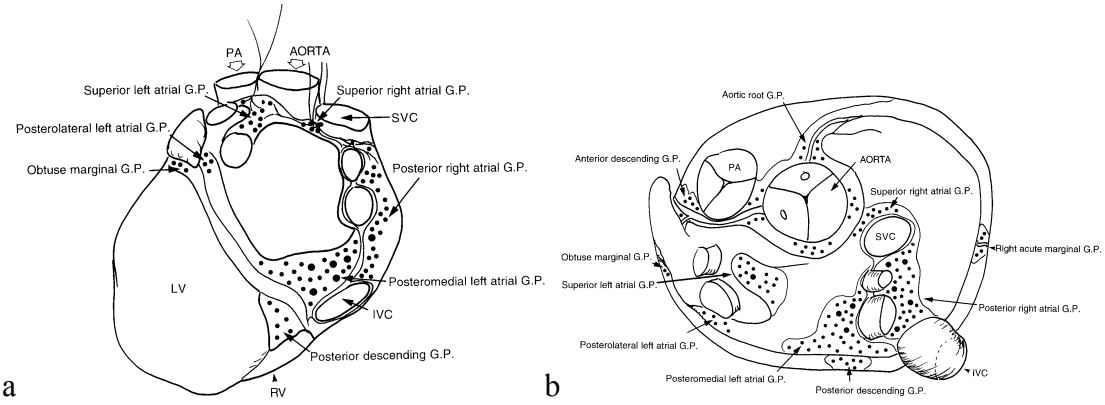

Figure 2-4 Anatomical locations of ganglionated plexuses as viewed posteriorly (a) and superiorly (b) (from Armour JA, The Anatomical record 1997; *247*(2): 289–298).

2.3 Imaging of Human Cardiac Sympathetic Innervation

Important developmental work in the 1970's by Beierwaltes et al at Michigan University led to the evolution of several radiotracers for the imaging of adrenal tumours. Of the later generation compounds, Iodine-123 meta- iodobenzylguanidine (I-123 mIBG) established itself as a robust radionuclide for the imaging of the adrenal medulla (22,23) (24-26). The utility of I-123 mIBG scintigraphy for imaging cardiac sympathetic innervation was established in a number of studies including some elegant experimental work by Sisson et al in dogs with phenol induced regional cardiac sympathetic denervation (27,28). Further work established the neuronal noradrenaline (NA) transporter, uptake-1, as the primary mechanism for uptake and storage of I-123 mIBG into cardiac sympathetic neurones (figure 2-5) (4,23). This important work formed the foundation for a seminal paper published by Sisson et al in 1987, describing the first detailed studies using I-123 mIBG to image cardiac sympathetic innervation in man (1,2). These early studies were followed by studies confirming abnormal I-123 mIBG uptake in subjects with diabetes and CAN (3-6). More recently, I-123 mIBG scintigraphy has been proposed as a prognostic tool in the risk stratification of heart failure (HF) and may also prove useful in determining which patients might benefit from implantable cardiac defibrillator (ICD) implantation (7-12).

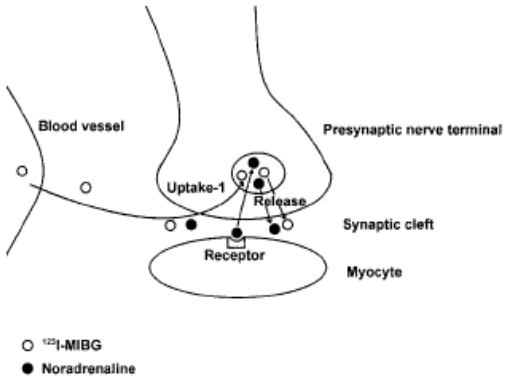

Figure 2-5 Release and uptake of NA and I-123 mIBG at the synaptic junction. (From Scott LA et al; J Nucl Med Technol 2004; 32:66–71)

2.4 The Pharmacology of I-123 mIBG

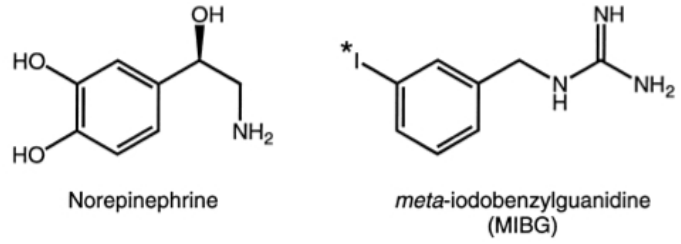

Figure 2-6 The molecular structures of noradrenaline (norepinephrine) and I-123 mIBG (from Raffel, DM et al; Nuclear Medicine and Biology. 2001; 28: 541-559).

I-123 mIBG is produced by modification of the NA analogue, guanethidine which is then radio-labelled with Iodine123 (figure 2-6). It is primarily taken up by cardiac sympathetic neurones via the pre-synaptic uptake-1 mechanism. Although a second mechanism, uptake-2 also exists, I-123 mIBG is not taken up via this mechanism at current recommended dosages. Iodine123 largely emits gamma photons with energies of 159 keV and has a half-life of 13.2 hours. It is not subject to metabolism by monoamine oxidase (MAO) or catechol-o-methyltransferase (COMT), thus permitting accumulation in cardiac sympathetic nerve terminals at higher concentrations than NA. I-123 mIBG is also taken up by the liver, lungs and spleen and is almost exclusively excreted via the kidneys. Several medications are known to interfere with the bio-kinetics of I-123 mIBG, an extensive list of which has been previously published (13-15). It is recommended that such medications be withheld prior to I-123 mIBG administration. Conventionally, subjects undergoing I-123 mIBG scintigraphy are given oral potassium perchlorate to block thyroid uptake. I-123 mIBG is administered intravenously at doses varying between 111-370 MBq at rest.

2.5 Imaging Protocol

2.5.1 Image Acquisition

Imaging protocols have differed significantly between studies using 123I-mIBG, which has made it difficult to compare studies. A number of factors have contributed to these discrepancies including choice of collimator, acquisition methods, dose of I-123 mIBG, and identifying regions of interest (ROI) for analysis (16,17). A recent proposal by the European Council of Nuclear Cardiology has provided detailed recommendations for the standardization of I-123 mIBG scintigraphy (13,18). General principles for imaging include the acquisition of planar and SPECT images at 15 minutes (early) and 240 minutes (late) following I-123 mIBG administration, using either a single or dual headed gamma camera. For planar images, the camera is positioned anteriorly and at 45 degrees left anterior oblique (LAO) projection, and images are acquired using a 128 x 128 matrix. For SPECT images, a 64 x 64 matrix is used and images are acquired over 180 degrees from right anterior oblique (RAO) to left posterior oblique allowing for regional assessment of uptake. A 20% window is centred over the 159-keV photopeak of I-123 for imaging. The majority of published studies have used low energy general purpose (LEGP) collimators however the use of medium energy (MEGP) collimators may improve accuracy by reducing scatter from the 0.529 MeV photon, which accounts for 1.4% of I-123 mIBG emission.

2.5.2 Image Analysis

Planar images (early and late) are used to quantitatively assess global uptake by means of calculating the relative I-123 mIBG uptake of the heart compared to the mediastinum using the heart to mediastinum ratio (HMR). This is achieved by drawing ROI over the heart and mediastinum and dividing the mean myocardial count per pixel in the myocardium by the mean mediastinal count per pixel to give the HMR (figure 2-7). The washout rate (WR), an index of sympathetic adrenergic activity and NA turnover can also be calculated from the planar images using the formula below.

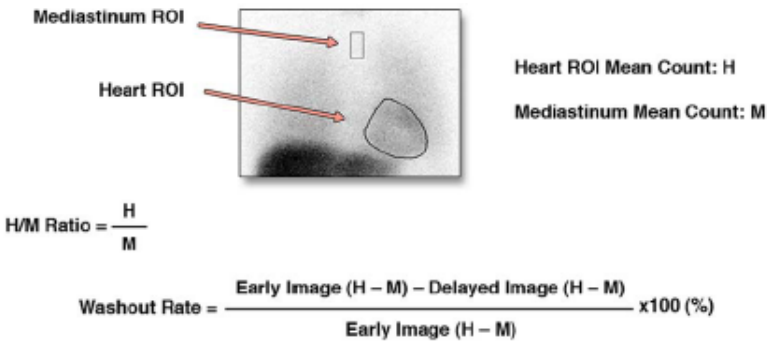

Figure 2-7 ROI and formulae for HMR and WR (from Carrió I, et al. JCMG 2011; 3(1): 92–100).

Regional uptake can be quantitatively and qualitatively assessed using single photon emission computed tomography (SPECT) derived images. Short, horizontal long and vertical long axis SPECT images (figure 2-8a) are reconstructed using sophisticated computer software packages to generate bulls-eye plots (figure 2-8b). Each wall segment can then be either semi-quantitatively assessed by assigning a visual score or quantitatively assessed by comparing counts between regions of the left ventricle.

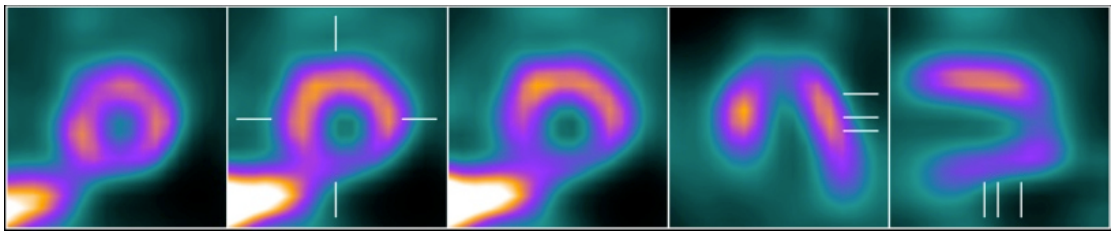
a.

b.

Figure 2-8 a) Short axis, vertical long axis and horizontal long axis slices of the left ventricle and b) Bulls-eye plot based on a AHA 17 segment left ventricular model [18].

2.6 Studies in Healthy Subjects

Several studies have investigated I-123 mIBG uptake in healthy adults. Gill et al studied cardiac I-123 mIBG uptake in 15 healthy adults and in six subjects post orthotopic cardiac transplantation (19,20). Regional I-123 mIBG uptake in normal subjects was higher in the anterior and lateral walls of the left ventricle compared to the inferior wall. Furthermore, uptake was slightly reduced at the apex and base, although these differences did not reach statistical significance. When healthy subjects were grouped according to age, older subjects had significantly reduced global uptake. In the transplant group, there was no evidence of tracer uptake, confirming complete cardiac denervation. Tsuchimochi et al investigated the effects of age and sex on I-123 mIBG uptake. Although there were no differences in global uptake with age, there was a reduction in the inferior to anterior wall count ratio, particularly in males (17,21).

Morozumi et al, investigated the relationship between I-123 mIBG uptake and autonomic function in healthy adult males. They reported regional heterogeneity in I-123 mIBG uptake in the septum, inferior and posterior walls compared with the anterior wall (22,23). Furthermore, WR and HMR correlated with tests of sympathetic function whereas inferior wall uptake correlated negatively with tests of parasympathetic function, suggesting that sympathetic activity may be mediated by vagal tone in the inferior wall. Heterogeneous patterns of innervation, particularly affecting posterior and inferior walls have been reported in other studies using healthy controls (24-26). Such findings of heterogeneous innervation of the healthy ventricle conflict with some studies using PET (positron emission tomography) imaging of sympathetic innervation which indicate homogenous tracer uptake (27,28).

Compared with 123-I mIBG, tracers used in PET are biologically more similar to NA and have more favourable physical properties for imaging. For example, 11C-metahydroxyephedrine (HED) has higher uptake-1 selectivity than I-123 mIBG, resulting in better differentiation between innervated and denervated myocardium. However, 123-I mIBG scintigraphy is well established in the clinical setting, particularly in the assessment of adrenal tumours and unlike PET imaging, is not limited by accessibility. Furthermore, in the assessment of cardiac sympathetic innervation, relatively few studies have been carried out using PET imaging compared to 123-I mIBG scintigraphy which correlates with clinical end points (7). Hence for our study, we used 123-I mIBG scintigraphy and devised an imaging protocol based on internationally recommended standards (13).

2.7 Studies in Diabetic Subjects

CAN is a recognised complication of diabetes, often present at diagnosis and is an independent predictor of morbidity and mortality (4,23). Several studies in diabetic cohorts have demonstrated the utility of I-123 mIBG scintigraphy for the detection of sympathetic denervation. Hattori et al studied I-123 mIBG uptake in 31 subjects with type 2 diabetes and 12 age-matched healthy controls. The authors reported a significant reduction in late HMR and inferior to anterior wall count ratio but not WR in the diabetic group (29). Sub group analysis according to the presence and severity of peripheral neuropathy, demonstrated a reduction in inferior wall uptake with worsening peripheral neuropathy. In addition, there were non-significant differences in late HMR and global WR in the sub-group with neuropathy compared to those without. Abnormal I-123 mIBG uptake has also been described both in patients with newly diagnosed and long-standing type 1 diabetes, and correlates with tests of cardiac autonomic function (30-33).

Stevens et al reported distal denervation and proximal hyper-innervation in diabetic subjects with severe CAN using PET imaging, suggesting a possible compensatory response to distal cardiac neuropathy (34). Poor glycaemic control has been shown to be associated with progression of cardiac neuropathy in a prospective 3-year study using PET with [11C]-meta-hydroxyephedrine ([11C]-HED) (35). Cardiac sympathetic dysinnervation may also play a role in diabetic cardiomyopathy. Indeed several early studies reported associations between mechanical cardiac dysfunction and reductions in I-123 mIBG uptake in diabetic subjects (33,36,37). More recently, Sacre et al reported an independent association between CAN and measures of myocardial functional reserve in a cohort of subjects with type 2 diabetes (38). In the sub-group who underwent I-123 mIBG scintigraphy, global uptake (HMR) correlated

with CAN, diastolic and peak systolic function. Regional uptake correlated with regional diastolic parameters exclusively in the anterior and lateral mid-wall segments.

2.8 Studies in Subjects with IGT

In the only published study using I-123 mIBG scintigraphy in a pre-diabetic cohort, Diakakis et al reported a reduction in HMR and increased WR in subjects with IGT compared with healthy controls. Regional analysis revealed severe defects in mIBG uptake involving the inferior wall and apex in almost half of the IGT group (39). They also reported a correlation between levels of circulating pro-inflammatory cytokines and WR suggesting a role for inflammation in the pathogenesis of cardiac autonomic neuropathy.

2.9 References

1. Sisson JC, Shapiro B, Meyers L, Mallette S, Mangner TJ, Wieland DM, et al. Metaiodobenzylguanidine to map scintigraphically the adrenergic nervous system in man. J Nucl Med. 1987 Oct;28(10):1625–36.

2. Armour JA. Functional anatomy of intrathoracic neurons innervating the atria and ventricles. HRTHM. Elsevier Inc; 2010 Jul 1;7(7):994–6.

3. Mäntysaari M, Kuikka J, Mustonen J, Tahvanainen K, Vanninen E, Länsimies E, et al. Noninvasive detection of cardiac sympathetic nervous dysfunction in diabetic patients using [123I]metaiodobenzylguanidine. Diabetes. 1992 Sep;41(9):1069–75.

4. Vinik AI, Ziegler D. Diabetic Cardiovascular Autonomic Neuropathy. Circulation. 2007 Jan 8;115(3):387–97.

5. Di Carli MF, Bianco-Batlles D, Landa ME, Kazmers A, Groehn H, Muzik O, et al. Effects of autonomic neuropathy on coronary blood flow in patients with diabetes mellitus. Circulation. 1999 Aug 24;100(8):813–9.

6. Standl E, Schnell O. A new look at the heart in diabetes mellitus: from ailing to failing. Diabetologia. 2000 Dec;43(12):1455–69.

7. Jacobson A, Senior R, Cerqueira M. Myocardial Iodine-123 Meta-Iodobenzylguanidine Imaging and Cardiac Events in Heart Failure. Results of the Prospective ADMIRE-HF (AdreView Myocardial Imaging for Risk Evaluation in Heart Failure) Study. J Am Coll Cardiol 2010;55:2212–21.

8. Wang Y, Seto S-W, Golledge J. Angiotensin II, sympathetic nerve activity and chronic heart failure. Heart Fail Rev. 2014 Mar;19(2):187–98.

9. Marshall A, Cheetham A, George RS, Mason M, Kelion AD. Cardiac iodine-123 metaiodobenzylguanidine imaging predicts ventricular arrhythmia in heart failure patients receiving an implantable cardioverter-defibrillator for primary prevention. Heart. 2012 Aug 17;98(18):1359–65.

10. Carrió I, Cowie MR, Yamazaki J, Udelson J, Camici PG. Cardiac Sympathetic Imaging With mIBG in Heart Failure. JCMG. 2011 Jan 14;3(1):92–100.

11. Verberne HJ, Brewster LM, Somsen GA, van Eck-Smit BLF. Prognostic value of myocardial 123I-metaiodobenzylguanidine (MIBG) parameters in patients with heart failure: a systematic review. European Heart Journal. 2008 Mar 20;29(9):1147–59.

12. Ketchum ES, Jacobson AF, Caldwell JH, Senior R, Cerqueira MD, Thomas GS, et al. Selective improvement in Seattle Heart Failure Model risk stratification using iodine-123 meta-iodobenzylguanidine imaging. J Nucl Cardiol. 2012 Oct;19(5):1007–16.

13. Flotats A, Carrió I, Agostini D, Guludec D, Marcassa C, Schaffers M, et al. Proposal for standardization of 123I-metaiodobenzylguanidine (MIBG) cardiac sympathetic imaging by the EANM Cardiovascular Committee and the European Council of Nuclear Cardiology. Eur J Nucl Med Mol Imaging. 2010 Jun 25;37(9):1802–12.

14. Boogers MJ, Borleffs CJW, Henneman MM, van Bommel RJ, van Ramshorst J, Boersma E, et al. Cardiac sympathetic denervation assessed with 123-iodine metaiodobenzylguanidine imaging predicts ventricular arrhythmias in implantable cardioverter-defibrillator patients. Journal of the American College of Cardiology. 2010 Jun 15;55(24):2769–77.

15. Bax JJ, Kraft O, Buxton AE, Fjeld JG, Parizek P, Agostini D, et al. 123I-mIBG Scintigraphy to Predict Inducibility of Ventricular Arrhythmias on Cardiac Electrophysiology Testing: A Prospective Multicenter Pilot Study. Circulation: Cardiovascular Imaging. 2008 Sep 16;1(2):131–40.

16. Chen W, Cao Q, Dilsizian V. Variation of Heart-to-Mediastinal Ratio in 123I-mIBG Cardiac Sympathetic Imaging: Its Affecting Factors and Potential Corrections. Curr Cardiol Rep. 2011 Jan 11;13(2):132–7.

17. Armour JA, Murphy DA, Yuan BX, Macdonald S, Hopkins DA. Gross and microscopic anatomy of the human intrinsic cardiac nervous system. Anat Rec. 1997 Feb;247(2):289–98.

18. Crick SJ, Wharton J, Sheppard MN, Royston D, Yacoub MH, Anderson RH, et al. Innervation of the human cardiac conduction system. A quantitative immunohistochemical and histochemical study. Circulation. 1994 Apr 1;89(4):1697–708.

19. Gill JS, Hunter GJ, Gane G, Camm AJ. Heterogeneity of the human myocardial sympathetic innervation: in vivo demonstration by iodine 123-labeled meta-iodobenzylguanidine scintigraphy. American Heart Journal. 1993 Aug 1;126(2):390–8.

20. Kimura K, Ieda M, Fukuda K. Development, Maturation, and Transdifferentiation of Cardiac Sympathetic Nerves. Circulation Research. 2012 Jan 19;110(2):325–36.

21. Tsuchimochi S, Tamaki N, Tadamura E, Kawamoto M, Fujita T, Yonekura Y, et al. Age and gender differences in normal myocardial adrenergic neuronal function evaluated by iodine-123-MIBG imaging. J Nucl Med. 1995 Jun;36(6):969–74.

22. Morozumi T, Kusuoka H, Fukuchi K. Myocardial iodine-123-metaiodobenzylguanidine images and autonomic nerve activity in normal subjects. J Nucl Med.1997;38:49-52.

23. Raffel DM, Wieland DM. Development of mIBG as a Cardiac Innervation Imaging Agent. JCMG. 2011 Jan 14;3(1):111–6.

24. Inobe Y, Kugiyama K, Miyagi H, Ohgushi M, Tomiguchi S, Takahashi M, et al. Long-lasting abnormalities in cardiac sympathetic nervous system in patients with coronary spastic angina: quantitative analysis with iodine 123 metaiodobenzylguanidine myocardial scintigraphy. American Heart Journal. 1997 Jul;134(1):112–8.

25. Newton TD, Augustine T, Arumugam P, Malik RA. Detection of medullary thyroid cancer with MIBG imaging for pheochromocytoma. Clin Nucl Med. 2008 May;33(5):328–9.

26. Somsen GA, Verberne HJ, Fleury E, Righetti A. Normal values and within-subject variability of cardiac I-123 MIBG scintigraphy in healthy individuals: implications for clinical studies. J Nucl Cardiol. 2004 Feb;11(2):126–33.

27. Schwaiger M, Kalff V, Rosenspire K, Haka MS, Molina E, Hutchins GD, et al. Noninvasive evaluation of sympathetic nervous system in human heart by positron emission tomography. Circulation. 1990 Aug 1;82(2):457–64.

28. Sisson JC, Lynch JJ, Johnson J, Jaques S, Wu D, Bolgos G, et al. Scintigraphic detection of regional disruption of adrenergic neurons in the heart. American Heart Journal. 1988 Jul;116(1 Pt 1):67–76.

29. Hattori N, Tamaki N, Hayashi T, Masuda I, Kudoh T, Tateno M, et al. Regional abnormality of iodine-123-MIBG in diabetic hearts. J Nucl Med. 1996 Dec;37(12):1985–90.

30. Schnell O, Muhr D, Weiss M, Dresel S, Haslbeck M, Standl E. Reduced myocardial 123I-metaiodobenzylguanidine uptake in newly diagnosed IDDM patients. Diabetes. 1996 Jun;45(6):801–5.

31. Schnell O, Kirsch CM, Stemplinger J, Haslbeck M, Standl E. Scintigraphic evidence for cardiac sympathetic dysinnervation in long-term IDDM patients with and without ECG-based autonomic neuropathy. Diabetologia. 1995 Nov;38(11):1345–52.

32. Langer A, Freeman MR, Josse RG, Armstrong PW. Metaiodobenzylguanidine imaging in diabetes mellitus: assessment of cardiac sympathetic denervation and its relation to autonomic dysfunction and silent myocardial ischemia. JAC. 1995 Mar 1;25(3):610–8.

33. Kreiner G, Wolzt M, Fasching P, Leitha T, Edlmayer A, Korn A, et al. Myocardial m-[123I]iodobenzylguanidine scintigraphy for the assessment of adrenergic cardiac innervation in patients with IDDM. Comparison with cardiovascular reflex tests and relationship to left ventricular function. Diabetes. 1995 May;44(5):543–9.

34. Stevens MJ, Raffel DM, Allman KC, Dayanikli F, Ficaro E, Sandford T, et al. Cardiac sympathetic dysinnervation in diabetes: implications for enhanced cardiovascular risk. Circulation. 1998 Sep 8;98(10):961–8.

35. Stevens MJ, Raffel DM, Allman KC, Schwaiger M, Wieland DM. Regression and progression of cardiac sympathetic dysinnervation complicating diabetes: an assessment by C-11 hydroxyephedrine and positron emission tomography. Metabolism. 1999 Jan;48(1):92–101.

36. Scognamiglio R, Avogaro A, Casara D, Crepaldi C, Marin M, Palisi M, et al. Myocardial dysfunction and adrenergic cardiac innervation in patients with insulin-dependent diabetes mellitus. JAC. 1998 Feb 1;31(2):404–12.

37. Sugiyama T. Is abnormal iodine-123-MIBG kinetics associated with left ventricular dysfunction in patients with diabetes mellitus? J Nucl Cardiol. 2000 Nov;7(6):562–8.

38. Sacre JW, Franjic B, Jellis CL, Jenkins C, Coombes JS, Marwick TH. Association of cardiac autonomic neuropathy with subclinical myocardial dysfunction in type 2 diabetes. JACC Cardiovasc Imaging. 2010 Dec;3(12):1207–15.

39. Diakakis G, Parthenakis F, Patrianakos A, Koukouraki S, Stathaki M, Karkavitsas N, et al. Myocardial sympathetic innervation in patients with impaired glucose tolerance: relationship to subclinical inflammation. Cardiovascular Pathology. 2008;17(3):172–7.

3 123I-mIBG Scintigraphy for the Assessment of Cardiac Sympathetic Innervation and the Relationship to Cardiac Autonomic Function in Healthy Adults Using Standardized Methods.

Omar Asghar, Parthiban Arumugam, Ian Armstrong, Simon Ray, Matthias Schmitt and Malik RA.

Contribution: Omar Asghar contributed to study concept and design of this study and was solely responsible for patient recruitment, data analysis, statistics and the writing of this chapter.

3.1 Abstract

Background: Global 123I-mIBG (MIBG) uptake is predictive of cardiovascular events and mortality in subjects with heart failure (HF). Normal variations in global and regional uptake however, are not well defined and few studies have addressed the functional relevance of MIBG uptake and distribution in healthy subjects.

Methods and Results: We undertook MIBG scintigraphy and cardiac autonomic function testing using standardized methodology in 15 healthy subjects (mean age 54.6±5.3 years, M:F 10:5) with no evidence of previous MI or ischaemic heart disease (IHD). Early heart to mediastinum ratio (HMR) was 1.67±0.13, late HMR 1.73±0.16 and washout rate (WR) 19.09±7.63% (4.20-31.30). Regional analysis revealed reduced tracer uptake at the apex, base and inferior wall in all subjects. Early and late HMR correlated negatively with RFa (r=-0.603; p=0.05 and -0.644; p=0.033) and E/I ratio (r=-0.616; p=0.043 and -0.676; p=0.022) and positively with LFa/RFa (r=0.711; p=0.014 and 0.784; p=0.004). WR correlated only with RFa (r=0.642, p=0.033).

Conclusion: Healthy adults demonstrate a heterogeneous pattern of cardiac innervation with reduced regional uptake of MIBG. Furthermore, HMR correlates with indices of cardiac sympathetic function, suggesting that it might not only be a useful prognostic marker but may also provide insight into the functional integrity of the cardiac autonomic nervous system.

Abbreviations

CAN: Cardiac autonomic neuropathy

HMR: Heart mediastinum ratio

LVMI: Left ventricular mass index

MIBG: 123I-meta-iodobenzylguanidine

SPECT: Single photon emission computed tomography

WR: Washout rate

3.2 Introduction

123I-meta-iodobenzylguanidine (MIBG) scintigraphy allows for the qualitative and quantitative global and regional assessment of cardiac sympathetic innervation and demonstrates cardiac denervation in a variety of pathologies [1]. Recently, MIBG has emerged as an important tool in the risk stratification of patients with heart failure (HF) [2, 3]. The utility of the late heart to mediastinum ratio (HMR) as a prognostic indicator in HF was demonstrated in the ADMIRE-HF study in which a late HMR <1.6 was associated with an event rate of 37% over two years for HF progression, arrhythmia or death [4]. More recently combined analyses of several studies using MIBG have shown considerably improved risk stratification for events in patients with heart failure [5], arrhythmic sudden cardiac death [6, 7], 5 year cardiac mortality [8] and long term prognosis [9]. In addition to measures of global innervation, single photon emission computed tomography (SPECT) derived innervation scores are predictive of ventricular arrhythmias and may be useful in the risk stratification of subjects undergoing implantable cardiac defibrillator implantation [10, 11]. However, in patients with Parkinson's disease and autonomic neuropathy, orthostatic symptoms and heart rate variability showed no relationship to cardiac MIBG uptake, suggesting a discordance between structure and function [12].

However, variations in global and regional uptake in healthy individuals are not well defined and indeed have urged the need for standardizing imaging protocols [13]. Early studies in healthy subjects were limited by variations in methodology and methods of interpretation and very few studies have addressed the functional relevance of MIBG uptake in healthy subjects. In a recent study however, an increase in cardiac presynaptic sympathetic activity was associated with reduced heart rate variability (HRV) in subjects with no evidence of myocardial ischaemia [14]. The purpose of this study was to define global and regional

cardiac sympathetic innervation in healthy adults using standardized methodology and to investigate the relationship with cardiac sympathetic function.

3.3 Methods

Global and regional cardiac sympathetic innervation, were quantified using MIBG scintigraphy in a cohort of healthy subjects. The study protocol was approved by the Central Manchester Research Ethics Committee. Written informed consent, according to the declaration of Helsinki, was obtained from all participants.

3.3.1 Patient Selection

Inclusion criteria were healthy male or female subjects aged 18-75 years. Exclusion criteria included any history of cardiac disease, diabetes, severe systemic disease (e.g. congestive cardiac failure, rheumatoid disease, systemic lupus erythematosus), chronic kidney disease, peripheral vascular disease, neuropathy and any contraindication to MIBG or CMR imaging.

3.3.2 Study Protocol

All study participants underwent an initial assessment including medical history; clinical examination and 12 lead ECG. Within two weeks of MIBG scintigraphy, all participants underwent CMR imaging to assess cardiac structure and function, to exclude previous MI with late Gadolinium enhancement (LGE). In addition, we performed adenosine stress CMR to exclude ischaemic heart disease. All medications known to affect the uptake of MIBG were omitted and thyroid blockade was achieved by oral administration of potassium perchlorate 170 mg on the evening prior to MIBG imaging.

Autonomic Function Testing

Cardiovascular autonomic function testing was carried out on the day of MIBG imaging. The ANX 3.0 autonomic monitoring system (ANSAR Medical Technologies, Inc., Philadelphia, PA) was used to perform spectral analysis of heart rate variability (HRV) during standard tests of cardiovascular reflexes [15]. We assessed parameters of HRV during expiration and inspiration (E/I), Valsalva maneuver (VM), response to standing (30:15 ratio) and postural drop in systolic blood pressure. In addition, the low frequency area (LFa) to respiratory frequency area (RFa) ratio; an estimate of sympathovagal balance, was determined.

3.3.3 I-123 mIBG Scintigraphy

Data Acquisition

123I-mIBG 185 MBq (AdreView-GE Healthcare) was administered intravenously by slow (1-2 min) injection through a peripheral venous cannula. All images were acquired using a Siemens Symbia T6 gamma camera (Siemens Healthcare) at 10 (early) and 240 minutes (late) post injection of MIBG. Planar images were acquired with a low energy high-resolution (LEHR) collimator, 159 keV ± 15% energy window, 128 × 128 image matrix, and zoom of 1.0 (pixel size 4.8 mm) for 15 minutes. SPECT images were acquired over a 180° orbit from the right anterior oblique to left posterior oblique positions with medium energy general purpose (MEGP) collimators, 159 keV ± 15% energy window, 64 × 64 image matrix, zoom of 1.45 (pixel size 6.6 mm) and 64 projections at 30 seconds per projection.

Data Analysis

Image processing was undertaken independently by a cardiology research fellow (OA) and an experienced nuclear cardiologist (PA); both blinded to clinical information. An average value of the two analyses was used except where there was a significant discrepancy (>10%) in which case images were reviewed and re-analysed. Global MIBG uptake was assessed in the early and late planar images by drawing an elliptical region of interest (ROI) over the whole heart and a 7×7 pixel square ROI in the upper mediastinum. The HMR was then calculated by dividing the mean myocardial count per pixel by the mean mediastinal count per pixel. Washout rate (WR), an index of sympathetic tone, was calculated from the planar data using the formula:

$$\text{Washout} = \frac{C_E - (C_L / df)}{C_E}$$

CE = myocardial count on early image, CL = myocardial count on late image, df = decay factor (physical decay of 123I-mIBG between early and late images).

SPECT images were processed to derive short and long axis (vertical and horizontal) slices using iterative reconstruction with resolution recovery (Siemens Flash 3D), with 6 iterations, 8 subsets and an 8.4 mm Gaussian post-filter. Segmental analysis was performed using a 17 segment left ventricular model. Tracer uptake (mean count per pixel) was expressed as a percentage of maximal tracer uptake and segments were assigned a score based on this percentage; <50% = 4, 50-59% = 3, 60-74% = 2 and >75% = 1. The total segmental score was calculated. In addition, we calculated a modified score (total segmental score - apex and inferior [apical, mid and basal] segments) to correct for reduced innervation in these regions.

3.3.4 Statistical Analysis

SPSS Statistics for Mac version 20 (IBM corporation, New York USA) was used for all statistical analysis. All data are expressed as mean ± SD and the Shapiro-Wilk test was used to determine normality of data. Pearson correlation was used to determine associations between HMR, WR, SPECT scores and indices of autonomic function.

3.4 Results

15 subjects (10 males, 5 females) underwent assessment however one male subject was excluded on the basis of an incidental finding of atrial flutter and LV impairment (LVEF 48%). The remaining 14 participants successfully completed the imaging protocol and CMR imaging did not reveal any abnormality in cardiac structure, function or stress perfusion. The demographic and clinical data are detailed in Table 3-1. LV mass (LVMI 51.1±10.7 g/m2) and ejection fraction (LVEF 61.0±6.4 %) were both within normal limits. There were no differences in LV mass (110.0±25.2 vs 84.0±16.6 g) or LVMI (52.6±11.3 vs 48.4±10.1 g/m2) between males and females.

3.4.1 Autonomic Function Testing

The results of autonomic function testing are summarized in Table 3-2. The E/I ratio was 1.2±0.1, Valsalva ratio 1.4±0.2, 30:15 ratio 1.2±0.1 and LFa/RFa ratio 2.4±2.5.

3.4.2 MIBG Scintigraphy

The results of MIBG scintigraphy are detailed in Table 3-3. A Bland Altman plot demonstrating inter-observer agreement for analysis of HMR is shown in figure 3-1. The early HMR was 1.67±0.13, late HMR 1.73±0.16 and WR 19.1±7.6 % (Figure 3-2). Qualitative assessment of the SPECT images revealed a consistent reduction of tracer uptake at the cardiac apex, base and inferior wall in all subjects (Figure 3-3). The total segmental score was 28±4 and modified score 20±3. Both early and late HMR correlated negatively with RFa (r=-0.603; p=0.05 and r=-0.644; p=0.033) and E/I ratio (r=-0.616; p=0.041 and r=-0.676; p=0.022) and positively with LFa/RFa (r=0.711; p=0.014 and r=0.784; p=0.004) (Figure 3-4). HMR did not correlate with any other indices of autonomic function. WR correlated only with RFa (r=0.642, p=0.033). Total segmental score (r=0.658; p=0.028) and modified score (r=0.713; p-0.014) both correlated with RFa.

3.5 Discussion

The human myocardium is predominantly innervated by sympathetic fibers in a distribution characterized by differences in nerve density between atria and ventricles, endocardium and epicardium with significant intra-ventricular regional variations [16-18]. Originally developed as a radionuclide for imaging adrenal tumours, MIBG has emerged as a promising tool for the assessment of the cardiac sympathetic nervous system [19]. Early observational studies using MIBG reported homogenous tracer uptake in young healthy subjects compared to reduced uptake at the apex and inferior wall in healthy older adults [20-22]. This heterogeneous pattern of uptake was confirmed in subsequent studies which also reported the effects of age and sex on tracer uptake [23-25]. More recently however, the ADMIRE-HF study failed to demonstrate an association between age and MIBG uptake in older healthy controls [26]. Studies using positron emission tomography (PET) with 11C-labeled

hydroxyephedrine ([11C]-HED) have reported similar homogenous uptake in young healthy adults and heterogeneity in older controls [27-29]. In our study we confirm regional heterogeneity in MIBG uptake predominantly affecting the apex, base and inferior wall in older healthy adults. Such findings are likely explained by the preferential sympathetic and parasympathetic innervation of the anterior and inferior walls respectively.

Whilst HMR shows considerable promise as a prognostic indicator in a variety of clinical contexts, there is to date no universally accepted normal range. Thus HMR values for healthy adults reported in the literature have varied between studies primarily due to differences in methodology and interpretation, rendering calls for the standardization of MIBG scintigraphy [13, 30, 31]. Although our imaging protocol was devised according to internationally recommended standards, we note that late HMR in our subjects was lower than that reported in ADMIRE-HF controls (1.77±0.23; range 1.09-2.40). This discrepancy could be explained by a number of factors. Our study involved a much smaller group with a narrower range of age and BMI than the ADMIRE-HF controls. Furthermore, in ADMIRE-HF, there was a trend towards a reduction in late HMR with age in control subjects, albeit non-significant [32]. A technical factor that may also have influenced HMR values is the degree of septal penetration of the collimators used. A recent study has suggested that LEHR collimators from Siemens and Philips provide comparable HMR results [33]. However, our experience of the LEHR collimators supplied by Siemens suggests that they exhibit a higher degree of septal penetration compared with LEHR collimators from GE. Hence this increased septal penetration would have reduced HMR in our subjects. Another explanation for higher HMR in ADMIRE-HF may be the range of cameras used in the study. This highlights the importance of understanding the performance of the particular manufacturer's collimators and demonstrates that normal ranges for HMR may not be transferable between manufacturers.

Spectral analysis of HRV and respiratory activity allow for real time, quantitative, independent and simultaneous measures of parasympathetic and sympathetic activity at rest and in response to physiological challenges. The low frequency component (LFa) of HRV relates to sympathetic activity, the respiratory frequency (RFa) corresponds to parasympathetic activity and the ratio of LFa/RFa is an index of sympathovagal balance. Morozumi et al reported a correlation between WR and the LF component of HRV in fifteen healthy male subjects [22] however in a more recent study, HRV did not correlate with MIBG for the detection of CAN in type 2 diabetic subjects [34]. A major flaw of the latter study was that 60% of all reported defects in MIBG uptake involved the inferior wall (46%) and apex (14%). Subsequently, 45% of subjects with normal HRV were labeled as having an abnormal 123I-mIBG study. In contrast, 92% with abnormal HRV had abnormalities in MIBG uptake. However, in a recent study of subjects without myocardial ischaemia, WR was inversely correlated with indices of HRV derived from ambulatory ECG recordings suggesting sympathetic over activity however this correlation was only significant in the very low frequency band (VLF) [14].

In our study, although HMR correlated negatively with RFa and positively with LFa/RFa as expected, WR correlated positively with RFa, a finding inconsistent with those of previous studies. This unexpected finding may be explained by the small numbers in our study and the possibility of a type 1 statistical error due the outliers in the group. Nevertheless, the nature of this relationship in the context of cardiac neuropathy remains to be established and requires further study.

Although our study population was small, we performed detailed structural and functional assessment by CMR imaging. Hence we were able to exclude clinical and subclinical cardiac disease and report normal LV mass and ejection fraction in these individuals. In addition, our robust MIBG methodology adds to the significance of our findings. Clearly, there is a need for further research to determine the functional significance of cardiac MIBG and establish it as a diagnostic tool and guide to therapeutic intervention

Sources of Funding

This study was funded by research grants from the NHS National Institutes for Health Research (FSF-R5-OA), NIH (R105991) and Juvenile Diabetes Research Foundation (8-2008-362).

Disclosures

None.

3.6 References

1. Carrió I, Flotats A (2010) Expanding indications for cardiac MIBG imaging of sympathetic activity. Eur J Nucl Med Mol Imaging 38:219–220.

2. Carrió I, Cowie MR, Yamazaki J, et al. (2011) Cardiac Sympathetic Imaging With mIBG in Heart Failure. JCMG 3:92–100.

3. Verberne HJ, Brewster LM, Somsen GA, van Eck-Smit BLF (2008) Prognostic value of myocardial 123I-metaiodobenzylguanidine (MIBG) parameters in patients with heart failure: a systematic review. European Heart Journal 29:1147–1159.

4. Jacobson A, Senior R, Cerqueira M. Myocardial Iodine-123 Meta-Iodobenzylguanidine Imaging and Cardiac Events in Heart Failure. Results of the Prospective ADMIRE-HF (AdreView Myocardial Imaging for Risk Evaluation in Heart Failure) Study. J Am Coll Cardiol 2010;55:2212–21.

5. Jain KK, Hauptman PJ, Spertus JA, et al. (2014) Incremental utility of iodine-123 meta-iodobenzylguanidine imaging beyond established heart failure risk models. Journal of cardiac failure 20:577–583.

6. Kelesidis I, Travin MI (2012) Use of cardiac radionuclide imaging to identify patients at risk for arrhythmic sudden cardiac death. J Nucl Cardiol 19:142–52.

7. Martins da Silva MI, Vidigal Ferreira MJ, Morão Moreira AP (2013) Iodine-123-metaiodobenzylguanidine scintigraphy in risk stratification of sudden death in heart failure. Rev Port Cardiol 32:509–516.

8. Nakajima K, Nakata T, Yamada T, et al. (2014) A prediction model for 5-year cardiac mortality in patients with chronic heart failure using ^{123}I-metaiodobenzylguanidine imaging. Eur J Nucl Med Mol Imaging 41:1673–1682.

9. Nakata T, Nakajima K, Yamashina S, et al. (2013) A Pooled Analysis of Multicenter Cohort Studies of. JCMG 6:772–784.

10. Bax JJ, Kraft O, Buxton AE, et al. (2008) 123I-mIBG Scintigraphy to Predict Inducibility of Ventricular Arrhythmias on Cardiac Electrophysiology Testing: A Prospective Multicenter Pilot Study. Circulation: Cardiovascular Imaging 1:131–140.

11. Boogers MJ, Borleffs CJW, Henneman MM, et al. (2010) Cardiac sympathetic denervation assessed with 123-iodine metaiodobenzylguanidine imaging predicts ventricular arrhythmias in implantable cardioverter-defibrillator patients. Journal of the American College of Cardiology 55:2769–2777.

12. Haensch C-A, Lerch H, Jörg J, Isenmann S (2009) Cardiac denervation occurs independent of orthostatic hypotension and impaired heart rate variability in Parkinson's disease. Parkinsonism Relat Disord 15:134–137.

13. Chen W, Cao Q, Dilsizian V (2011) Variation of Heart-to-Mediastinal Ratio in 123I-mIBG Cardiac Sympathetic Imaging: Its Affecting Factors and Potential Corrections. Curr Cardiol Rep 13:132–137.

14. Simula S, Vanninen E, Hedman A, et al. (2012) Myocardial (123) I-metaiodobenzylguanidine washout and heart rate variability in asymptomatic subjects. Ann Noninvasive Electrocardiol 17:8–13.

15. Spallone V, Ziegler D, Freeman R, et al. (2011) Cardiovascular autonomic neuropathy in diabetes: clinical impact, assessment, diagnosis, and management. Diabetes Metab Res Rev 27.

16. Kawano H, Okada R, Yano K (2003) Histological study on the distribution of autonomic nerves in the human heart. Heart Vessels 18:32–39.

17. Kimura K, Ieda M, Fukuda K (2012) Development, Maturation, and Transdifferentiation of Cardiac Sympathetic Nerves. Circulation Research 110:325–336.

18. Armour JA (2010) Functional anatomy of intrathoracic neurons innervating the atria and ventricles. HRTHM 7:994–996.

19. Raffel DM, Wieland DM (2011) Development of mIBG as a Cardiac Innervation Imaging Agent. JCMG 3:111–116.

20. Gill JS, Hunter GJ, Gane G, Camm AJ (1993) Heterogeneity of the human myocardial sympathetic innervation: in vivo demonstration by iodine 123-labeled meta-iodobenzylguanidine scintigraphy. American Heart Journal 126:390–398.

21. Tsuchimochi S, Tamaki N, Tadamura E, et al. (1995) Age and gender differences in normal myocardial adrenergic neuronal function evaluated by iodine-123-MIBG imaging. J Nucl Med 36:969–974.

22. Morozumi T, Kusuoka H, Fukuchi K. Myocardial iodine-123-metaiodobenzylguanidine images and autonomic nerve activity in normal subjects. J Nucl Med.1997;38:49-52.

23. Sakata K, Iida K, Mochizuki N, et al. (2009) Physiological changes in human cardiac sympathetic innervation and activity assessed by (123)I-metaiodobenzylguanidine (MIGB) imaging. Circ J 73:310–315.

24. Sakata K, Shirotani M, Yoshida H, Kurata C (2014) Physiological fluctuation of the human left ventricle sympathetic nervous system assessed by iodine-123-MIBG. J Nucl Med 39:1667–1671.

25. D'Alto M, Maurea S, Basso A, et al. (1998) [The heterogeneity of myocardial sympathetic innervation in normal subjects: an assessment by iodine-123 metaiodobenzylguanidine scintigraphy]. Cardiologia 43:1231–1236.

26. Jacobson AF, Chen J, Verdes L, et al. (2013) Impact of age on myocardial uptake of ^{123}I-mIBG in older adult subjects without coronary heart disease. J Nucl Cardiol 20:406–414.

27. Schwaiger M, Kalff V, Rosenspire K, et al. (1990) Noninvasive evaluation of sympathetic nervous system in human heart by positron emission tomography. Circulation 82:457–464.

28. Munch G, Nguyen NTB, Nekolla S, et al. (2000) Evaluation of Sympathetic Nerve Terminals With [11C]Epinephrine and [11C]Hydroxyephedrine and Positron Emission Tomography. Circulation 101:516–523.

29. Stevens MJ, Raffel DM, Allman KC, et al. (1998) Cardiac sympathetic dysinnervation in diabetes: implications for enhanced cardiovascular risk. Circulation 98:961–968.

30. Flotats A, Carrió I, Agostini D, et al. (2010) Proposal for standardization of 123I-metaiodobenzylguanidine (MIBG) cardiac sympathetic imaging by the EANM Cardiovascular Committee and the European Council of Nuclear Cardiology. Eur J Nucl Med Mol Imaging 37:1802–1812.

31. Bombardieri E, Aktolun C, Baum RP, et al. (2003) 131I/123I-metaiodobenzylguanidine (MIBG) scintigraphy: procedure guidelines for tumour imaging. Eur J Nucl Med Mol Imaging 30:BP132–9.

32. Chen J, Verdes L, Folks RD, et al. (2010) 08455. JAC 55:A89.E844.

33. Verschure DO, de Wit TC, Bongers V, et al. (2015) ^{123}I-MIBG heart-to-mediastinum ratio is influenced by high-energy photon penetration of collimator septa from liver and lung activity. Nucl Med Commun 36:279–285.

34. Scholte AJHA, Schuijf JD, Delgado V, et al. (2010) Cardiac autonomic neuropathy in patients with diabetes and no symptoms of coronary artery disease: comparison of 123I-metaiodobenzylguanidine myocardial scintigraphy and heart rate variability. Eur J Nucl Med Mol Imaging 37:1698–1705.

Age (Years)	54.6±5.4
BMI (Kg/m2)	27.0±3.1
Systolic BP (mm Hg)	118±11
Diastolic BP (mm Hg)	72±10
Fasting Glucose (mg/dl)	86.4±9.0
HbA1c (%)	5.3±1.5
Total Chol (mg/dl)	90.0±13.5
LDLc (mg/dl)	52.2±10.8
HDLc (mg/dl)	28.8±7.2
Triglyceride (mg/dl)	29.8±9.0
LVMI (g/m2)	51.1±10.7
LVEF (%)	61.0±6.4

Table 3-1. Clinical and CMR characteristics of study subjects. (Data are expressed as Mean ± SD).

Early HMR	1.67±0.13
Late HMR	1.73±0.16
Washout Rate (%)	19.1±7.6
Total Segmental Score	28.4±4.0
Modified Segmental Score	20.1±3.2

Table 3-2 MIBG global and regional analysis. (Data are expressed as Mean ± SD).

E/I ratio	1.2±0.1
Valsalva ratio	1.4±0.2
30:15 ratio	1.2±0.1
LFa/RFa	2.4±2.5

Table 3-3 HRV indices of autonomic function. (Data are expressed as Mean ± SD).

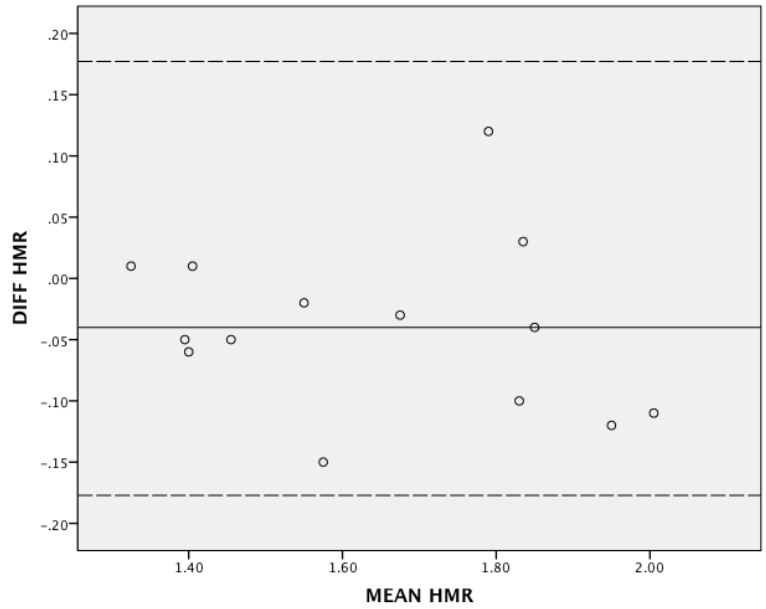

Figure 3-1 Bland Altman plot demonstrating inter-observer agreement (β= -0.176) for HMR with 95% limits of agreement (dashed lines).

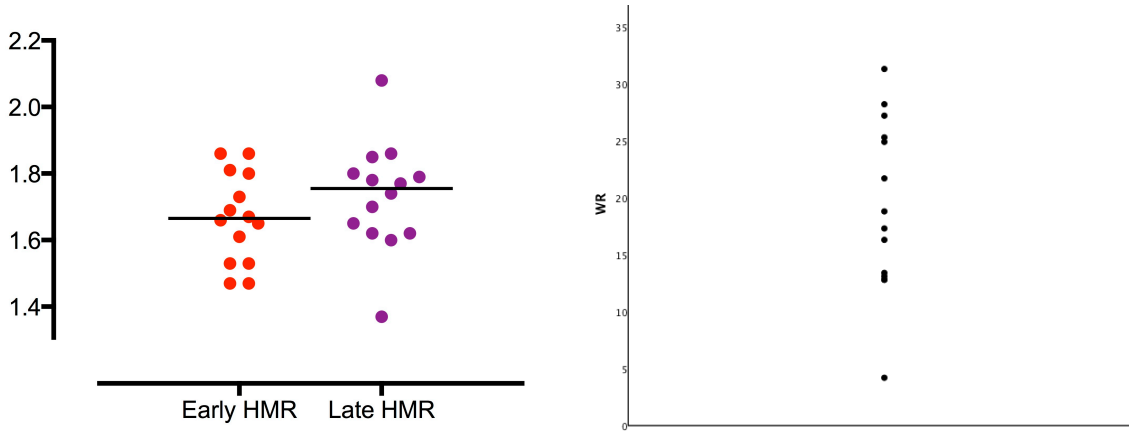

A B

Figure 3-2 Scatter plots of HMR (A) and WR (B).

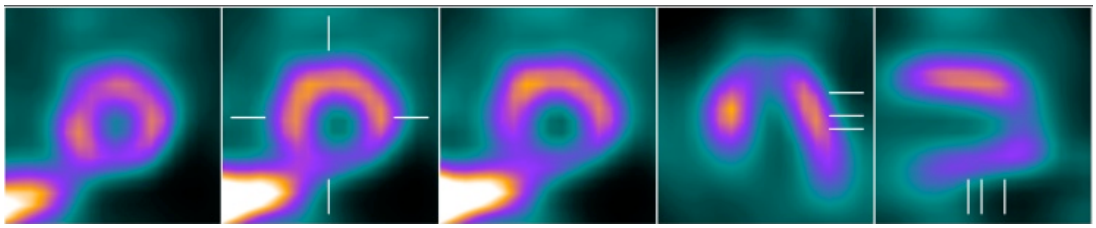

A

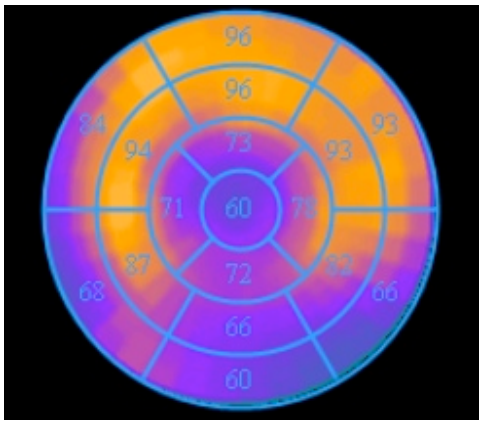

B

Figure 3-3 A) SPECT reconstructed images and B) bull's eye plot of the normal innervation pattern. Note the reduced tracer uptake at the apex, base and inferior wall.

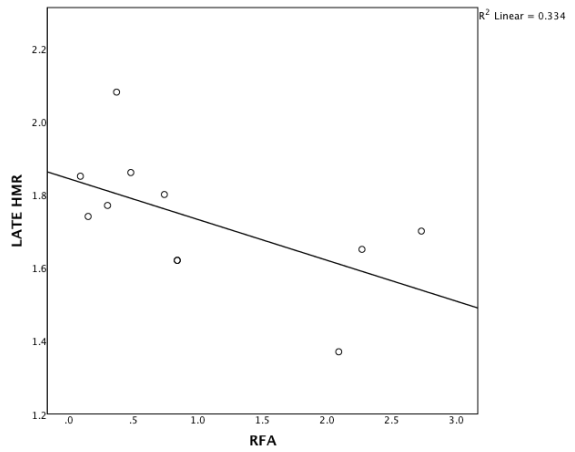

A

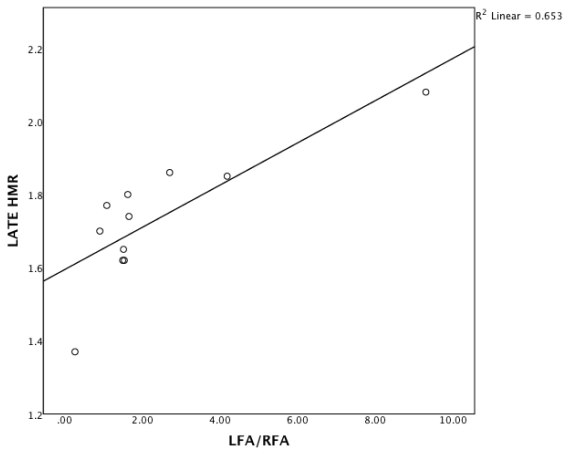

B

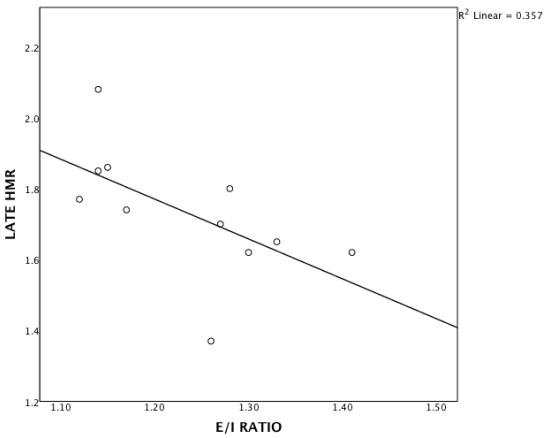

C

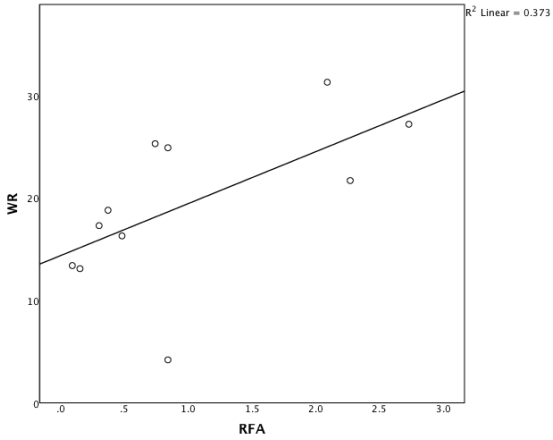

D

Figure 3-4 Correlations of late HMR with RFa (A), LFa/RFa (B), E/I (C) and WR with RFA (D).

4 Individuals With Impaired Glucose Tolerance Demonstrate Normal Cardiac Sympathetic Innervation Using I-123 mIBG Scintigraphy

Omar Asghar, Parthiban Arumugam, Ian Armstrong, Simon Ray, Matthias Schmitt and Malik RA.

Contribution: Omar Asghar contributed to study concept and design of this study and was solely responsible for patient recruitment, data analysis, statistics and the writing of this chapter.

An amended version of this paper has been published in the Journal of Nuclear Cardiology.

4.1 Abstract

Background: Impaired glucose tolerance (IGT) is associated with an increased risk of type 2 diabetes (T2DM) and cardiovascular disease. Some but not all studies have reported cardiac autonomic dysfunction in subjects with IGT and there is only one direct study of cardiac innervation in subjects with IGT. The purpose of this study was to assess global and regional cardiac sympathetic innervation and cardiac autonomic function in individuals with IGT.

Methods and Results: We undertook 123I-mIBG scintigraphy and cardiac autonomic function in 15 subjects with IGT and 15 age and sex matched healthy controls. Early heart to mediastinum ratio (HMR) (1.71±0.17 vs 1.67±0.13, p=0.49), late HMR (1.73±0.18 vs 1.73±0.16, p=0.97) and washout rate (WR) (18.6±4.2 vs 19.1±7.6 %, p=0.84), did not differ between subjects with IGT and control subjects. More detailed regional analysis revealed reduced tracer uptake at the apex, base and in inferior wall in both subjects with IGT and controls. Two subjects with IGT had reduced uptake in the anterior wall. There were no differences in total segmental score (53.3±8.4 vs 56.6±4.0, p=0.193), modified score (46.2±6.0 vs 48.5±3.3, p=0.215) and tests of cardiac autonomic function between the groups.

Conclusion: Global and regional measures of MIBG uptake and washout as well as cardiac autonomic function did not differ between subjects with IGT and healthy controls.

4.2 Introduction

Impaired glucose tolerance (IGT) is a clinically silent, altered state of glycaemia and a precursor to type 2 diabetes mellitus (T2DM). Epidemiological data suggest that IGT may be an independent predictor of cardiovascular (CV) morbidity and mortality (1-3). This increased risk has been attributed to the early development of cardiovascular disease (CVD) as reported in several observational studies demonstrating sub-clinical structural and functional cardiovascular abnormalities in IGT (4-11). However, there is a substantial body of evidence demonstrating that microvascular complications also develop in subjects with IGT (12). Of relevance cardiac autonomic neuropathy (CAN) is an independent predictor of mortality in patients with T2DM (13).

Cardiac autonomic neuropathy has been reported in subjects with IGT (14,15), although in our recent study, subjects with IGT had a significant abnormality in warm and cold thresholds, intraepidermal nerve fiber density and corneal nerve morphology, but no abnormality in heart rate variability with deep breathing (HRVdb) (16). Furthermore, in a recent study patients with T2DM were shown to have higher resting muscle sympathetic nerve activity, arterial norepinephrine levels and lower plasma norepinephrine clearance with reduced neuronal reuptake compared to subjects with IGT (17). These data therefore suggest the need for more precise assessment of autonomic innervation in subjects with IGT, before they are labeled as having significant cardiac autonomic neuropathy.

Imaging of the cardiac sympathetic nerves has emerged as a powerful prognostic indicator for heart failure (HF) and ventricular arrhythmias (18-22). 123I-meta-iodobenzylguanidine (MIBG) scintigraphy allows for the global and regional assessment of cardiac sympathetic innervation and has been used to demonstrate cardiac sympathetic denervation in diabetic subjects (23). Furthermore, the prognostic utility of MIBG scintigraphy in diabetic subjects

was demonstrated in the ADMIRE-HF study in which a heart to mediastinum ratio (HMR) ≤1.6 carried a threefold increase in the risk of HF progression over 2 years of follow up (24,25). In addition, studies using MIBG scintigraphy in patients with T1DM and T2DM have demonstrated associations between CAN, myocardial blood flow and mechanical dysfunction (26-28). To date there have been no such studies in subjects with IGT.

4.3 Methods

Global and regional cardiac sympathetic innervation was quantified using MIBG scintigraphy in a well-defined cohort of subjects with IGT and healthy controls. The study protocol was approved by the Central Manchester Research Ethics Committee. Written informed consent, according to the declaration of Helsinki, was obtained from all participants on enrolment to the study.

4.3.1 Patient Selection

Inclusion criteria were male or female subjects aged 18-75 years with a diagnosis of IGT (glucose 7.8-11.1 mmol/l, 2 hours post oral glucose challenge), identified from our institutional database. In addition, we invited healthy males and females aged 18-75 to act as controls. All positive responders underwent repeat oral glucose tolerance testing (OGTT) on induction to the study to confirm glycaemic status. Prior to MIBG scintigraphy, all participants underwent CMR imaging to exclude previous myocardial infarction, ischaemic heart disease, heart failure and structural heart disease. Exclusion criteria included any history of diabetes, cardiac disease, severe systemic disease (e.g. congestive cardiac failure, rheumatoid disease, SLE), chronic kidney disease (serum creatinine >250 umol/l), peripheral vascular disease or neuropathy.

4.3.2 Study Protocol

All study participants underwent an initial assessment including medical history, clinical examination and 12 lead ECG. All medications known to affect the uptake of MIBG were omitted and thyroid blockade was achieved by oral administration of potassium perchlorate 500mg on the evening prior to imaging. Cardiovascular autonomic function testing was carried out on the day of imaging.

Autonomic Function Testing

The ANX 3.0 autonomic monitoring system (ANSAR Medical Technologies, Inc., Philadelphia, PA) was used to perform spectral analysis of heart rate variability (HRV) during standard tests of cardiovascular reflexes. We assessed parameters of HRV during expiration and inspiration (E/I), Valsalva maneuver (VM), response to standing (30:15 ratio) and postural drop in systolic blood pressure. In addition, the low frequency area (LFa) to respiratory frequency area (RFa) ratio; an estimate of sympathovagal balance, was determined.

4.3.3 I-123 mIBG Scintigraphy

Data Acquisition

123I-mIBG 185MBq (AdreView-GE Healthcare) was administered intravenously by slow (1-2 min) injection through a peripheral venous cannula. All images were acquired using a Siemens Symbia T6 gamma camera (Siemens Healthcare) at 10 (early) and 240 minutes (late) post injection of MIBG. Planar images were acquired with a low energy high-resolution collimator, 159 keV ± 15% energy window, 128 × 128 image matrix, and zoom of 1.0 (pixel size 4.8 mm) for 15 minutes. SPECT images were acquired over a 180° orbit from the right

anterior oblique to left posterior oblique positions with medium energy general purpose collimators, 159 keV ± 15% energy window, 64 × 64 image matrix, zoom of 1.45 (pixel size 6.6 mm) and 64 projections at 30 seconds per projection.

Data Analysis

Image processing was undertaken by a cardiology research fellow (OA) and an experienced nuclear cardiologist who were blinded to clinical information. Average values were used except where there was a significant discrepancy between the two analyses in which case images were reviewed and re-analysed. Global MIBG uptake was assessed in the early and late planar images by drawing regions of interest (ROI) over the whole heart and the upper mediastinum. The heart to mediastinum ratio (HMR) was then calculated by dividing the mean myocardial count per pixel by the mean mediastinal count per pixel. Washout rate (WR), an index of sympathetic tone, was derived using the planar images by calculating the percentage of tracer release between early and late images.

SPECT images were processed to derive short and long axis (vertical and horizontal) slices using iterative reconstruction with resolution recovery (Siemens Flash 3D), with 6 iterations, 8 subsets and an 8.4 mm Gaussian post-filter. Segmental analysis was performed using a 17 segment left ventricular model and tracer uptake (mean count per pixel) was determined and expressed as a percentage of maximal tracer uptake. Each segment was assigned a score based on tracer uptake; <50% = 1, 50-59% = 2, 60-74% = 3 and >75% = 4. The total segmental score was calculated in addition to a modified score, which excluded the apical and inferior wall segments.

4.3.4 Statistical Analysis

SPSS Statistics for Mac version 20 (IBM corporation, New York USA) was used for all statistical analysis. All data are expressed as mean ± SD and the Shapiro-Wilk test was used to determine normality of data. The unpaired T test was used to compare normally distributed data between groups and the Mann Whitney U test was used for non-parametric data. A two-tailed P-value of less than 0.05 was considered statistically significant.

4.4 Results

15 subjects with IGT (10 males, 5 females) and 15 healthy control subjects (10 males, 5 females) underwent assessment. One male control subject was excluded on the basis of an incidental ECG finding of atrial flutter and LV impairment (LVEF 48%) on CMR. The remaining participants successfully completed the imaging protocol and CMR imaging did not reveal any abnormality in cardiac structure, function or stress perfusion. In the IGT group, two subjects were taking statin therapy and one subject was taking an angiotensin converting enzyme inhibitor.

The demographic and clinical data are detailed in Table 4-1. Both groups were age and sex matched. Subjects with IGT had a significantly greater BMI (32.4±6.3 vs 27.0±3.1 Kg/m2, $p<0.05$) and triglycerides (2.0±0.9 vs 1.1±0.5 mmol/l, $p<0.05$) and lower HDL cholesterol (1.2±0.4 vs 1.6±0.4 mmol/l, $p<0.05$) compared to healthy controls. There were no differences in LVEF (61.1±5.4 vs 61.0±6.4 %, $p=0.96$) or left ventricular mass index (LVMI) (47.6±8.8 vs 51.1±10.7 g/m2, $p=0.32$) between the two groups.

4.4.1 Autonomic Function Testing

There were no differences in autonomic function indices between the groups: (E/I ratio: 1.2±0.1 vs 1.2±0.1, p=0.13), (Valsalva ratio: 1.2±0.3 vs 1.4±0.2, p=0.08), (30:15 ratio: 1.2±01 vs 1.2±0.1, p=0.37), (LFa/RFa ratio: 2.1±2.3 vs 2.4±2.5, p=0.79) (Table 4-2).

4.4.2 I-123 mIBG Scintigraphy

There were no differences in early HMR (1.71±0.17 vs 1.67±0.13, p=0.49), late HMR (1.73±0.18 vs 1.73±0.16, p=0.97) and WR (18.6±4.2 vs 19.1±7.6 %, p=0.84) between subjects with IGT and controls (Table 4-3 and figures 4-2, 4-3). Qualitative assessment of the SPECT images revealed a consistent reduction of tracer uptake in subjects with IGT and in control subjects at the cardiac apex, base and inferior wall. Furthermore, in two of the IGT group, there was reduced tracer uptake in the anterior wall (Figure 4-3) however these deficits did not significantly impact on HMR which was greater than 1.6 in both cases. There were no significant differences in the total segmental score (53.3±8.4 vs 56.6±4.0, p=0.193) and modified score (46.2±6.0 vs 48.5±3.3, p=0.215) in subjects with IGT compared to controls.

4.5 Discussion

CAN is a recognised complication of both T1DM and T2DM, often present at diagnosis in T2DM and is an independent predictor of morbidity and mortality (13,29). Abnormal MIBG uptake has been shown in subjects with newly diagnosed and long duration type 1 DM and correlates with tests of cardiac autonomic function (30-33). Similar findings have been reported in studies using [11C]-HED PET imaging (34). More recently, Sacre et al reported an independent association between CAN and measures of myocardial functional reserve in

subjects with T2DM (26). In a sub set of patients who underwent MIBG scintigraphy, HMR correlated with CAN and parameters of diastolic and systolic function.

In the only study published to date in subjects with IGT, late HMR was significantly reduced compared to healthy controls (35). They reported regional defects in innervation, predominantly in the apex and inferior wall in the vast majority (20/22) of the IGT cohort. In the present study we show that these are in fact normal findings in healthy subjects as previously described in the literature (36-40). Another major limitation of their study was the highly selected nature of the IGT cohort in which most subjects had a positive family history of DM. In contrast, we demonstrate normal global and regional MIBG uptake in a cohort of uncomplicated subjects from primary care with IGT, compared to age and sex matched healthy controls. Although HMR in our healthy controls was lower than in ADMIRE-HF (1.76±0.23; range 1.09-2.40), the age range and BMI of our control subjects were narrower. The disparity in HMR may also be explained by differences in imaging protocols between the studies. Our imaging protocol was based on internationally recommended standards (41,42) however in ADMIRE-HF, they used a higher MIBG dose (370MBq), low energy high resolution (LEHR) collimators (43), filtered back projection (FBP) for SPECT image processing and qualitative regional assessment. Iterative reconstruction and resolution recovery methods for SPECT in or study allowed us to use a lower (185MBq) MIBG dose thus reducing activity to the patient in our study. The choice of collimator is a well recognised cause of variability in HMR and in our study, we used a MEGP collimator which reduces scatter thus improving spatial resolution and provides superior image contrast (44,45). Given the relatively wide range of late HMR values in the IGT and control groups, the possibility of a type II statistical error could not be excluded.

Using spectral analysis of HRV, we also confirm normal autonomic function in our IGT group who underwent a robust cardiac assessment including detailed structural and functional cardiac phenotyping using gold standard imaging modalities, notably CMR. Previous studies have reported conflicting findings for the presence of CAN in subjects with IGT. In the Finnish Diabetes Prevention Study of 268 subjects with IGT, the prevalence of parasympathetic and sympathetic dysfunction was 25 and 5% respectively however the presence of parasympathetic dysfunction was associated with age and obesity (46). Similarly, Putz et al reported the presence of CAN in subjects with IGT however their cohort did not undergo any cardiovascular assessment to exclude cardiovascular disease (14). Our findings are consistent with those reported by Isak et al who did not find any differences in HRV in a group of subjects with IGT compared to age-matched healthy controls (47).

In summary subjects with IGT and an adverse CV risk profile had no evidence of cardiac autonomic neuropathy. We have now gone one step further and show no evidence of either regional or global sympathetic denervation using MIBG scintigraphy. CAN may represent a late manifestation of IGT and abnormalities in cardiac MIBG scintigraphy may not become apparent until advanced CAN.

Sources of Funding

This study was funded by research grants from the NHS National Institutes for Health Research (FSF-R5-OA), NIH (R105991) and Juvenile Diabetes Research Foundation (8-2008-362).

Disclosures

None.

4.6 References

1. Ford ES, Zhao G, Li C. Pre-Diabetes and the Risk for Cardiovascular Disease. JAC. 2031 Feb 13;55(13):1310–7.

2. Levitzky Y, Pencina M, D'Agostino R, Meigs J, Murabito J, Vasan R, et al. Impact of Impaired Fasting Glucose on Cardiovascular Disease:: The Framingham Heart Study. Journal of the American College of Cardiology. 2008;51(3):264–70.

3. Levitan EB, Song Y, Ford ES, Liu S. Is Nondiabetic Hyperglycemia a Risk Factor for Cardiovascular Disease?: A Meta-analysis of Prospective Studies. Archives of internal medicine. American Medical Association; 2004 Oct 25;164(19):2147–55.

4. Rutter MK. Impact of Glucose Intolerance and Insulin Resistance on Cardiac Structure and Function: Sex-Related Differences in the Framingham Heart Study. Circulation. 2003 Jan 28;107(3):448–54.

5. Henry R, Paulus W, Kamp O, Kostense P, Spijkerman A, Dekker J, et al. Deteriorating glucose tolerance status is associated with left ventricular dysfunction-the Hoorn Study. Neth J Med. 2008;66:110–7.

6. Henry R, Kamp O, Kostense P, Spijkerman A, Dekker J, van Eijck R, et al. Left ventricular mass increases with deteriorating glucose tolerance, especially in women: independence of increased arterial stiffness or decreased flow-mediated dilation. Diabetes Care. 2004;27(2):522.

7. Witteles R, Fowler M. Insulin-Resistant Cardiomyopathy:: Clinical Evidence, Mechanisms, and Treatment Options. Journal of the American College of Cardiology. 2008;51(2):93–102.

8. Velagaleti RS, Gona P, Chuang ML, Salton CJ, Fox CS, Blease SJ, et al. Relations of Insulin Resistance and Glycemic Abnormalities to Cardiovascular Magnetic Resonance Measures of Cardiac Structure and Function: The Framingham Heart Study. Circulation: Cardiovascular Imaging. 2010 May 1;3(3):257–63.

9. Okura H, Inoue H, Tomon M, Nishiyama S, Yoshikawa T, Yoshida K, et al. Impaired glucose tolerance as a determinant of early deterioration of left ventricular diastolic function in middle-aged healthy subjects. The American Journal of Cardiology. 2000;85(6):790.

10. Ilercil A. Relationship of impaired glucose tolerance to left ventricular structure and function: The Strong Heart Study. American Heart Journal. 2001 Jun 1;141(6):992–8.

11. Chaturvedi N. A comparison of left ventricular abnormalities associated with glucose intolerance in African Caribbeans and Europeans in the UK. Heart. 2001 Jun 1;85(6):643–8.

12. Singleton J, Smith A, Russell J, Feldman E. Microvascular complications of impaired glucose tolerance. Diabetes. 2003;52(12):2867.

13. Pop-Busui R, Evans GW, Gerstein HC, Fonseca V, Fleg JL, Hoogwerf BJ, et al. Effects of cardiac autonomic dysfunction on mortality risk in the Action to Control Cardiovascular Risk in Diabetes (ACCORD) trial. Diabetes Care. 2010 Jul;33(7):1578–84.

14. Putz Z, Tabak AG, Toth N, Istenes I, Nemeth N, Gandhi RA, et al. Noninvasive Evaluation of Neural Impairment in Subjects With Impaired Glucose Tolerance. Diabetes Care. 2009 Jan 1;32(1):181–3.

15. Stein PK, Barzilay JI, Domitrovich PP, Chaves PM, Gottdiener JS, Heckbert SR, et al. The relationship of heart rate and heart rate variability to non-diabetic fasting glucose levels and the metabolic syndrome: the Cardiovascular Health Study. Diabetic Medicine. 2007 Aug;24(8):855–63.

16. Asghar O, Petropoulos IN, Alam U, Jones W, Jeziorska M, Marshall A, et al. Corneal confocal microscopy detects neuropathy in subjects with impaired glucose tolerance. Diabetes Care. 2014 Sep;37(9):2643–6.

17. Straznicky NE, Grima MT, Sari CI, Eikelis N, Lambert EA, Nestel PJ, et al. Neuroadrenergic dysfunction along the diabetes continuum: a comparative study in obese metabolic syndrome subjects. Diabetes. 2012 Oct;61(10):2506–16.

18. Boogers MJ, Borleffs CJW, Henneman MM, van Bommel RJ, van Ramshorst J, Boersma E, et al. Cardiac sympathetic denervation assessed with 123-iodine metaiodobenzylguanidine imaging predicts ventricular arrhythmias in implantable cardioverter-defibrillator patients. Journal of the American College of Cardiology. 2010 Jun 15;55(24):2769–77.

19. Carrió I, Cowie MR, Yamazaki J, Udelson J, Camici PG. Cardiac Sympathetic Imaging With mIBG in Heart Failure. JCMG. 2011 Jan 14;3(1):92–100.

20. Verberne HJ, Brewster LM, Somsen GA, van Eck-Smit BLF. Prognostic value of myocardial 123I-metaiodobenzylguanidine (MIBG) parameters in patients with heart failure: a systematic review. European Heart Journal. 2008 Mar 20;29(9):1147–59.

21. Kasama S, Toyama T, Sumino H, Nakazawa M, Matsumoto N, Sato Y, et al. Prognostic Value of Serial Cardiac 123I-MIBG Imaging in Patients with Stabilized Chronic Heart Failure and Reduced Left Ventricular Ejection Fraction. J Nucl Med. 2008 May 15;49(6):907–14.

22. Bax JJ, Kraft O, Buxton AE, Fjeld JG, Parizek P, Agostini D, et al. 123I-mIBG Scintigraphy to Predict Inducibility of Ventricular Arrhythmias on Cardiac Electrophysiology Testing: A Prospective Multicenter Pilot Study. Circulation: Cardiovascular Imaging. 2008 Sep 16;1(2):131–40.

23. Hattori N, Tamaki N, Hayashi T, Masuda I, Kudoh T, Tateno M, et al. Regional abnormality of iodine-123-MIBG in diabetic hearts. J Nucl Med. 1996 Dec;37(12):1985–90.

24. Gerson MC, Caldwell JH, Ananthasubramaniam K, Clements IP, Henzlova MJ, Amanullah A, et al. Influence of diabetes mellitus on prognostic utility of imaging of myocardial sympathetic innervation in heart failure patients. Circulation: Cardiovascular Imaging. 2011 Mar;4(2):87–93.

25. Nagamachi S, Fujita S, Nishii R, Futami S, Tamura S, Mizuta M, et al. Prognostic value of cardiac I-123 metaiodobenzylguanidine imaging in patients with non–insulin-dependent diabetes mellitus. J Nucl Cardiol. 2006 Jan;13(1):34–42.

26. Sacre JW, Franjic B, Jellis CL, Jenkins C, Coombes JS, Marwick TH. Association of cardiac autonomic neuropathy with subclinical myocardial dysfunction in type 2 diabetes. JACC Cardiovasc Imaging. 2010 Dec;3(12):1207–15.

27. Schnell O. Cardiac sympathetic innervation and blood flow regulation of the diabetic heart. Diabetes Metab Res Rev. 2001;17(4):243–5.

28. Hattori N, Rihl J, Bengel F, Nekolla S. Cardiac autonomic dysinnervation and myocardial blood flow in long-term Type 1 diabetic patients. Diabetic …. 2003.

29. Vinik AI, Ziegler D. Diabetic Cardiovascular Autonomic Neuropathy. Circulation. 2007 Jan 8;115(3):387–97.

30. Schnell O, Muhr D, Weiss M, Dresel S, Haslbeck M, Standl E. Reduced myocardial 123I-metaiodobenzylguanidine uptake in newly diagnosed IDDM patients. Diabetes. 1996 Jun;45(6):801–5.

31. Schnell O, Kirsch CM, Stemplinger J, Haslbeck M, Standl E. Scintigraphic evidence for cardiac sympathetic dysinnervation in long-term IDDM patients with and without ECG-based autonomic neuropathy. Diabetologia. 1995 Nov;38(11):1345–52.

32. Langer A, Freeman MR, Josse RG, Armstrong PW. Metaiodobenzylguanidine imaging in diabetes mellitus: assessment of cardiac sympathetic denervation and its relation to autonomic dysfunction and silent myocardial ischemia. JAC. 1995 Mar 1;25(3):610–8.

33. Kreiner G, Wolzt M, Fasching P, Leitha T, Edlmayer A, Korn A, et al. Myocardial m-[123I]iodobenzylguanidine scintigraphy for the assessment of adrenergic cardiac innervation in patients with IDDM. Comparison with cardiovascular reflex tests and relationship to left ventricular function. Diabetes. 1995 May;44(5):543–9.

34. Stevens MJ, Raffel DM, Allman KC, Dayanikli F, Ficaro E, Sandford T, et al. Cardiac sympathetic dysinnervation in diabetes: implications for enhanced cardiovascular risk. Circulation. 1998 Sep 8;98(10):961–8.

35. Diakakis G, Parthenakis F, Patrianakos A, Koukouraki S, Stathaki M, Karkavitsas N, et al. Myocardial sympathetic innervation in patients with impaired glucose tolerance: relationship to subclinical inflammation. Cardiovascular Pathology. 2008;17(3):172–7.

36. Gill JS, Hunter GJ, Gane G, Camm AJ. Heterogeneity of the human myocardial sympathetic innervation: in vivo demonstration by iodine 123-labeled meta-iodobenzylguanidine scintigraphy. American Heart Journal. 1993 Aug 1;126(2):390–8.

37. Tsuchimochi S, Tamaki N, Tadamura E, Kawamoto M, Fujita T, Yonekura Y, et al. Age and gender differences in normal myocardial adrenergic neuronal function evaluated by iodine-123-MIBG imaging. J Nucl Med. 1995 Jun;36(6):969–74.

38. Somsen GA, Verberne HJ, Fleury E, Righetti A. Normal values and within-subject variability of cardiac I-123 MIBG scintigraphy in healthy individuals: implications for clinical studies. J Nucl Cardiol. 2004 Feb;11(2):126–33.

39. Morozumi T, Kusuoka H, Fukuchi K. Myocardial iodine-123-metaiodobenzylguanidine images and autonomic nerve activity in normal subjects. J Nucl Med.1997;38:49-52.

40. Kimura K, Ieda M, Fukuda K. Development, Maturation, and Transdifferentiation of Cardiac Sympathetic Nerves. Circulation Research. 2012 Jan 19;110(2):325–36.

41. Flotats A, Carrió I, Agostini D, Guludec D, Marcassa C, Schaffers M, et al. Proposal for standardization of 123I-metaiodobenzylguanidine (MIBG) cardiac sympathetic imaging by the EANM Cardiovascular Committee and the European Council of Nuclear Cardiology. Eur J Nucl Med Mol Imaging. 2010 Jun 25;37(9):1802–12.

42. Bombardieri E, Aktolun C, Baum RP, Bishof-Delaloye A, Buscombe J, Chatal JF, et al. 131I/123I-metaiodobenzylguanidine (MIBG) scintigraphy: procedure guidelines for tumour imaging. European Journal of Nuclear Medicine and Molecular Imaging. 2003. pp. BP132–9.

43. Jacobson AF, Lombard J, Banerjee G, Camici PG. 123I-mIBG Scintigraphy to predict risk for adverse cardiac outcomes in heart failure patients: Design of two prospective multicenter international trials. J Nucl Cardiol. 2009 Jan 20;16(1):113–21.

44. Nakajima K, Okuda K, Yoshimura M, Matsuo S, Wakabayashi H, Imanishi Y, et al. Multicenter cross-calibration of I-123 metaiodobenzylguanidine heart-to-mediastinum ratios to overcome camera-collimator variations. J Nucl Cardiol. 2014 Oct;21(5):970–8.

45. Verberne HJ, Habraken JBA, van Eck-Smit BLF, Agostini D, Jacobson AF. Variations in 123I-metaiodobenzylguanidine (MIBG) late heart mediastinal ratios in chronic heart failure: a need for standardisation and validation. Eur J Nucl Med Mol Imaging. 2008 Mar;35(3):547–53.

46. Laitinen T, Lindström J, Eriksson J, Ilanne-Parikka P, Aunola S, Keinanen-Kiukaanniemi S, et al. Cardiovascular autonomic dysfunction is associated with central obesity in persons with impaired glucose tolerance. Diabet Med. 2011 Jun;28(6):699–704.

47. Isak B, Oflazoglu B, Tanridag T, Yitmen I, Us O. Evaluation of peripheral and autonomic neuropathy among patients with newly diagnosed impaired glucose tolerance. Diabetes Metab Res Rev. 2008 Oct;24(7):563–9.

	CONTROL	IGT	P
Age (Years)	54.6±5.4	56.9±9.0	0.41
BMI (Kg/m2)	27.0±3.1	32.4±6.3	0.007
Systolic BP (mm Hg)	118±11	124±14	0.17
Diastolic BP (mm Hg)	72±10	74±10	0.63
Fasting Glucose (mmol/l)	4.8±0.5	6.0±0.8	<0.001
2h Glucose (mmol/l)	5.3±1.3	9.4±1.3	<0.001
HbA1c (%)	5.3±1.5	5.9±0.5	0.18
Total Chol (mmol/l)	5.0±0.75	4.8±1.4	0.49
LDLc (mmol/l)	2.9±0.6	2.8±1.1	0.94
HDLc (mmol/l)	1.6±0.4	1.2±0.4	0.022
Triglyceride (mmol/l)	1.1±0.5	2.0±0.9	0.003
LVMI (g/m2)	51.1±10.7	47.6±8.8	0.32
LVEF (%)	61.0±6.4	61.1±5.4	0.96

Table 4-1 Clinical and CMR characteristics of study subjects. (Data are expressed as Mean ± SD).

	CONTROL	IGT	P
Early HMR	1.67±0.13	1.71±0.17	0.49
Late HMR	1.73±0.16	1.73±0.18	0.97
Washout Rate (%)	19.1±7.6	18.6±4.2	0.84
Total Segmental Score	56.6±4.0	53.3±8.4	0.19
Modified Segmental Score	48.5±3.3	46.2±6.0	0.22

Table 4-2 MIBG global and regional analysis. (Data are expressed as Mean ± SD).

	CONTROL	IGT	P
E/I ratio	1.2±0.1	1.12±0.1	0.13
Valsalva ratio	1.4±0.2	1.2±0.3	0.09
30:15 ratio	1.2±0.1	1.2±0.1	0.37
LFa/RFa	2.4±2.5	2.1±2.3	0.79

Table 4-3 HRV indices of autonomic function. (Data are expressed as Mean ± SD).

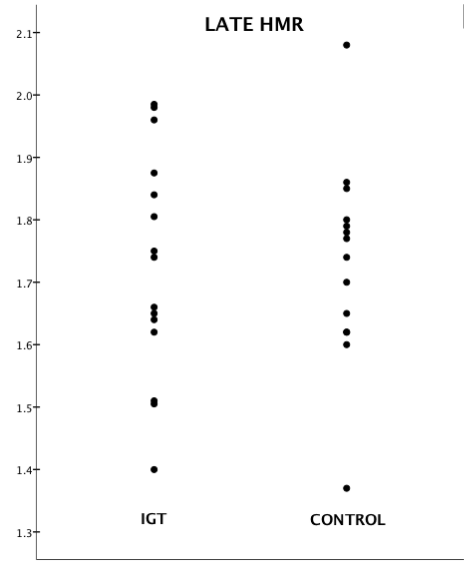

Figure 4-1 Scatter plot of late HMR in IGT vs Controls

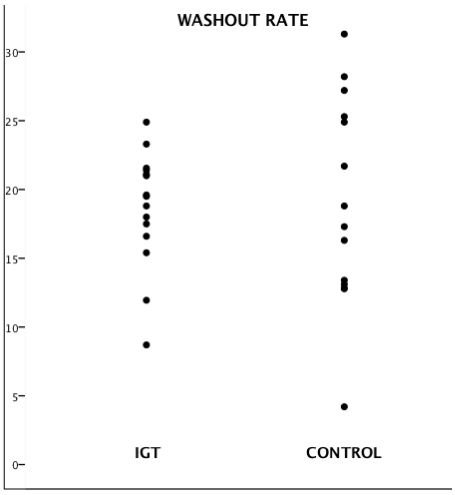

Figure 4-2 Scatter plot of WR in IGT and Controls.

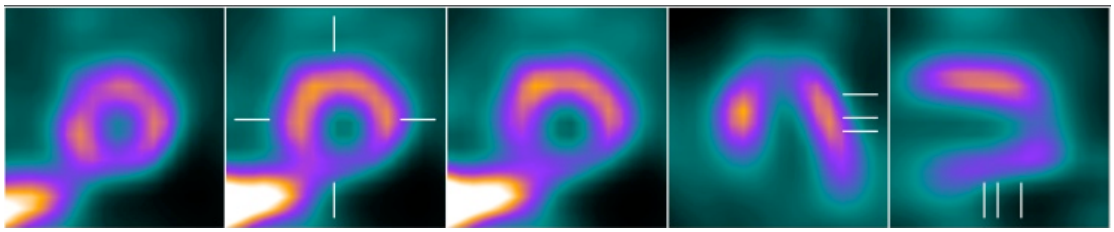

A

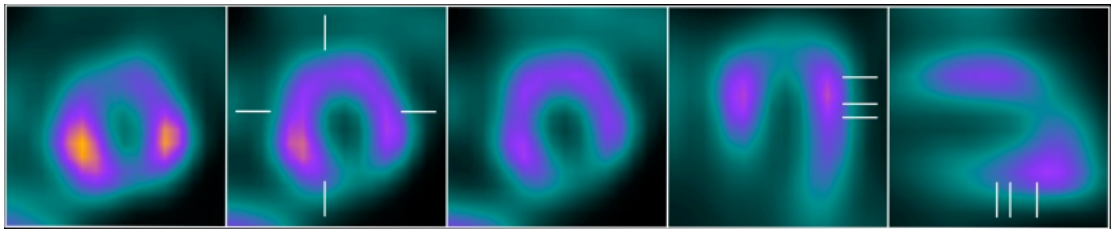

B

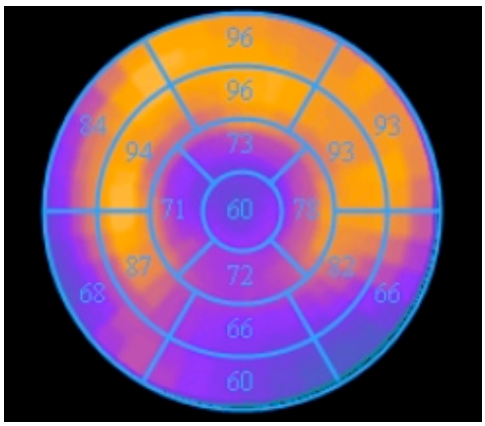

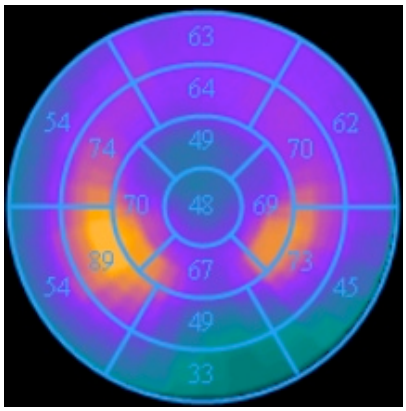

C D

Figure 4-3SPECT reconstructed images and bull's eye plots of a control subject with a normal innervation pattern (A and C) and a subject with IGT (B and D). Note the reduced tracer uptake particularly in the anterior and lateral segments despite normal global uptake (late HMR 1.88).

5 Subjects with Extreme Duration Type 1 Diabetes are Protected from Sympathetic Denervation and Cardiac Autonomic Neuropathy.

Omar Asghar, Parthiban Arumugam, Ian Armstrong, Simon Ray, Matthias Schmitt and Rayaz Malik.

Contribution: Omar Asghar contributed to study concept and design of this study and was solely responsible for patient recruitment, data analysis, statistics and the writing of this chapter.

5.1 Abstract

Objective: To determine whether medalists exhibit cardiac sympathetic denervation on MIBG scintigraphy and cardiac autonomic neuropathy.Research Design and Methods: We assessed cardiac sympathetic innervation in 15 subjects with type 1 diabetes of extreme duration and 15 healthy adults using standardised MIBG scintigraphy and cardiovascular reflex tests. Prior to MIBG imaging, CMR imaging was performed in all subjects to exclude abnormalities of cardiac structure, function and perfusion.

Results: There were no differences in global uptake (early HMR 1.67±0.18 vs 1.67±0.13; P=0.987), (late HMR 1.61±0.22 vs 1.73±0.16, P=0.105) or washout rate (WR) (22.0±6.9 vs 19.1±7.6%; P=0.302) between the diabetic group and controls. Regional assessment revealed reduced MIBG uptake at the cardiac apex, base and inferior wall in diabetic subjects and controls which were more pronounced in the diabetic group. The inferior (6.6±3.1 vs 9.2±1.4; P=0.009), apical (11.5±4.1 vs 15.8±2.7; P=0.003) and basal (17.1±2.4 vs 18.9±1.8; P=0.041) uptake scores were significantly lower in the diabetic group. Diabetic patients had a lower Valsalva ratio (1.2±0.2 vs 1.4±0.2; P=0.009) and RFa (0.5±0.9 vs 1.1±1.0, P=0.028) but there were no differences in resting heart rate (74±12 vs 65±11 bpm; P=0.124), QTc (400±18 vs 386±23 ms; P=0.073), E/I ratio (1.2±0.2 vs 1.2±0.1; P=0.109), 30:15 ratio (1.1±0.3 vs 0.9±0.5; P=0.781), LFa (0.8±1.3 vs 1.2±1.3; P=0.705) and LFa/RFa (2.5±2.2 vs 2.3±2.7; P=0.975) between the groups.

Conclusions: Subjects with type 1 diabetes of extreme duration of diabetes exhibit normal global uptake and washout of MIBG and only minimal cardiac autonomic dysfunction.

5.2 Introduction

The term "medalists" has been used to represent a unique group of individuals who have survived over 50 years of type 1 diabetes. The Joslin 50 year Medalist study identified a sub-group of this cohort (escapers) who had remained free of micro and macrovascular complications (1,2). A major limitation of this study however was that the definition of cardiovascular disease (CVD) was based on clinical history alone. Furthermore, peripheral neuropathy but not cardiac autonomic neuropathy (CAN) were assessed. CAN is a common complication of both type 1 and 2 diabetes and a strong independent risk factor for CV morbidity and mortality (3,4). This elevated risk may be attributable to features of advanced CAN, including cardiac arrhythmias, silent myocardial ischemia (SMI), lack of hypoglycaemia awareness and sudden cardiac death.

Imaging of the cardiac sympathetic nerves has emerged as a powerful prognostic indicator for heart failure (HF) and ventricular arrhythmias (5-9). 123I-meta-iodobenzylguanidine (MIBG) scintigraphy allows for the global and regional assessment of cardiac sympathetic innervation and has been used to demonstrate cardiac sympathetic denervation in subjects with type 2 diabetes (4,10). The prognostic utility of MIBG scintigraphy in diabetic (predominantly type 2) subjects was demonstrated in the ADMIRE-HF study in which a heart to mediastinum ratio (HMR) $\leq$1.6 carried a threefold increase in the risk of HF progression over 2 years of follow up (11). In addition, studies of MIBG in diabetic (type 1 and 2) subjects have demonstrated associations between CAN and impaired myocardial blood flow (12-16) and CAN and mechanical dysfunction (17). There are currently no data on cardiac innervation and CAN in medalists.

The aim of this study was to assess global and regional cardiac sympathetic innervation and autonomic function in a cohort of individuals with extreme duration type 1 diabetes.

5.3 Research Design and Methods

We performed assessment of cardiac sympathetic innervation using MIBG scintigraphy and cardiac autonomic function tests in a cohort of subjects with type 1 diabetes of extreme duration and healthy controls. The study protocol was approved by the Central Manchester Research Ethics Committee. Written informed consent, according to the declaration of Helsinki, was obtained from all participants on enrolment to the study.

5.3.1 Patient Selection

We invited subjects aged 18-75 years with type 1 diabetes of extreme duration (>45 years) identified from our local institutional diabetic database. In addition, we invited healthy males and females aged 18-75 to act as controls. Exclusion criteria included any history of cardiac disease, severe systemic disease (e.g. congestive cardiac failure, rheumatoid disease, SLE), chronic kidney disease (serum creatinine >250 umol/l), peripheral vascular disease or any contraindication to MIBG scintigraphy or CMR imaging (including adenosine stress and gadolinium contrast).

5.3.2 Study Protocol

All study participants underwent an initial assessment including medical history, clinical examination and 12 lead ECG. Healthy control subjects underwent oral glucose tolerance testing (OGTT) on induction to the study to confirm normoglycemia. Within two weeks of MIBG scintigraphy, all participants underwent CMR imaging to exclude previous myocardial infarction (MI), ischemic heart disease, HF and structural heart disease. All medications known to affect the uptake of MIBG were omitted and thyroid blockade was achieved by oral administration of potassium perchlorate 500mg on the evening prior to MIBG imaging. Cardiovascular autonomic function testing was carried out on the day of MIBG imaging.

Autonomic Function Testing

The ANX 3.0 autonomic monitoring system (ANSAR Medical Technologies, Inc., Philadelphia, PA) was used to perform spectral analysis of heart rate variability (HRV) during standard tests of cardiovascular reflexes. We assessed parameters of HRV during expiration and inspiration (E/I), Valsalva maneuver (VM), response to standing (30:15 ratio) and postural drop in systolic blood pressure. In addition, the low frequency area (LFa) to respiratory frequency area (RFa) ratio; an estimate of sympathovagal balance, was determined.

5.3.3 I-123 mIBG Scintigraphy

Data Acquisition

123I-mIBG 185MBq (AdreView-GE Healthcare) was administered intravenously by slow (1-2 min) injection through a peripheral venous cannula. All images were acquired using a Siemens Symbia T6 gamma camera (Siemens Healthcare) at 10 (early) and 240 minutes (late) post injection of MIBG. Planar images were acquired with a low energy high-resolution collimator, 159 keV ± 15% energy window, 128 × 128 image matrix, and zoom of 1.0 (pixel size 4.8 mm) for 15 minutes. SPECT images were acquired over a 180° orbit from the right anterior oblique to left posterior oblique positions with medium energy general purpose collimators, 159 keV ± 15% energy window, 64 × 64 image matrix, zoom of 1.45 (pixel size 6.6 mm) and 64 projections at 30 seconds per projection.

Data Analysis

Image processing was undertaken by a cardiology research fellow (OA) and an experienced nuclear cardiologist (IA), blinded to clinical information. Average values were used except where there was a significant discrepancy between the two analyses in which case images were reviewed and re-analysed. Global MIBG uptake was assessed in the early and late planar images by drawing regions of interest (ROI) over the whole heart and the upper mediastinum. The heart to mediastinum ratio (HMR) was then calculated by dividing the mean myocardial count per pixel by the mean mediastinal count per pixel. Washout rate (WR), an index of sympathetic tone, was derived using the planar images by calculating the percentage of tracer release between early and late images.

SPECT images were processed to derive short and long axis (vertical and horizontal) slices using iterative reconstruction with resolution recovery (Siemens Flash 3D), with 6 iterations, 8 subsets and an 8.4 mm Gaussian post-filter. Segmental analysis was performed using a 17 segment left ventricular model and tracer uptake (mean count per pixel) was determined and expressed as a percentage of maximal tracer uptake. Each segment was assigned a score based on tracer uptake; <50% = 1, 50-59% = 2, 60-74% = 3 and >75% = 4. We compared total segmental score, modified total score (total - apical and inferior segments) and individual wall scores (anterior, apical, inferior and basal) between the groups.

5.3.4 Statistical Analysis

SPSS Statistics for Mac version 20 (IBM corporation, New York USA) was used for all statistical analysis. All data are expressed as mean ± SD and the Shapiro-Wilk test was used to determine normality of data. The unpaired T test was used to compare normally distributed

data between groups and the Mann Whitney U test was used for non-parametric data. A two-tailed P-value of less than 0.05 was considered statistically significant.

5.4 Results

We recruited 15 subjects with type 1 diabetes of extreme duration and 15 healthy control subjects. Two subjects were excluded (1 from each group) from the study due to incidental findings on CMR imaging of LV impairment and severe left ventricular hypertrophy respectively. A further subject from the medalist group demonstrated late gadolinium enhancement in a limited area of the apical septum consistent with an old sub-endocardial MI but remained in the study. All other study participants (medalists: 6 male, 9 female; controls: 9 males, 5 females) exhibited normal cardiac structure, function and stress perfusion on CMR imaging and successfully completed the imaging protocol.

5.4.1 Demographic, Clinical and Cardiac Data (Table 5-1)

The mean duration of diabetes was 48.3±5.4 years (median 50.0 years) and the mean HbA1c over 16 years was 8.5±1.0% (69±11 mmol/mol) indicating moderate to poor long-term glycemic control, but good lipid profile (chol 4.7±0.3, HDLc 1.8±0.5, LDLc 2.2±0.5, Trig 1.1±0.4 mmol/l) and renal function eGFR (76±17ml/kg/min). Eight of the fourteen medalists had a history of retinopathy and 12 medalists were taking statin and angiotensin converting enzyme (ACE) inhibitor therapy in addition to insulin. None of the control group were taking any regular medication. The diabetic subjects were older (61.9±7.3 vs 51.5±5.4 years; P=0.006) and had lower diastolic (61±14 vs 72±10 mm Hg; P=0.021) but slightly higher systolic (120±15 vs 118±11; P=0.045) blood pressure than controls. There were no differences in BMI, lipids or eGFR between the groups. LVMI was lower in the diabetic

group (41.0±6.4 vs 51.1±10.7 g/m2, P=0.007) and there were no differences in LVEF (63.1±6.9 vs 61.0±6.4%; P=0.425).

5.4.2 Autonomic Function Testing (Table 5-1)

There were no differences in resting heart rate (74±12 vs 65±11 bpm; P=0.124), QTc (400±18 vs 386±23 ms; P=0.073), E/I ratio (1.2±0.2 vs 1.2±0.1; P=0.109), 30:15 ratio (1.1±0.3 vs 0.9±0.5; P=0.781), LFa (0.8±1.3 vs 1.2±1.3; P=0.705) and LFa/RFa (2.5±2.2 vs 2.3±2.7; P=0.975) between the groups. However, diabetic patients had a lower Valsalva ratio (1.2±0.2 vs 1.4±0.2; P=0.009) and RFa (0.5±0.9 vs 1.1±1.0, P=0.028) compared to controls.

5.4.3 I-123 mIBG Scintigraphy (Table 5-1)

There were no differences in early HMR (1.67±0.18 vs 1.67±0.13; P=0.987), late HMR (1.61±0.22 vs 1.73±0.16, P=0.105) (Figure 5-1) and WR (22.0±6.9 vs 19.1±7.6%; P=0.302) (Figure 5-2) between diabetic subjects and controls. Qualitative assessment of the SPECT images revealed a consistent reduction of tracer uptake at the cardiac apex, base and inferior wall in all subjects however these changes were more pronounced in the diabetic group (Figure 5-3). Total segmental score was higher in the diabetic group compared with controls (38.9±9.0 vs 30.5±5.2; P=0.006) however there was no difference in modified total score (16.6±4.5 vs 14.1±3.0; P=0.104). The inferior (6.6±3.1 vs 9.2±1.4; P=0.009), apical (11.5±4.1 vs 15.8±2.7; P=0.003) and basal (17.1±2.4 vs 18.9±1.8; P=0.041) scores were significantly lower with no difference in the anterior wall score (9.6±1.5 vs 10.2±1.3; p=0.23) comparing the diabetic patients with the control subjects.

5.5 Conclusions

Medalists represent a unique group of patients with an extreme duration of Type 1 diabetes. This is the first study to investigate in detail, the presence and extent of cardiac sympathetic innervation and cardiac autonomic function in such a group of individuals with type 1 diabetes of extreme duration.

In the present study we show that despite such an extreme duration of diabetes these patients have no evidence of CAD and indeed they have a lower left ventricular mass index and normal left ventricular ejection fraction which may be attributable to the optimal blood pressure and lipid profile, but not the glycemic control.

CAN is a recognised complication of DM, often present at diagnosis and is an independent predictor of morbidity and mortality (3,4). However, again despite the long duration of moderate glycemic control, in the present study the majority of cardiac parasympathetic autonomic function tests were normal. There was a borderline abnormal Valsalva ratio and RFa, suggestive of minimal parasympathetic dysfunction. However, LFa and the LFA/RFa ratio were normal indicating no evidence of cardiac sympathetic dysfunction in these patients with an extreme duration of diabetes.

Abnormal MIBG uptake has been demonstrated in both recently diagnosed and long duration type 1 diabetes (18-20). Stevens et al investigated cardiac innervation in patients with T1 diabetes with and without diabetic autonomic neuropathy (DAN), diagnosed using standard cardiovascular reflex tests (21). Using [11C]-HED PET imaging, they reported the presence of innervation defects in 40% of subjects without clinical DAN, which was characterized by distal deficits in tracer retention with preservation of the proximal myocardial segments. Whilst in subjects with severe DAN, there was evidence of proximal hyperinnervation but

normal sympathetic tone, suggesting a compensatory proximal reinnervation in response to distal neuronal loss in severe DAN. Using MIBG scintigraphy we demonstrate that global MIBG uptake and washout are comparable to healthy controls. Whilst there is a more pronounced regional heterogeneity in MIBG uptake in diabetic patients, this pattern is consistent with that observed in healthy controls. There was no difference in total and modified uptake scores on SPECT analysis, and although there was a significantly lower uptake in the inferior, basal and apical segments in the diabetic group this was similar in pattern to the control group. This regional heterogeneity in the control group is consistent with previously published data in healthy adults (22-25). The further reduction in regional uptake in our diabetic group may simply be explained by the effects of age, as they were older and the effects of age on MIBG have been previously reported (26,27). Irrespective of regional defects, HMR was comparable to healthy controls and HMR has been shown to be of prognostic significance in type 2 diabetic subjects (28). Despite almost half a century of persistent hyperglycemia these patients show no evidence of cardiac sympathetic denervation. Poor glycemic control is associated with a reduction in MIBG uptake (29), hence our findings provide further evidence of protection from complications in this unique group of patients.

A perceived weakness of the current study may be the small study population, however we have undertaken detailed structural and functional cardiac phenotyping using gold standard imaging modalities, notably CMR and MIBG scintigraphy (30). These data are also consistent with our recent detailed echocardiographic study, which also demonstrated protection from systolic dysfunction and only mild diastolic dysfunction and myocardial fibrosis in medalists (31).

In summary, type 1 diabetes patients with an extreme duration of diabetes exhibit normal global uptake and washout of MIBG and only minimal cardiac autonomic dysfunction. Further research is clearly indicated to identify the protective mechanisms in this unique group of individuals.

Acknowledgements

O.A. designed the study, wrote the manuscript, performed data analysis and researched the data. P.A. designed the imaging protocols and performed data analysis. I.A. designed the imaging protocols and processed data. S.G.R. assisted with study design and protocol. M.S. designed the CMR aspect of the study. R.A.M. reviewed and edited the manuscript, assisted with study design and was the principal investigator for the study. None of the authors had any conflict of interest. The study was funded by research grants from the NHS National Institutes for Health Research (FSF-R5-OA), NIH (R105991) and Juvenile Diabetes Research Foundation (8-2008-362).

5.6 References

1. Sun JK, Keenan HA, Cavallerano JD, Asztalos BF, Schaefer EJ, Sell DR, et al. Protection From Retinopathy and Other Complications in Patients With Type 1 Diabetes of Extreme Duration: The Joslin 50-Year Medalist Study. Diabetes Care. 2011 Mar 29;34(4):968–74.

2. Bain SC, Gill GV, Dyer PH, Jones AF, Murphy M, Jones KE, et al. Characteristics of Type 1 diabetes of over 50 years duration (the Golden Years Cohort). Diabetic Medicine. 2003 Oct;20(10):808–11.

3. Vinik AI, Ziegler D. Diabetic Cardiovascular Autonomic Neuropathy. Circulation. 2007 Jan 8;115(3):387–97.

4. Pop-Busui R, Evans GW, Gerstein HC, Fonseca V, Fleg JL, Hoogwerf BJ, et al. Effects of cardiac autonomic dysfunction on mortality risk in the Action to Control Cardiovascular Risk in Diabetes (ACCORD) trial. Diabetes Care. 2010 Jul;33(7):1578–84.

5. Boogers MJ, Borleffs CJW, Henneman MM, van Bommel RJ, van Ramshorst J, Boersma E, et al. Cardiac sympathetic denervation assessed with 123-iodine metaiodobenzylguanidine imaging predicts ventricular arrhythmias in implantable cardioverter-defibrillator patients. Journal of the American College of Cardiology. 2010 Jun 15;55(24):2769–77.

6. Carrió I, Cowie MR, Yamazaki J, Udelson J, Camici PG. Cardiac Sympathetic Imaging With mIBG in Heart Failure. JCMG. 2011 Jan 14;3(1):92–100.

7. Verberne HJ, Brewster LM, Somsen GA, van Eck-Smit BLF. Prognostic value of myocardial 123I-metaiodobenzylguanidine (MIBG) parameters in patients with heart failure: a systematic review. European Heart Journal. 2008 Mar 20;29(9):1147–59.

8. Kasama S, Toyama T, Sumino H, Nakazawa M, Matsumoto N, Sato Y, et al. Prognostic Value of Serial Cardiac 123I-MIBG Imaging in Patients with Stabilized Chronic Heart Failure and Reduced Left Ventricular Ejection Fraction. J Nucl Med. 2008 May 15;49(6):907–14.

9. Bax JJ, Kraft O, Buxton AE, Fjeld JG, Parizek P, Agostini D, et al. 123I-mIBG Scintigraphy to Predict Inducibility of Ventricular Arrhythmias on Cardiac Electrophysiology Testing: A Prospective Multicenter Pilot Study. Circulation: Cardiovascular Imaging. 2008 Sep 16;1(2):131–40.

10. Hattori N, Tamaki N, Hayashi T, Masuda I, Kudoh T, Tateno M, et al. Regional abnormality of iodine-123-MIBG in diabetic hearts. J Nucl Med. 1996 Dec;37(12):1985–90.

11. Gerson MC, Caldwell JH, Ananthasubramaniam K, Clements IP, Henzlova MJ, Amanullah A, et al. Influence of diabetes mellitus on prognostic utility of imaging of myocardial sympathetic innervation in heart failure patients. Circulation: Cardiovascular Imaging. 2011 Mar;4(2):87–93.

12. Schnell O. Cardiac sympathetic innervation and blood flow regulation of the diabetic heart. Diabetes Metab Res Rev. 2001;17(4):243–5.

13. Hattori N, Rihl J, Bengel F, Nekolla S. Cardiac autonomic dysinnervation and myocardial blood flow in long-term Type 1 diabetic patients. Diabetic Medicine. 2003;20;375-381.

14. Di Carli MF, Bianco-Batlles D, Landa ME, Kazmers A, Groehn H, Muzik O, et al. Effects of autonomic neuropathy on coronary blood flow in patients with diabetes mellitus. Circulation. 1999 Aug 24;100(8):813–9.

15. Allman KC, Stevens MJ, Wieland DM, Hutchins GD, Wolfe ER, Greene DA, et al. Noninvasive assessment of cardiac diabetic neuropathy by carbon-11 hydroxyephedrine and positron emission tomography. JAC. 1993 Nov 1;22(5):1425–32.

16. Di Carli M, Tobes M, Mangner T. Effects of cardiac sympathetic innervation on coronary blood flow. N Engl J Med 1997;336:1208-15.

17. Sacre JW, Franjic B, Jellis CL, Jenkins C, Coombes JS, Marwick TH. Association of cardiac autonomic neuropathy with subclinical myocardial dysfunction in type 2 diabetes. JACC Cardiovasc Imaging. 2010 Dec;3(12):1207–15.

18. Schnell O, Muhr D, Weiss M, Dresel S, Haslbeck M, Standl E. Reduced myocardial 123I-metaiodobenzylguanidine uptake in newly diagnosed IDDM patients. Diabetes. 1996 Jun;45(6):801–5.

19. Schnell O, Kirsch CM, Stemplinger J, Haslbeck M, Standl E. Scintigraphic evidence for cardiac sympathetic dysinnervation in long-term IDDM patients with and without ECG-based autonomic neuropathy. Diabetologia. 1995 Nov;38(11):1345–52.

20. Kreiner G, Wolzt M, Fasching P, Leitha T, Edlmayer A, Korn A, et al. Myocardial m-[123I]iodobenzylguanidine scintigraphy for the assessment of adrenergic cardiac innervation in patients with IDDM. Comparison with cardiovascular reflex tests and relationship to left ventricular function. Diabetes. 1995 May;44(5):543–9.

21. Stevens MJ, Raffel DM, Allman KC, Dayanikli F, Ficaro E, Sandford T, et al. Cardiac sympathetic dysinnervation in diabetes: implications for enhanced cardiovascular risk. Circulation. 1998 Sep 8;98(10):961–8.

22. Gill JS, Hunter GJ, Gane G, Camm AJ. Heterogeneity of the human myocardial sympathetic innervation: in vivo demonstration by iodine 123-labeled meta-iodobenzylguanidine scintigraphy. American Heart Journal. 1993 Aug 1;126(2):390–8.

23. Tsuchimochi S, Tamaki N, Tadamura E, Kawamoto M, Fujita T, Yonekura Y, et al. Age and gender differences in normal myocardial adrenergic neuronal function evaluated by iodine-123-MIBG imaging. J Nucl Med. 1995 Jun;36(6):969–74.

24. Somsen GA, Verberne HJ, Fleury E, Righetti A. Normal values and within-subject variability of cardiac I-123 MIBG scintigraphy in healthy individuals: implications for clinical studies. J Nucl Cardiol. 2004 Feb;11(2):126–33.

25. Morozumi T, Kusuoka H, Fukuchi K. Myocardial iodine-123-metaiodobenzylguanidine images and autonomic nerve activity in normal subjects. Journal of Nuclear Medicine 38; 49-52.

26. Sakata K, Iida K, Mochizuki N, Ito M, Nakaya Y. Physiological changes in human cardiac sympathetic innervation and activity assessed by (123)I-metaiodobenzylguanidine (MIGB) imaging. Circ J. 2009 Feb;73(2):310–5.

27. Sakata K, Shirotani M, Yoshida H, Kurata C. Physiological fluctuation of the human left ventricle sympathetic nervous system assessed by iodine-123-MIBG. J Nucl Med. 2014 Oct 28;39(10):1667–71.

28. Nagamachi S, Fujita S, Nishii R, Futami S, Tamura S, Mizuta M, et al. Prognostic value of cardiac I-123 metaiodobenzylguanidine imaging in patients with non–insulin-dependent diabetes mellitus. J Nucl Cardiol. 2006 Jan;13(1):34–42.

29. Ziegler D, Weise F, Langen KJ, Piolot R, Boy C, Hübinger A, et al. Effect of glycaemic control on myocardial sympathetic innervation assessed by [123I]metaiodobenzylguanidine scintigraphy: a 4-year prospective study in IDDM patients. Diabetologia. 1998 Apr;41(4):443–51.

30. Flotats A, Carrió I, Agostini D, Guludec D, Marcassa C, Schaffers M, et al. Proposal for standardization of 123I-metaiodobenzylguanidine (MIBG) cardiac sympathetic imaging by the EANM Cardiovascular Committee and the European Council of Nuclear Cardiology. Eur J Nucl Med Mol Imaging. 2010 Jun 25;37(9):1802–12.

31. Fagan A, Asghar O, Pearce K, Stout M, Ray SG, Schmitt M, et al. Medalists With Extreme Duration of Type 1 Diabetes Exhibit Only Mild Diastolic Dysfunction and Myocardial Fibrosis. Diabetes Care. 2015 ed. 38:e1–e2.

	CONTROL	DIABETES	P
Age (Years)	51.5±5.4	61.9±7.3	0.006
Diabetes Duration (years)	-	48.3±5.4	-
BMI (Kg/m^2)	27.0±3.1	28.2±4.4	0.417
Systolic BP (mm Hg)	118±11	120±15	0.045
Diastolic BP (mm Hg)	72±10	61±14	0.021
HbA1c (%/mmol/mol)	5.8±0.4/40±4	8.3±0.9/67±10	<0.001
Total Chol (mmol/l)	5.0±0.9	4.6±1.2	0.150
LDLc (mmol/l)	2.8±0.8	2.1±1.1	0.048
HDLc (mmol/l)	1.5±0.5	1.9±0.8	0.210
Triglyceride (mmol/l)	1.1±0.5	0.9±0.5	0.285
eGFR (ml/kg/min)	81.0±9.0	73.0±20.0	0.454
LVMI (g/m^2)	51.1±10.7	41±6.4	0.007
LVEF (%)	61.0±6.4	63.1±6.9	0.425
HR	65±11	74±12	0.124
E/I ratio	1.2±0.1	1.2±0.2	0.109
Valsalva ratio	1.4±0.2	1.2±0.2	0.009
30:15 ratio	0.9±0.5	1.1±0.3	0.781
LFa	1.2±1.3	0.8±1.3	0.705
RFa	1.1±1.0	0.5±0.9	0.028
LFa/RFa	2.3±2.7	2.5±2.2	0.975
Early HMR	1.67±0.13	1.67±0.18	0.987
Late HMR	1.73±0.16	1.61±0.22	0.105
Washout Rate (%)	19.1±7.6	22.0±6.9	0.302
Total Segmental Score	30.5±5.2	38.9±9.0	0.006
Modified Segmental Score	14.1±3.0	16.6±4.5	0.104
Inferior Wall Score	9.2±1.4	6.6±3.1	0.009
Apical Score	15.8±2.7	11.5±4.1	0.003
Basal Score	18.9±1.8	17.1±2.4	0.041
Anterior Wall Score	10.2±1.3	9.6±1.5	0.23

Table 5-1 Clinical characteristics, CMR and MIBG parameters characteristics of study subjects. (Data are expressed as Mean ± SD).

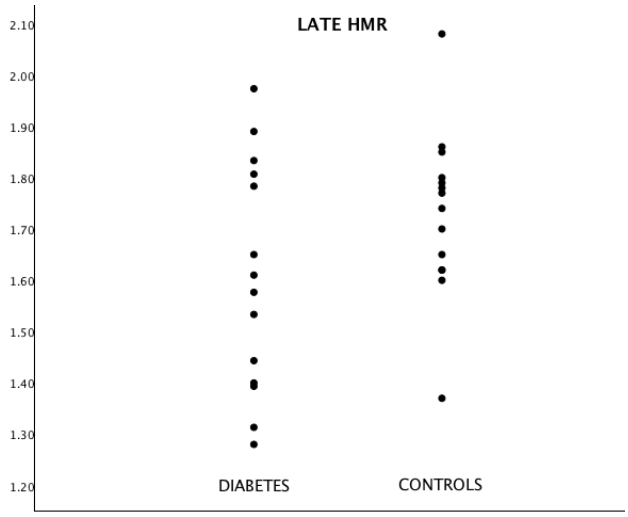

Figure 5-1 Scatter plot of late HMR in Diabetic subjects and Controls.

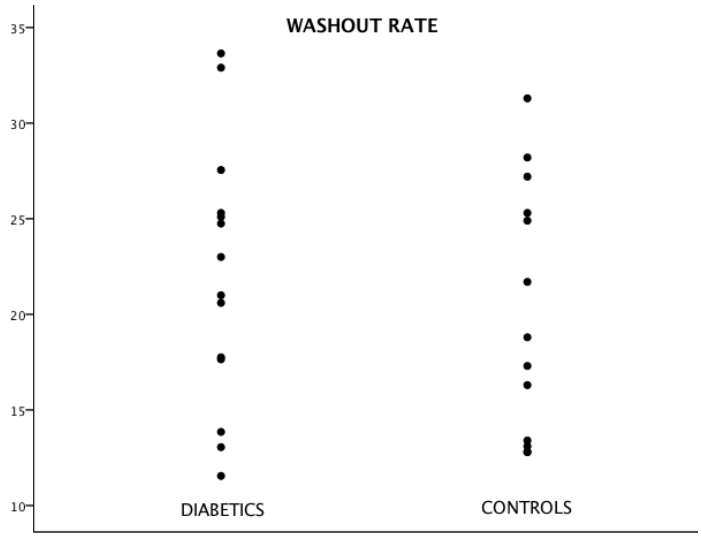

Figure 5-2 Scatter plot of WR in Diabetic Subjects and Controls.

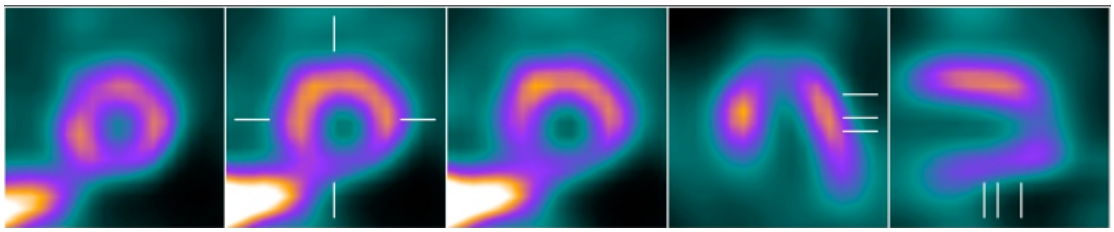

A

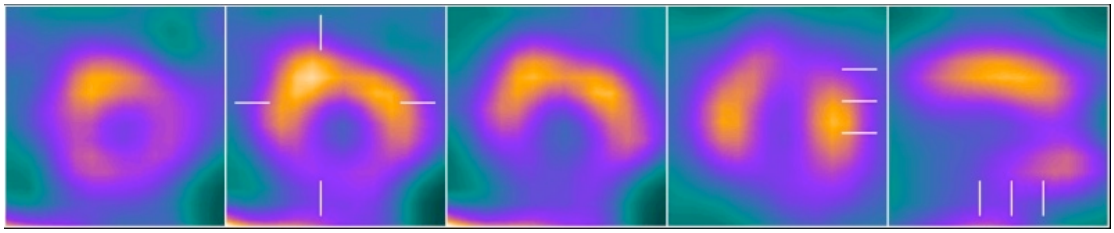

B

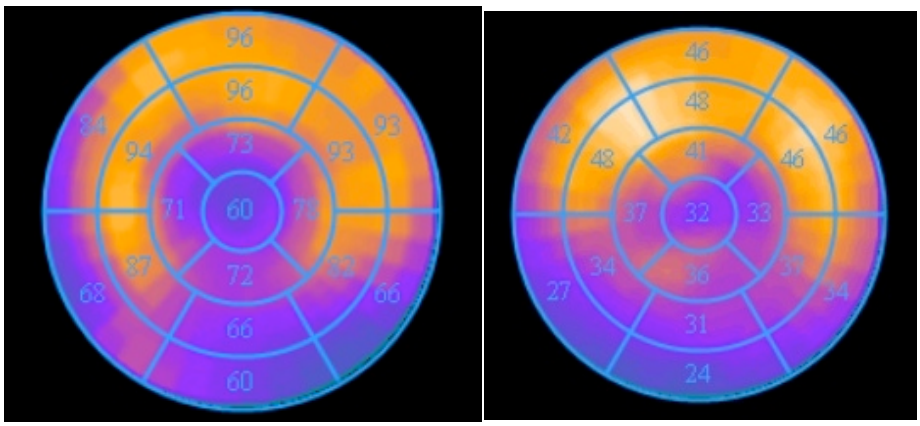

C D

Figure 5-3 SPECT reconstructed images and bull's eye plots of a control subject with a normal innervation pattern (A and C) and a subject with diabetes of extreme duration (B and D). Note the exaggerated reduction in tracer uptake in the apical, inferior and basal segments in the diabetic subject (late HMR 1.58).

6 Cardiac Magnetic Resonance Imaging Demonstrates Normal Cardiac Structure and Function and Myocardial Perfusion in Subjects with Impaired Glucose Tolerance.

Omar Asghar, Christopher Miller, Simon Ray, Matthias Schmitt and Rayaz Malik.

Contribution: Omar Asghar contributed to study concept and design, patient recruitment, data analysis, statistics and was the sole author of this chapter. The CMR methodology and analyses were the work of Christopher Miller.

6.1 Abstract

Background: Impaired glucose tolerance (IGT), a precursor to type 2 diabetes (T2DM), is considered to carry an adverse cardiovascular risk. Previous echocardiographic studies have reported structural and functional cardiac abnormalities in subjects with IGT. However no studies to date have used CMR to undertake detailed cardiovascular phenotyping in these subjects.

Methods and Results: Multiparametric CMR was undertaken in 18 subjects with IGT and 14 healthy age matched controls to quantify left ventricular mass, volumes and function, myocardial blood flow (MBF) at rest and during pharmacological stress, deformation and fibrosis. There were no differences in LVEF (61.1±5.4 vs 61.0±6.4 %, p=0.96), LVMI (51.1±10.7 vs 47.6±8.8 g/m2, P=0.32) or ECV (0.26±0.05 vs 0.27±0.05 %, P=0.63) between IGT and controls. Resting (0.83±0.16 vs 0.75±0.17 ml/min/g, P=0.17) and stress (2.02±0.48 vs 2.07±0.42 ml/min/g, P=0.76) MBF and perfusion ratio (rest/stress) (2.43±0.45 vs 2.81±0.47 ml/min/g, P=0.12) did not differ between subjects with IGT and controls. Radial (-34.3±11.6 vs -36.2±17.7, P=0.73), circumferential (-22.3±2.6 vs -21.7±6.2, P=0.74) and longitudinal (-16.0±10.8 vs -19.6±3.6, P=0.20) strain, and extra cellular volume (ECV) were comparable (0.26±0.05 vs 0.27±0.05 %, p=0.63) in both groups.

Conclusion: Subjects with IGT exhibit normal cardiac structure and function with no evidence of fibrosis or an abnormality of myocardial microvascular perfusion, when assessed using comprehensive multiparametric CMR imaging.

6.2 Introduction

Diabetes mellitus (DM) is a strong independent predictor of heart failure (HF) (1). Furthermore, glycemia and insulin resistance are both predictive of incident HF, independent of diabetes status (2-4). Such evidence supports the paradigm for the existence of a distinct cardiomyopathy specific to DM (5,6). The pathophysiological substrate of diabetic cardiomyopathy (DC) involves metabolic derangement, neurohormonal activation, and microvascular inflammation (7,8) which leads to cardiomyocyte hypertrophy, diffuse interstitial and perivascular fibrosis (5,9,10). The functional manifestations of cardiac remodeling in DC begin with diastolic dysfunction and progress to systolic dysfunction and HF.

Impaired glucose tolerance (IGT) is a clinically silent, altered state of glycemia and a precursor to type 2 DM (T2DM) (11). Epidemiological data suggest that IGT may be an independent predictor of cardiovascular (CV) morbidity and mortality (12-14). This increased risk may be attributable to the early development of cardiovascular disease (CVD) in subjects with IGT, although the exact time of onset and risk factors are unknown (15).

Relatively few studies have assessed cardiac structure and function in IGT. Of these, the majority employed 2D echocardiography as the imaging modality (16-19). More advanced echocardiographic techniques such as tissue Doppler imaging (TDI) and speckle tracking echocardiography (STE) have enabled the assessment of left ventricular torsion, long axis, radial and circumferential deformation and hence the detection of early, sub-clinical cardiac dysfunction (20). However, cardiac magnetic resonance (CMR) is the gold standard modality for cardiac imaging and assessment and unlike echocardiography, is not limited by geometric assumptions, operator or patient factors and provides high spatial and temporal resolution with excellent reproducibility. This is particularly useful in the research setting whereby it

substantially reduces the sample sizes required in order to detect true clinical differences (21). The applications of CMR are rapidly expanding and allow for multiparametic assessment of the heart including volumetric analysis (22), diastology (1,23), deformation (24-26), myocardial blood flow (27), tissue characterization and fibrosis (28) and inflammation (29). The only detailed CMR study to date evaluated patients with T2DM and showed decreases in peak filling rate, mitral peak E velocities and peak E velocity to peak A velocity ratios, with further worsening in those with coronary atherosclerosis (30).

To date, there are no CMR studies in subjects with IGT. We have therefore undertaken a comprehensive multiparametric CMR imaging study to quantify myocardial blood flow (MBF), volumetrics, deformation and fibrosis in a cohort of subjects with IGT and healthy controls.

6.3 Methods

6.3.1 Study Population

We recruited 18 adult subjects with IGT from our institution and 15 age and sex matched healthy control subjects. Exclusion criteria included any history of cardiac disease, severe systemic disease, peripheral vascular disease, chronic kidney disease (eGFR $\leq$35 mls/min/1.73m2) and any contraindication to CMR imaging. Participants with a contraindication to adenosine were excluded from the perfusion assessment part of the study. The study was approved by the Central Manchester Research and Ethics committee and written informed consent was obtained from all participants, according to the declaration of Helsinki.

6.3.2 Clinical and Metabolic Assessment

Clinical assessment included medical history, clinical examination and resting 12 lead ECG. All study participants underwent a repeat oral glucose tolerance test (OGTT) on induction to the study, to confirm glycemic status. Renal function, HbA1c, lipids, blood count and haematocrit were assessed. All participants were instructed to abstain from caffeine intake for a minimum of 12 hours prior to CMR imaging.

6.3.3 CMR Protocol

Details of our imaging and analysis protocols have been previously described (22,24,31,32).

Image Acquisition

CMR was performed using a 1.5T scanner (Avanto; Siemens Healthcare, Germany) equipped with a 32 element phased array coil. Steady-state free precession cine images were acquired in standard long axis views and a short axis stack covering the left ventricle (LV). Tagged short axis images at the LV base, mid cavity and apex were acquired using a segmented k-space fast gradient echo sequence with spatial modulation of magnetization in orthogonal planes. MBF was assessed during pharmacological (vasodilator) stress with intravenous adenosine (140 μg/kg/min) via a large peripheral vein for 3-minutes prior to, and during, data acquisition. A 0.05 mmol/Kg bolus of gadolinium-based contrast agent (gadopentetate dimeglumine; Gd-DTPA; Magnevist; Bayer Healthcare, Germany) was administered intravenously at 5ml/s followed by a 30 ml saline flush. Rest imaging was performed 10 minutes after stress imaging with a further 0.05 mmol/Kg bolus of contrast agent. Following rest imaging, a further 0.1 mmol/Kg of contrast agent was administered (top-up). A short axis, single-shot modified Look Locker inversion recovery (MOLLI) sequence was acquired at mid ventricular level pre and 15 minutes post contrast top-up. Standard late gadolinium

enhancement (LGE) imaging was performed at least 10 minutes following the top-up of contrast with spoiled gradient echo segmented inversion recovery and phased sensitive inversion recovery segmented gradient echo sequences.

CMR Image Analysis

Off line image analysis was carried out by a cardiology research fellow (OA) under the supervision of an experienced operator (CM), blinded to clinical information. Left ventricular (LV) mass, volumes and ejection fraction (EF) were derived from SSFP images using CMRtools (Cardiovascular Imaging Solutions, London, UK) and our previously described methods (22). Peak systolic circumferential strain and strain rate were calculated from tagged mid cavity short axis slices using InTag (CREATIS; Université de Lyon, France) (20,24). We also used 2D Cardiac Performance Analysis MR (TomTec Imaging Systems GmbH, Munich, Germany) to derive longitudinal, radial and circumferential strain and strain rate. For T1 relaxation time measurements and MBF quantification, we used Osirix Imaging Software (Pixmeo; Switzerland) to trace epicardial and endocardial borders, draw a region of interest in the blood pool and to identify the right ventricular insertion point (27,32). Extracellular volume fraction (ECV) was quantified to provide a measure of myocardial fibrosis.

6.4 Statistical Analysis

SPSS Statistics for Mac version 20 (IBM corporation, New York USA) was used for all statistical analysis. All data are expressed as mean ± standard deviation (SD) and the Shapiro-Wilk test was used to determine normality of data. The unpaired T test was used to compare normally distributed data between groups and the Mann Whitney U test was used for non-parametric data. A two-tailed P-value of less than 0.05 was considered statistically significant.

6.5 Results

18 subjects with IGT (11 males, 7 females) and 15 healthy controls (10 males, 5 females) were assessed. In the control group, one subject was found to be in atrial flutter on ECG and therefore underwent volumetric analysis only. In the IGT group, 2 subjects had a contraindication to adenosine and did not undergo MBF assessment. We were unable to assess MBF in a further 2 IGT subjects due to problems with image post processing, therefore 4 IGT subjects were excluded from MBF assessment. Qualitative analysis of rest and stress perfusion was normal in all subjects.

6.5.1 Baseline characteristics

Both groups were matched for age (54.6±5.4 vs 56.8±9.2 years, P=0.45). Subjects with IGT had a significantly greater BMI (32.5±6.5 vs 27.0±3.1 Kg/m2, P<0.05), triglycerides (2.0±1.0 vs 1.1±0.5 mmol/l, P<0.05) and lower HDL cholesterol (1.2±0.4 vs 1.6±0.4 mmol/l, P<0.05) with no difference in systolic BP (118±11 vs 126±12 mmHg, P=0.08), HbA1c (5.7±0.4 vs 5.8±0.4%, P=0.46), total cholesterol (5.0±0.74 vs 4.7±1.4 mmol/l, P=0.49) or LDLc (2.9±0.6 vs 2.8±1.1 mmol/l, P=0.96) (Table 1).

6.5.2 CMR Data

There were no differences in left ventricular ejection fraction (LVEF) (61.1±5.4 vs 61.0±6.4 %, P=0.96) or left ventricular mass, indexed to body surface area (BSA) (51.1±10.7 vs 47.6±8.8 g/m2, P=0.32), height1.7 (39.7±7.3 vs 40.1±6.0 g/m2, P=0.878) and Ht2.7 (22.9±3.7 vs 23.5±3 g/m2, P=0.682) between the two groups. Concentricity index was similar in both groups (0.59±0.13 vs 0.58±0.11, P=0.744) (Table 2).

T1 Mapping

ECV was comparable in both groups (0.26±0.05 vs 0.27±0.05 %, P=0.63) (Table 2). There was no evidence of LGE in any of the subjects.

Myocardial Blood Flow

There were no differences in resting MBF (0.83±0.16 vs 0.75±0.17 ml/min/g, P=0.17), stress MBF (2.02±0.48 vs 2.07±0.42 ml/min/g, P=0.76) or perfusion ratio (rest/stress) (2.43±0.45 vs 2.81±0.47 ml/min/g, P=0.12) between subjects with IGT and controls (Table 3).

Myocardial Deformation

There were no differences in radial (-34.3±11.6 vs -36.2±17.7, P=0.73), circumferential (-22.3±2.6 vs -21.7±6.2, P=0.74) or longitudinal (-16.0±10.8 vs -19.6±3.6, P=0.20) strain between the IGT and control groups when assessed using either method (Table 4).

6.6 Discussion

CMR data on cardiac structure and function in IGT are limited. Several population-based echocardiographic studies have reported increased LVM in subjects with IGT. In the Framingham Heart Study, LVM and wall thickness (LVWT) increased with worsening glucose tolerance and were more pronounced in female participants free of CVD (16). Similarly, in the Hoorn study, LVM was associated with glycemic status only in females with IGT (17). The Strong Heart Study (SHS) also reported increased LVM and LVWT in American Indians with IGT (18). Although, LVMI was found to be abnormal in subjects with normal glucose tolerance, this was accounted for by obesity and hypertension, particularly in Afrocaribbean's (19). In the current study, LVEF, LVMI and concentricity were comparable between subjects with IGT and healthy age matched controls. This challenges the findings of

the Multi Ethnic Study of Atherosclerosis (MESA) and the Framingham Offspring cohort study, where CMR showed an association between LV mass and glycemic indices in subjects with impaired fasting glucose (IFG) and DM (33,34). However, in these studies the methodology for deriving LVM and volumes was subject to a number of limitations as using short axis slices alone presents difficulty in determining the true basal LV slice, end-diastole and end-systole. Furthermore, it is not clear whether their analyses included papillary muscles and trabeculae in their cavity volumes rather than within the mass. We have used validated 3D modeling methods for volumetric and structural analysis which provides accurate and reproducible measurement of LV mass and volumes (22). Furthermore, we used 3 different methods to calculate LVMI, to adjust for the increased BMI in our IGT group and are therefore confident that our data are robust and meaningful.

Diastolic dysfunction is one of the earliest detectable cardiac functional abnormalities and is characterized by a reduction in longitudinal and radial myocardial deformation and an increase in LV torsion (20). TDI and STE techniques are recent developments in echocardiography which allow for load independent assessment of diastolic function by means of measuring long axis, circumferential and radial function (20). Using TDI, it is possible to perform accurate tracking of myocardial tissue displacement and the measurement of regional velocity and strain (20). STE tracks myocardial speckles and can be utilized to assess longitudinal, radial and circumferential myocardial deformation in addition to torsion (20). Long axis function was shown to be reduced both at rest and during exercise in diabetic subjects without evidence of ischemic heart disease (35,36). Studies using STE in diabetic subjects have reported impaired longitudinal but preserved radial and circumferential contraction in asymptomatic males with T2DM free of CVD (37). Asymptomatic patients with T2DM have demonstrated significant reductions in circumferential, radial and longitudinal function, compared with age-matched controls (38). Sacre et al reported an

association between CAN and regional impairment of left ventricular diastolic function on CMR, which corresponded with areas of dysinnervation on MIBG scintigraphy in subjects with T2DM (39). To date, studies in IGT cohorts have been limited by relatively insensitive measures of diastolic dysfunction (40-43). Larghat et al assessed LV structure and function using CMR in subjects with T2DM, pre-diabetes (defined by FPG and HbA1c) and healthy age matched control subjects who underwent coronary angiography for investigation of chest pain (44). They reported differences in LV mass, torsion angle and myocardial perfusion reserve in the T2DM group compared with healthy controls but no differences were found between diabetic and pre-diabetic subjects. In young adults [mean age 31.8(6.6) years] with a short duration of T2DM [4.7(4.0) years], CMR has shown preserved cardiac volumes and function and normal circumferential strain and myocardial perfusion reserve with no evidence of myocardial fibrosis when compared to BMI matched controls (45). The data in the current study is similar as it shows no differences in radial, circumferential and longitudinal strain and strain rates between subjects with IGT and healthy controls.

Coronary microvascular dysfunction is a feature of pre-diabetes and insulin resistance (46). Quantitative CMR assessment of MBF is an emerging technology which shows much promise and is an attractive validated alternative to positron emission tomography (PET) in the assessment of microvascular dysfunction (27). To date, there are no published studies of CMR MBF in subjects with T2DM or IGT. We report normal resting and stress MBF in subjects with IGT indicating that these individuals do not have evidence of myocardial microvascular disease.

Although extensively studied in animal models of DM, the need for endomyocardial biopsy has limited the study of myocardial fibrosis in man (10). Fischer et al demonstrated interstitial fibrosis in myocardial biopsy, but did not differentiate subjects with IGT from

those with diabetes (47). Integrated back scatter assessment has been used to show myocardial fibrosis in subjects with T2DM and metabolic syndrome (48-50). T1 mapping has been utilised to demonstrate fibrosis associated with impaired systolic and diastolic function and biomarkers of fibrosis in patients with type 1 and 2 diabetes (51-53). Quantitative assessment of myocardial extracellular volume (ECV), a surrogate of myocardial fibrosis, shows much promise and has been recently validated in man (32,54,55). In the only such study published to date, diabetic subjects showed ECV expansion (56). In the present study we show no differences in ECV between subjects with IGT and healthy controls, suggesting that this may be a late abnormality.

We conclude that subjects with IGT exhibit a normal structural and functional cardiac phenotype with no evidence of fibrosis or microvascular disease when assessed by detailed and comprehensive multiparametric CMR. Whilst these data conflict with existing data in subjects with IGT, these studies used echocardiography, which is clearly less sensitive than CMR. Longitudinal studies with larger study populations are required to establish if and when individuals with IGT develop the early pathognomonic features of diabetic cardiomyopathy and how these changes progress with glycaemic status.

Sources of Funding

This study was funded by research grants from the NHS National Institutes for Health Research (FSF-R5-OA), NIH (R105991) and Juvenile Diabetes Research Foundation (8-2008-362).

Disclosures

None.

6.7 References

1. From AM, Scott CG, Chen HH. The development of heart failure in patients with diabetes mellitus and pre-clinical diastolic dysfunction a population-based study. Journal of the American College of Cardiology. 2010 Jan 26;55(4):300–5.

2. Held C, Gerstein HC, Yusuf S, Zhao F, Hilbrich L, Anderson C, et al. Glucose levels predict hospitalization for congestive heart failure in patients at high cardiovascular risk. Circulation. 2007 Mar 20;115(11):1371–5.

3. Arnlöv J, Lind L, Sundström J, Andrén B, Vessby B, Lithell H. Insulin resistance, dietary fat intake and blood pressure predict left ventricular diastolic function 20 years later. Nutr Metab Cardiovasc Dis. 2005 Aug;15(4):242–9.

4. Arnlöv J, Lind L, Zethelius B, Andrén B, Hales CN, Vessby B, et al. Several factors associated with the insulin resistance syndrome are predictors of left ventricular systolic dysfunction in a male population after 20 years of follow-up. American Heart Journal. 2001 Oct;142(4):720–4.

5. Asghar O, Al-Sunni A, Khavandi K, Khavandi A, Withers S, Greenstein A, et al. Diabetic cardiomyopathy. Clinical Science. 2009 May;116(10):741–60.

6. Witteles R, Fowler M. Insulin-Resistant Cardiomyopathy:: Clinical Evidence, Mechanisms, and Treatment Options. Journal of the American College of Cardiology. 2008;51(2):93–102.

7. Bell D. Diabetic cardiomyopathy. Diabetes Care. 2003;26(10):2949.

8. Horwich TB, Fonarow GC. Glucose, Obesity, Metabolic Syndrome, and Diabetes. JAC. Elsevier Inc; 2010 Jan 26;55(4):283–93.

9. van Heerebeek L, Hamdani N, Handoko ML, Falcao-Pires I, Musters RJ, Kupreishvili K, et al. Diastolic Stiffness of the Failing Diabetic Heart: Importance of Fibrosis, Advanced Glycation End Products, and Myocyte Resting Tension. Circulation. 2008 Jan 1;117(1):43–51.

10. Asbun J, Villarreal F. The pathogenesis of myocardial fibrosis in the setting of diabetic cardiomyopathy. Journal of the American College of Cardiology. 2006;47(4):693–700.

11. Tabák AG, Herder C, Rathmann W et al. Prediabetes: a high-risk state for diabetes development. The Lancet. Elsevier Ltd; 2012 Jun 16;379(9833):2279–90.

12. Coutinho M, Gerstein HC, Wang Y, Yusuf S. The relationship between glucose and incident cardiovascular events. A metaregression analysis of published data from 20 studies of 95,783 individuals followed for 12.4 years. Diabetes Care. 1999 Feb;22(2):233–40.

13. Levitan EB, Song Y, Ford ES, Liu S. Is Nondiabetic Hyperglycemia a Risk Factor for Cardiovascular Disease?: A Meta-analysis of Prospective Studies. Archives of internal medicine. American Medical Association; 2004 Oct 25;164(19):2147–55.

14. Ford ES, Zhao G, Li C. Pre-Diabetes and the Risk for Cardiovascular Disease. JAC. 2031 Feb 13;55(13):1310–7.

15. De Marco M, de Simone G, Roman MJ, Chinali M, Lee ET, Calhoun D, et al. Cardiac Geometry and Function in Diabetic or Prediabetic Adolescents and Young Adults: The Strong Heart Study. Diabetes Care. 2011 Sep 23;34(10):2300–5.

16. Rutter MK. Impact of Glucose Intolerance and Insulin Resistance on Cardiac Structure and Function: Sex-Related Differences in the Framingham Heart Study. Circulation. 2003 Jan 28;107(3):448–54.

17. Henry R, Kamp O, Kostense P, Spijkerman A, Dekker J, van Eijck R, et al. Left ventricular mass increases with deteriorating glucose tolerance, especially in women: independence of increased arterial stiffness or decreased flow-mediated dilation. Diabetes Care. 2004;27(2):522.

18. Ilercil A. Relationship of impaired glucose tolerance to left ventricular structure and function: The Strong Heart Study. American Heart Journal. 2001 Jun 1;141(6):992–8.

19. Chaturvedi N. A comparison of left ventricular abnormalities associated with glucose intolerance in African Caribbeans and Europeans in the UK. Heart. 2001 Jun 1;85(6):643–8.

20. Oh JK, Park SJ, Nagueh SF. Established and Novel Clinical Applications of Diastolic Function Assessment by Echocardiography. Circulation: Cardiovascular Imaging. 2011 Jul 19;4(4):444–55.

21. Keenan NG, Pennell DJ. CMR of Ventricular Function. Echocardiography. 2007 Feb;24(2):185–93.

22. Miller CA, Jordan P, Borg A, Argyle R, Clark D, Pearce K, et al. Quantification of left ventricular indices from SSFP cine imaging: Impact of real-world variability in analysis methodology and utility of geometric modeling. J Magn Reson Imaging. 2012 Nov 2;37(5):1213–22.

23. Paelinck B, Lamb H. Assessment of Diastolic Function by Cardiac MRI. Cardiovascular Magnetic Resonance Imaging. 2008;:415–28.

24. Miller CA, Borg A, Clark D, Steadman CD, McCann GP, Clarysse P, et al. Comparison of local sine wave modeling with harmonic phase analysis for the assessment of myocardial strain. J Magn Reson Imaging. 2012 Dec 12;38(2):320–8.

25. Young AA, Cowan BR. Evaluation of left ventricular torsion by cardiovascular magnetic resonance. J Cardiovasc Magn Reson. 2012;14:49.

26. Götte M, Germans T, Rüssel I, Zwanenburg J, Marcus J, van Rossum A, et al. Myocardial Strain and Torsion Quantified by Cardiovascular Magnetic Resonance Tissue Tagging: Studies in Normal and Impaired Left Ventricular Function. Journal of the American College of Cardiology. 2006;48(10):2002–11.

27. Miller CA, Naish JH, Ainslie MP, Tonge C, Tout D, Arumugam P, et al. Voxel-wise quantification of myocardial blood flow with cardiovascular magnetic resonance: effect of variations in methodology and validation with positron emission tomography. Journal of Cardiovascular Magnetic Resonance. Journal of Cardiovascular Magnetic Resonance; 2014 Jan 24;16(1):1–15.

28. Won S, Davies-Venn C, Liu S, Bluemke DA. Noninvasive imaging of myocardial extracellular matrix for assessment of fibrosis. Current Opinion in Cardiology. 2013 May;28(3):282–9.

29. Baksi AJ, Pennell DJ. T2* imaging of the heart: methods, applications, and outcomes. Top Magn Reson Imaging. 2014 Feb;23(1):13–20.

30. Graça B, Donato P, Ferreira MJ, Castelo-Branco M, Caseiro-Alves F. Left Ventricular Diastolic Function in Type 2 Diabetes Mellitus and the Association With Coronary Artery Calcium Score: A Cardiac MRI Study. American Journal of Roentgenology. 2014 Jun;202(6):1207–14.

31. Miller CA, Naish JH, Shaw SM, Yonan N, Williams SG, Clark D, et al. Multiparametric cardiovascular magnetic resonance surveillance of acute cardiac allograft rejection and characterisation of transplantation-associated myocardial injury: a pilot study. 2014 Jul 20;:1–11.

32. Miller CA, Naish JH, Bishop P, Coutts G, Clark D, Zhao S, et al. Comprehensive Validation of Cardiovascular Magnetic Resonance Techniques for the Assessment of Myocardial Extracellular Volume. Circulation: Cardiovascular Imaging. 2013 May 21;6(3):373–83.

33. Bertoni A, Goff D, D Agostino R, Liu K, Hundley W, Lima J, et al. Diabetic Cardiomyopathy and Subclinical Cardiovascular Disease. Diabetes Care. 2006;29(3):588.

34. Velagaleti RS, Gona P, Chuang ML, Salton CJ, Fox CS, Blease SJ, et al. Relations of Insulin Resistance and Glycemic Abnormalities to Cardiovascular Magnetic Resonance Measures of Cardiac Structure and Function: The Framingham Heart Study. Circulation: Cardiovascular Imaging. 2010 May 1;3(3):257–63.

35. Ha J-W, Lee H-C, Kang E-S, Ahn C-M, Kim J-M, Ahn J-A, et al. Abnormal left ventricular longitudinal functional reserve in patients with diabetes mellitus: implication for detecting subclinical myocardial dysfunction using exercise tissue Doppler echocardiography. Heart. 2007 Dec;93(12):1571–6.

36. Fang Z, Najos-Valencia O, Leano R, Marwick T. Patients with early diabetic heart disease demonstrate a normal myocardial response to dobutamine* 1. Journal of the American College of Cardiology. 2003;42(3):446–53.

37. Ng ACT, Delgado V, Bertini M, Meer RWVD, Rijzewijk LJ, Shanks M, et al. Findings from Left Ventricular Strain and Strain Rate Imaging in Asymptomatic Patients With Type 2 Diabetes Mellitus. AJC. 2009 Jan 11;104(10):1398–401.

38. Nakai H, Takeuchi M, Nishikage T, Lang RM, Otsuji Y. Subclinical left ventricular dysfunction in asymptomatic diabetic patients assessed by two-dimensional speckle tracking echocardiography: correlation with diabetic duration. European Journal of Echocardiography. 2009 Dec 1;10(8):926–32.

39. Sacre JW, Franjic B, Jellis CL, Jenkins C, Coombes JS, Marwick TH. Association of cardiac autonomic neuropathy with subclinical myocardial dysfunction in type 2 diabetes. JACC Cardiovasc Imaging. 2010 Dec;3(12):1207–15.

40. Henry R, Paulus W, Kamp O, Kostense P, Spijkerman A, Dekker J, et al. Deteriorating glucose tolerance status is associated with left ventricular dysfunction-the Hoorn Study. Neth J Med. 2008;66:110–7.

41. Okura H, Inoue H, Tomon M, Nishiyama S, Yoshikawa T, Yoshida K, et al. Impaired glucose tolerance as a determinant of early deterioration of left ventricular diastolic function in middle-aged healthy subjects. The American Journal of Cardiology. 2000;85(6):790.

42. Fujita M, Asanuma H, Kim J, Liao Y, Hirata A, Tsukamoto O, et al. Impaired glucose tolerance: a possible contributor to left ventricular hypertrophy and diastolic dysfunction. International Journal of Cardiology. 2007 May 16;118(1):76–80.

43. Shimabukuro M, Higa N, Asahi T, Yamakawa K, Oshiro Y, Higa M, et al. Impaired glucose tolerance, but not impaired fasting glucose, underlies left ventricular diastolic dysfunction. Diabetes Care. 2011 Mar;34(3):686–90.

44. Larghat AM, Swoboda PP, Biglands JD, Kearney MT, Greenwood JP, Plein S. The microvascular effects of insulin resistance and diabetes on cardiac structure, function, and perfusion: a cardiovascular magnetic resonance study. European Heart Journal - Cardiovascular Imaging [Internet]. 2014 Aug 12.

45. Khan JN, Wilmot EG, Leggate M, Singh A, Yates T, Nimmo M, et al. Subclinical diastolic dysfunction in young adults with Type 2 diabetes mellitus: a multiparametric contrast-enhanced cardiovascular magnetic resonance pilot study assessing potential mechanisms. European Heart Journal - Cardiovascular Imaging. 2014 Oct 24;15(11):1263–9.

46. Schelbert HR. Coronary Circulatory Function Abnormalities in Insulin Resistance. JAC. American College of Cardiology Foundation; 2009 Feb 3;53(5):S3–S8.

47. Fischer VW, Fischer VW, Fischer VW, Fischer VW, Barner HB, Barner HB, et al. Pathomorphologic aspects of muscular tissue in diabetes mellitus. Human pathology [Internet]. 1984 Dec;15(12):1127–36.

48. Fang Z, Yuda S, Anderson V, Short L, Case C, Marwick T. Echocardiographic detection of early diabetic myocardial disease* 1. Journal of the American College of Cardiology. 2003;41(4):611–7.

49. Kosmala W, Przewlocka-Kosmala M, Szczepanik-Osadnik H, Mysiak A, O'Moore-Sullivan T, Marwick TH. A Randomized Study of the Beneficial Effects of Aldosterone Antagonism on LV Function, Structure, and Fibrosis Markers in Metabolic Syndrome. JCMG. Elsevier Inc; 2011 Dec 1;4(12):1239–49.

50. Marwick TH, Raman SV, Carrió I, Bax JJ. Recent Developments in Heart Failure Imaging. JCMG. 2011 Jan 14;3(4):429–39.

51. Ng ACT, Auger D, Delgado V, van Elderen SGC, Bertini M, Siebelink HM, et al. Association Between Diffuse Myocardial Fibrosis by Cardiac Magnetic Resonance Contrast-Enhanced T1 Mapping and Subclinical Myocardial Dysfunction in Diabetic Patients: A Pilot Study. Circulation: Cardiovascular Imaging. 2012 Jan 17;5(1):51–9.

52. Jellis C, Wright J, Kennedy D, Sacre J, Jenkins C, Haluska B, et al. Association of Imaging Markers of Myocardial Fibrosis with Metabolic and Functional Disturbances in Early Diabetic Cardiomyopathy. Circulation: Cardiovascular Imaging. 2011 Sep 23.

53. Messroghli DR, Radjenovic A, Kozerke S, Higgins DM, Sivananthan MU, Ridgway JP. Modified Look-Locker inversion recovery (MOLLI) for high-resolutionT1 mapping of the heart. Magn Reson Med. 2004;52(1):141–6.

54. Flett AS, Hayward MP, Ashworth MT, Hansen MS, Taylor AM, Elliott PM, et al. Equilibrium Contrast Cardiovascular Magnetic Resonance for the Measurement of Diffuse Myocardial Fibrosis: Preliminary Validation in Humans. Circulation. 2010 Jul 12;122(2):138–44.

55. Aus dem Siepen F, Buss SJ, Messroghli D, Andre F, Lossnitzer D, Seitz S, et al. T1 mapping in dilated cardiomyopathy with cardiac magnetic resonance: quantification of diffuse myocardial fibrosis and comparison with endomyocardial biopsy. European Heart Journal - Cardiovascular Imaging. 2014 Sep 22.

56. Wong TC, Piehler KM, Kang IA, Kadakkal A, Kellman P, Schwartzman DS, et al. Myocardial extracellular volume fraction quantified by cardiovascular magnetic resonance is increased in diabetes and associated with mortality and incident heart failure admission. European Heart Journal. 2014 Mar;35(10):657–64.

	CONTROL	IGT	P
Age (Years)	54.6±5.4	56.8±9.2	0.45
BMI (Kg/m^2)	27.0±3.1	32.5±6.5	0.007
Systolic BP (mm Hg)	118±11	126±12	0.08
Diastolic BP (mm Hg)	72±10	75±10	0.51
Fasting Glucose (mmol/l)	4.8±0.5	5.9±0.8	<0.001
2h Glucose (mmol/l)	5.3±1.3	9.5±1.3	<0.001
HbA1c (%)	5.7±0.4	5.8±0.4	0.46
Total Chol (mmol/l)	5.0±0.74	4.7±1.4	0.49
LDLc (mmol/l)	2.9±0.6	2.8±1.1	0.96
HDLc (mmol/l)	1.6±0.4	1.2±0.4	0.035
Triglyceride (mmol/l)	1.1±0.5	2.0±1.0	0.005

Table 6-1 Clinical data. (Data are expressed as Mean ± SD).

	CONTROL	IGT	P
LVMI (BSA) g/m^2	51.1±10.7	47.6±8.8	0.32
LVMI (Ht$^{1.7}$) g/m^2	39.7±7.3	40.1±6.0	0.878
LVMI (Ht$^{2.7}$) g/m^2	22.9±3.7	23.5±3	0.682
CONCENTRICITY	0.59±0.13	0.58±0.11	0.744
LVEF (%)	61.0±6.4	61.1±5.4	0.96
rMBF	0.75±0.17	0.83±0.16	0.17
sMBF	2.07±0.42	2.02±0.48	0.76
R/S MBF	2.81±0.47	2.43±0.45	0.12
ECV	0.27±0.05	0.26±0.05	0.63

Table 6-2 CMR data. (Data are expressed as Mean ± SD)

	CONTROL	IGT	P
LONG ST	-16.0±10.8	-19.6±3.6	0.20
LONG SR	0.9±0.9	1.24±0.3	0.10
RAD ST	-34.3±11.6	-36.2±17.7	0.73
RAD SR	1.3±0.7	1.6±0.5	0.11
CIRC ST	-22.3±2.6	-21.7±6.2	0.74
CIRC SR	2.7±5.7	1.3±0.4	0.29
IN TAG	-19.2±2.3	-19.2±3.0	0.98

Table 6-3 Myocardial deformation data. (Data are expressed as Mean ± SD).

7 Subjects with Extreme Duration Type 1 Diabetes Exhibit No Structural or Functional Abnormality on Cardiac Magnetic Resonance Imaging.

Omar Asghar, Christopher Miller, Simon Ray, Matthias Schmitt and Rayaz Malik.

Contribution: Omar Asghar contributed to study concept and design, patient recruitment, data analysis, statistics and was the sole author of this chapter. The CMR methodology and analyses were the work of Christopher Miller.

7.1 Abstract

Background: A subgroup of Individuals with type 1 diabetes of extreme duration (Medalists), appear to be free of long-term diabetic complications however the degree of protection from cardiovascular disease is not established.

Methods and Results: We performed multiparametric cardiac magnetic resonance (CMR) imaging in 13 subjects with diabetes of extreme duration (47.4±5.1 years) and 14 healthy controls, to assess cardiac structure, volumetrics, myocardial deformation, diffuse fibrosis and myocardial blood flow. There were no differences in ejection fraction (LVEF) (63.1±6.9 vs 61.0±6.4 %, P=0.425), however LVMI was significantly lower in the diabetic group when indexed to body surface area (BSA) (41.0±6.4 vs 51.1±10.7 g/m2, P=0.007) and Ht1.7 (32.8±6.2 vs 39.5±7.5 g/m2, P=0.02) but not Ht2.7 (22.0±3.7 vs 22.8±3.8 g/m2, P=0.065). Concentricity index was similar in both groups (0.51±0.08 vs 0.58±0.13, P=0.115). Extracellular volume (ECV) was higher in the diabetic group compared to control subjects (0.32±0.04 vs 0.27±0.05 %, P=0.01). There were no significant differences in resting myocardial blood flow (MBF) (0.86±0.24 vs 0.75±0.17 ml/min/g, P=0.177), stress MBF (1.80±0.35 vs 2.07±0.42 ml/min/g, P=0.094). However, MBF ratio (stress/rest) was significantly lower in the diabetic group compared to control subjects (2.16±0.66 vs 2.81±0.47 ml/min/g, P=0.006). There were no differences in radial (-32.1±17.7 vs -34.3±11.6; P=0.707), circumferential (-24.9±5.2 vs -22.3±2.6; P=0.109) or longitudinal (-18.9±5.5 vs -16.0±10.8, P=0.394) strain between the diabetic group and controls.

Conclusion: Individuals with type 1 diabetes of extreme duration exhibit normal cardiac structure and function with only mild alterations in ECV and coronary perfusion reserve.

7.2 Introduction

Medalists represent a unique group of individuals who have survived over 50 years of type 1 diabetes (T1DM). The Joslin 50 year Medalist study further identified a sub-group of medalists (escapers) who had remained free of micro and macrovascular complications (1,2). However, their definition of cardiovascular disease (CVD) was based on clinical history alone and the true cardiovascular phenotype of medalists is not known.

In contrast, a recent Swedish registry study of patients with Type 1 diabetes has shown that the multivariable-adjusted hazard ratios were markedly increased for death (2-8 fold) and more specifically for death from cardiovascular causes (3-10 fold) compared with controls, even in patients with an HbA1c <6.9% (HR-2.36) (3). Diabetes is of course a strong independent predictor of heart failure (HF) independent of coronary heart disease (CHD) and hypertension (4). Diabetic cardiomyopathy (DC) describes a distinct pathophysiological process, characterized by metabolic derangement, neurohormonal activation, and microvascular inflammation (5,6) giving rise to cardiomyocyte hypertrophy, diffuse interstitial and perivascular fibrosis (7-9). Echocardiography has been deployed to show early diastolic dysfunction, characterized by alterations in longitudinal, circumferential and radial myocardial function and left ventricular (LV) torsion (10). Furthermore, long axis dysfunction, the earliest detectable abnormality in diastolic function, is reduced both at rest and during exercise in diabetic subjects without evidence of ischemic heart disease (11-14).

Recent advances in cardiac magnetic resonance (CMR) imaging have allowed multi-parametric assessment of the heart including volumetric analysis (15), diastology (16), deformation (17-19), myocardial blood flow (20), tissue characterization (21) and inflammation (22). We have undertaken a comprehensive multi-parametric CMR imaging

study to establish the structural and functional cardiac phenotype in a cohort of subjects with extreme duration T1DM and healthy controls.

7.3 Research Design and Methods

7.3.1 Patient Selection

We studied subjects aged 18-75 years with T1DM of extreme duration (>45 years) and healthy males and females aged 18-75. Exclusion criteria included any history of cardiac disease, severe systemic disease (e.g. congestive cardiac failure, rheumatoid disease, SLE), chronic kidney disease (eGFR ≤35 mls/min/1.73m2), peripheral vascular disease or any contraindication to CMR imaging (including adenosine stress and gadolinium contrast). The study protocol was approved by the Central Manchester Research Ethics Committee. Written informed consent, according to the declaration of Helsinki, was obtained from all participants on enrolment to the study.

7.3.2 Study Protocol

All study participants underwent an initial assessment including medical history, clinical examination and 12 lead ECG. Renal function, HbA1c, lipids, blood count and haematocrit (for extracellular volume [ECV] calculation) were assessed. In addition, healthy control subjects underwent an oral glucose tolerance test (OGTT) to confirm normoglycemia. All participants were instructed to abstain from caffeine intake for a minimum of 12 hours prior to CMR imaging.

7.3.3 CMR Protocol

Details of our imaging and analysis protocols have been previously described (15,17,23,24).

Image Acquisition

CMR was performed using a 1.5T MR scanner (Avanto; Siemens Healthcare, Germany) equipped with a 32 element phased array coil. Steady-state free precession (SSFP) cine images were acquired in standard long axis views and a short axis stack covering the left ventricle (LV). Tagged short axis images at the LV base, mid cavity and apex were acquired using a segmented k-space fast gradient echo sequence with spatial modulation of magnetization in orthogonal planes. Myocardial blood flow (MBF) was assessed during pharmacological (vasodilator) stress with intravenous adenosine (140 μg/kg/min) via a large peripheral vein for 3-minutes prior to, and during, data acquisition. A 0.05 mmol/Kg bolus of gadolinium-based contrast agent (gadopentetate dimeglumine; Gd-DTPA; Magnevist; Bayer Healthcare, Germany) was administered intravenously at 5ml/s followed by a 30 ml saline flush. Rest imaging was performed 10 minutes after stress imaging with a further 0.05 mmol/Kg bolus of contrast agent. Following rest imaging, a further 0.1 mmol/Kg of contrast agent was administered (top-up). A short axis, single-shot modified Look Locker inversion recovery sequence was acquired at mid ventricular level pre and 15 minutes post contrast top-up. Standard late gadolinium enhancement (LGE) imaging was performed at least 10 minutes following the top-up of contrast with spoiled gradient echo segmented inversion recovery and phased sensitive inversion recovery segmented gradient echo sequences.

CMR Image Analysis

Off line image analysis was carried out by a cardiology research fellow (OA) under the supervision of an experienced operator (CM), blinded to clinical information. Left ventricular (LV) mass, volumes and ejection fraction (EF) were derived from SSFP images using CMRtools (Cardiovascular Imaging Solutions, London, UK) and our previously described methods (15). Peak systolic circumferential strain and strain rate were calculated from tagged mid cavity short axis slices using InTag (CREATIS; Université de Lyon, France) (17). We also used 2D Cardiac Performance Analysis MR (TomTec Imaging Systems GmbH, Munich, Germany) to derive longitudinal, radial and circumferential strain and strain rate. For T1 relaxation time measurements and MBF quantification, we used Osirix Imaging Software (Pixmeo; Switzerland) to trace epicardial and endocardial borders, draw a region of interest in the blood pool and to identify the right ventricular insertion point (20,24).

7.3.4 Statistical Analysis

SPSS Statistics for Mac version 20 (IBM corporation, New York USA) was used for all statistical analysis. All data are expressed as mean ± standard deviation (SD) and the Shapiro-Wilk test was used to determine normality of data. The unpaired T test was used to compare normally distributed data between groups and the Mann Whitney U test was used for non-parametric data. A two-tailed P-value of less than 0.05 was considered statistically significant.

7.4 Results

14 subjects with T1DM of extreme duration (5 male, 9 female) and 15 healthy control subjects (10 males, 5 females) were studied. One subject from the control group was excluded from the study due to an incidental finding of LV impairment and one diabetic patient became claustrophobic in the scanner and was unable to continue. A further diabetic patient was unable to tolerate adenosine and was not included in the MBF part of the study. Therefore 13 diabetic and 14 control subjects completed the imaging protocol.

7.4.1 Demographic, Clinical and Cardiac Data (Tables 7-1 and 7-2)

The mean duration of diabetes was 47.4±5.1 years (median 48.0 years) and the mean HbA1c over 16 years was 8.5±1.0% (69±11 mmol/mol) indicating moderate to poor long-term glycemic control, but a good lipid profile (Chol 4.7±0.3, HDLc 1.8±0.5, LDLc 2.2±0.5, Trig 1.1±0.4 mmol/l) and renal function (eGFR 76±17ml/kg/min). Eight of the fourteen medalists had a history of retinopathy and 12 medalists were taking statin and angiotensin converting enzyme (ACE) inhibitor therapy in addition to insulin. None of the control group were taking any regular medication. The patients with diabetes were older (61.8±7.6 vs 54.6±5.4 years; P=0.009) and had a lower diastolic (60±14 vs 72±10 mmHg; P=0.014) but slightly higher systolic (128±15 vs 118±11 mmHg; P=0.051) blood pressure than controls. LDLc (2.1±1.0 vs 2.9±0.6 mmol/l; P=0.035) was lower and HDLc (2.1±0.7 vs 1.6±0.4 mmol/l, P=0.027) was higher in diabetic patients compared to controls. There were no differences in BMI, triglycerides or eGFR between the groups.

7.4.2 Volumetric Data

There were no differences in LV ejection fraction (LVEF) (63.1±6.9 vs 61.0±6.4 %, P=0.425), however LV mass index (LVMI) was significantly lower in the diabetic group when indexed to BSA (41.0±6.4 vs 51.1±10.7 g/m2, P=0.007) and Ht1.7 (32.8±6.2 vs 39.5±7.5 g/m2, P=0.02) but not when indexed to Ht2.7 (22.0±3.7 vs 22.8±3.8 g/m2, P=0.065). Concentricity index was similar in both groups (0.51±0.08 vs 0.58±0.13, P=0.115).

7.4.3 T1 Mapping

ECV was higher in the diabetic group compared to control subjects (0.32±0.04 vs 0.27±0.05 %, P=0.01).

7.4.4 Myocardial Blood Flow

There were no significant differences in resting MBF (0.86±0.24 vs 0.75±0.17 ml/min/g, P=0.177), stress MBF (1.80±0.35 vs 2.07±0.42 ml/min/g, P=0.094). However, MBF ratio (stress/rest) was significantly lower in the diabetic group compared to control subjects (2.16±0.66 vs 2.81±0.47 ml/min/g, P=0.006).

7.4.5 Myocardial Deformation

There were no differences in radial (-32.1±17.7 vs -34.3±11.6; P=0.707), circumferential (-24.9±5.2 vs -22.3±2.6; P=0.109) or longitudinal (-18.9±5.5 vs -16.0±10.8, P=0.394) strain between the diabetic group and controls.

7.5 Discussion

Medalists represent a unique group of patients with an extreme duration of T1DM and a variable degree of microvascular and macrovascular complications. As such they constitute a special phenotype, which merits further study, especially given the excess cardiovascular mortality in patients with T1DM, even in those with good glycemic control (3). Detailed cardiac studies in medalist cohorts identifying the exact phenotype are lacking. This is the first study to investigate in detail, cardiac structure, function and myocardial blood flow in a cohort of patients with an extreme duration of diabetes, including medalists (8/13).

In the present study we show that extreme duration patients with T1DM have no evidence of CHD and normal LVEF, but a lower LVMI. We have employed robust, validated and reproducible 3D modeling methods for volumetric and structural analyses by using long axis in addition to short axis slices and threshold-based contouring to identify myocardium (15). Furthermore, we have used 3 different methods to calculate LVMI to adjust for BMI. These data are not consistent with the reported association between HbA1c and CMR findings in the DCCT cohort, although LVMI was higher and LVEF was lower, only in patients with prior CVD, and there was no difference between the conventional and intensively treated patients (25). This is interesting in the context of the recent analysis showing markedly increased mortality in T1DM (8%) v controls (2.9%) and a clear relationship between poorer glycemic control and renal impairment with worse outcomes (3). In the present study, there is clearly protection from the development of left ventricular hypertrophy and a reduction in ejection fraction in these patients.

We have found no differences in longitudinal, radial and circumferential function in patients with extreme duration T1DM. Whilst the majority of previous studies have used echocardiography to show early diastolic dysfunction in patients with T2DM, a recent CMR study has shown diastolic dysfunction in young adults with T2DM (26) and a reduction in left ventricular longitudinal myocardial deformation has also been demonstrated in children with T1DM (27). A lack of CMR evidence of diastolic dysfunction is in keeping with our recent echocardiographic study also showing only mild evidence of diastolic dysfunction (28) and therefore clearly warrants further study.

Studies in patients with T1DM have demonstrated a reduction in MBF in association with sympathetic dysfunction (29,30). Quantitative CMR assessment of MBF is an emerging technology which shows much promise and is an attractive validated alternative to positron emission tomography (PET) in the assessment of microvascular dysfunction (20). To date, there are no published studies of CMR derived MBF in diabetic subjects. We have found no differences in resting and stress MBF between patients with extreme duration T1DM and controls, however, the stress/rest ratio, an index of coronary microvascular perfusion reserve, was significantly lower in the diabetic group. Coronary microvascular dysfunction may partly be mediated through cardiac autonomic dysfunction, however, our study subjects patients had minimal evidence of cardiac autonomic neuropathy and we did not find any correlation between myocardial perfusion reserve and markers of cardiac autonomic function (unpublished data).

Although extensively studied in animal models of diabetes, the need for endomyocardial biopsy has limited the study of myocardial fibrosis in man (9,31). Previous studies have

demonstrated myocardial fibrosis in subjects with T2DM and metabolic syndrome using integrated back scatter (32-34). In a recent study correlating histology with CMR, the latter was shown to be a highly accurate, non-invasive assessment of regional myocardial fibrosis using LGE and diffuse interstitial myocardial fibrosis, using post-contrast T1 mapping (35). Furthermore, T1 mapping using CMR, has shown that fibrosis is associated with impaired systolic and diastolic function and biomarkers of fibrosis in patients with T1DM and T2DM (36-38). Quantitative assessment of myocardial ECV, a surrogate of myocardial fibrosis, shows much promise and has been recently validated in man (24,39,40). In the only study published to date using ECV quantification in diabetic subjects, diabetes (T1 and T2DM) was associated with ECV expansion, HF admission to hospital and death (41). We report an increase in ECV in our patients with T1DM compared to healthy controls. However, the clinical relevance of this mild degree of myocardial fibrosis is questionable given the absence of LV mechanical dysfunction, microvascular and autonomic dysfunction.

A perceived weakness of the current study may be the small study population, however we believe the detailed structural and functional cardiac phenotyping in this unique cohort of extreme duration patients with T1DM presents novel data. It confirms that these unique individuals are indeed protected from the long-term complications of diabetes, warranting further studies to establish the basis of this protection.

Sources of Funding

This study was funded by research grants from the NHS National Institutes for Health Research (FSF-R5-OA), NIH (R105991) and Juvenile Diabetes Research Foundation (8-2008-362).

Disclosures

None

7.6 References

1. Sun JK, Keenan HA, Cavallerano JD, Asztalos BF, Schaefer EJ, Sell DR, et al. Protection From Retinopathy and Other Complications in Patients With Type 1 Diabetes of Extreme Duration: The Joslin 50-Year Medalist Study. Diabetes Care. 2011 Mar 29;34(4):968–74.

2. Bain SC, Gill GV, Dyer PH, Jones AF, Murphy M, Jones KE, et al. Characteristics of Type 1 diabetes of over 50 years duration (the Golden Years Cohort). Diabetic Medicine. 2003 Oct;20(10):808–11.

3. Lind M, Svensson A-M, Kosiborod M, Gudbjörnsdottir S, Pivodic A, Wedel H, et al. Glycemic Control and Excess Mortality in Type 1 Diabetes. N Engl J Med. 2014 Nov 20;371(21):1972–82.

4. From AM, Scott CG, Chen HH. The development of heart failure in patients with diabetes mellitus and pre-clinical diastolic dysfunction a population-based study. Journal of the American College of Cardiology. 2010 Jan 26;55(4):300–5.

5. Bell D. Diabetic cardiomyopathy. Diabetes Care. 2003;26(10):2949.

6. Horwich TB, Fonarow GC. Glucose, Obesity, Metabolic Syndrome, and Diabetes. JAC. Elsevier Inc; 2010 Jan 26;55(4):283–93.

7. Asghar O, Al-Sunni A, Khavandi K, Khavandi A, Withers S, Greenstein A, et al. Diabetic cardiomyopathy. Clinical Science. 2009 May;116(10):741–60.

8. van Heerebeek L, Hamdani N, Handoko ML, Falcao-Pires I, Musters RJ, Kupreishvili K, et al. Diastolic Stiffness of the Failing Diabetic Heart: Importance of Fibrosis, Advanced Glycation End Products, and Myocyte Resting Tension. Circulation. 2008 Jan 1;117(1):43–51.

9. Asbun J, Villarreal F. The pathogenesis of myocardial fibrosis in the setting of diabetic cardiomyopathy. Journal of the American College of Cardiology. 2006;47(4):693–700.

10. Oh JK, Park SJ, Nagueh SF. Established and Novel Clinical Applications of Diastolic Function Assessment by Echocardiography. Circulation: Cardiovascular Imaging. 2011 Jul 19;4(4):444–55.

11. Ha J-W, Lee H-C, Kang E-S, Ahn C-M, Kim J-M, Ahn J-A, et al. Abnormal left ventricular longitudinal functional reserve in patients with diabetes mellitus: implication for detecting subclinical myocardial dysfunction using exercise tissue Doppler echocardiography. Heart. 2007 Dec;93(12):1571–6.

12. Fang Z, Najos-Valencia O, Leano R, Marwick T. Patients with early diabetic heart disease demonstrate a normal myocardial response to dobutamine* 1. Journal of the American College of Cardiology. 2003;42(3):446–53.

13. Ng ACT, Delgado V, Bertini M, Meer RWVD, Rijzewijk LJ, Shanks M, et al. Findings from Left Ventricular Strain and Strain Rate Imaging in Asymptomatic Patients With Type 2 Diabetes Mellitus. AJC. 2009 Jan 11;104(10):1398–401.

14. Nakai H, Takeuchi M, Nishikage T, Lang RM, Otsuji Y. Subclinical left ventricular dysfunction in asymptomatic diabetic patients assessed by two-dimensional speckle tracking echocardiography: correlation with diabetic duration. European Journal of Echocardiography. 2009 Dec 1;10(8):926–32.

15. Miller CA, Jordan P, Borg A, Argyle R, Clark D, Pearce K, et al. Quantification of left ventricular indices from SSFP cine imaging: Impact of real-world variability in analysis methodology and utility of geometric modeling. J Magn Reson Imaging. 2012 Nov 2;37(5):1213–22.

16. Paelinck B, Lamb H. Assessment of Diastolic Function by Cardiac MRI. Cardiovascular Magnetic Resonance Imaging. 2008;:415–28.

17. Miller CA, Borg A, Clark D, Steadman CD, McCann GP, Clarysse P, et al. Comparison of local sine wave modeling with harmonic phase analysis for the assessment of myocardial strain. J Magn Reson Imaging. 2012 Dec 12;38(2):320–8.

18. Young AA, Cowan BR. Evaluation of left ventricular torsion by cardiovascular magnetic resonance. J Cardiovasc Magn Reson. 2012;14:49.

19. Götte M, Germans T, Rüssel I, Zwanenburg J, Marcus J, van Rossum A, et al. Myocardial Strain and Torsion Quantified by Cardiovascular Magnetic Resonance Tissue Tagging:: Studies in Normal and Impaired Left Ventricular Function. Journal of the American College of Cardiology. 2006;48(10):2002–11.

20. Miller CA, Naish JH, Ainslie MP, Tonge C, Tout D, Arumugam P, et al. Voxel-wise quantification of myocardial blood flow with cardiovascular magnetic resonance: effect of variations in methodology and validation with positron emission tomography. Journal of Cardiovascular Magnetic Resonance. Journal of Cardiovascular Magnetic Resonance; 2014 Jan 24;16(1):1–15.

21. Won S, Davies-Venn C, Liu S, Bluemke DA. Noninvasive imaging of myocardial extracellular matrix for assessment of fibrosis. Current Opinion in Cardiology. 2013 May;28(3):282–9.

22. Baksi AJ, Pennell DJ. T2* imaging of the heart: methods, applications, and outcomes. Top Magn Reson Imaging. 2014 Feb;23(1):13–20.

23. Miller CA, Naish JH, Shaw SM, Yonan N, Williams SG, Clark D, et al. Multiparametric cardiovascular magnetic resonance surveillance of acute cardiac allograft rejection and characterisation of transplantation-associated myocardial injury: a pilot study. 2014 Jul 20;1–11.

24. Miller CA, Naish JH, Bishop P, Coutts G, Clark D, Zhao S, et al. Comprehensive Validation of Cardiovascular Magnetic Resonance Techniques for the Assessment of Myocardial Extracellular Volume. Circulation: Cardiovascular Imaging. 2013 May 21;6(3):373–83.

25. Genuth SM, Backlund J-YC, Bayless M, Bluemke DA, Cleary PA, Crandall J, et al. Effects of prior intensive versus conventional therapy and history of glycemia on cardiac function in type 1 diabetes in the DCCT/EDIC. Diabetes. 2013 Oct;62(10):3561–9.

26. Khan JN, Wilmot EG, Leggate M, Singh A, Yates T, Nimmo M, et al. Subclinical diastolic dysfunction in young adults with Type 2 diabetes mellitus: a multiparametric contrast-enhanced cardiovascular magnetic resonance pilot study assessing potential mechanisms. European Heart Journal - Cardiovascular Imaging. 2014 Oct 24;15(11):1263–9.

27. Labombarda F, Leport M, Morello R, Ribault V, Kauffman D, Brouard J, et al. Longitudinal left ventricular strain impairment in type 1 diabetes children and adolescents: a 2D speckle strain imaging study. Diabetes Metab. 2014 Sep;40(4):292–8.

28. Fagan A, Asghar O, Pearce K, Stout M, Ray SG, Schmitt M, et al. Medalists With Extreme Duration of Type 1 Diabetes Exhibit Only Mild Diastolic Dysfunction and Myocardial Fibrosis. Diabetes Care. 2015 ed. 38:e1–e2.

29. Pop-Busui R, Kirkwood I, Schmid H, Marinescu V, Schroeder J, Larkin D, et al. Sympathetic dysfunction in type 1 diabetes. Journal of the American College of Cardiology. 2004 Dec;44(12):2368–74.

30. Hattori N, Rihl J, Bengel F, Nekolla S. Cardiac autonomic dysinnervation and myocardial blood flow in long-term Type 1 diabetic patients. Diabetic Medicine. 2003;20;375-381.

31. Fischer VW, Fischer VW, Fischer VW, Fischer VW, Barner HB, Barner HB, et al. Pathomorphologic aspects of muscular tissue in diabetes mellitus. Human pathology [Internet]. 1984 Dec;15(12):1127–36.

32. Fang Z, Yuda S, Anderson V, Short L, Case C, Marwick T. Echocardiographic detection of early diabetic myocardial disease* 1. Journal of the American College of Cardiology. 2003;41(4):611–7.

33. Kosmala W, Przewlocka-Kosmala M, Szczepanik-Osadnik H, Mysiak A, O'Moore-Sullivan T, Marwick TH. A Randomized Study of the Beneficial Effects of Aldosterone Antagonism on LV Function, Structure, and Fibrosis Markers in Metabolic Syndrome. JCMG. Elsevier Inc; 2011 Dec 1;4(12):1239–49.

34. Marwick TH, Raman SV, Carrió I, Bax JJ. Recent Developments in Heart Failure Imaging. JCMG. 2011 Jan 14;3(4):429–39.

35. Iles LM, Ellims AH, Llewellyn H, Hare JL, Kaye DM, McLean CA, et al. Histological validation of cardiac magnetic resonance analysis of regional and diffuse interstitial myocardial fibrosis. European Heart Journal - Cardiovascular Imaging. 2014 Oct 28.

36. Ng ACT, Auger D, Delgado V, van Elderen SGC, Bertini M, Siebelink HM, et al. Association Between Diffuse Myocardial Fibrosis by Cardiac Magnetic Resonance Contrast-Enhanced T1 Mapping and Subclinical Myocardial Dysfunction in Diabetic Patients: A Pilot Study. Circulation: Cardiovascular Imaging. 2012 Jan 17;5(1):51–9.

37. Jellis C, Wright J, Kennedy D, Sacre J, Jenkins C, Haluska B, et al. Association of Imaging Markers of Myocardial Fibrosis with Metabolic and Functional Disturbances in Early Diabetic Cardiomyopathy. Circulation: Cardiovascular Imaging. 2011 Sep 23.

38. Messroghli DR, Radjenovic A, Kozerke S, Higgins DM, Sivananthan MU, Ridgway JP. Modified Look-Locker inversion recovery (MOLLI) for high-resolutionT1 mapping of the heart. Magn Reson Med. 2004;52(1):141–6.

39. Flett AS, Hayward MP, Ashworth MT, Hansen MS, Taylor AM, Elliott PM, et al. Equilibrium Contrast Cardiovascular Magnetic Resonance for the Measurement of Diffuse Myocardial Fibrosis: Preliminary Validation in Humans. Circulation. 2010 Jul 12;122(2):138–44.

40. Aus dem Siepen F, Buss SJ, Messroghli D, Andre F, Lossnitzer D, Seitz S, et al. T1 mapping in dilated cardiomyopathy with cardiac magnetic resonance: quantification of diffuse myocardial fibrosis and comparison with endomyocardial biopsy. European Heart Journal - Cardiovascular Imaging. 2014 Sep 22.

41. Wong TC, Piehler KM, Kang IA, Kadakkal A, Kellman P, Schwartzman DS, et al. Myocardial extracellular volume fraction quantified by cardiovascular magnetic resonance is increased in diabetes and associated with mortality and incident heart failure admission. European Heart Journal. 2014 Mar;35(10):657–64.

	CONTROL	DIABETES	P
Age (Years)	54.6±5.4	61.8±7.6	0.009
Diabetes Duration (Years)	-	47.4±5.1	-
BMI (Kg/m^2)	27.0±3.1	28.1±4.5	0.48
Systolic BP (mm Hg)	118±11	128±15	0.051
Diastolic BP (mm Hg)	72±10	60±14	0.014
HbA1c (%)	5.7±0.4	8.3±1.0	<0.0001
Total Chol (mmol/l)	5.0±0.74	4.6±1.0	0.227
LDLc (mmol/l)	2.9±0.6	2.1±1.0	0.035
HDLc (mmol/l)	1.6±0.4	2.1±0.7	0.027
Triglyceride (mmol/l)	1.1±0.5	0.9±0.4	0.265
eGFR (ml/Kg/min)	81±9	72±20	0.135

Table 7-1 Clinical data. (Data are expressed as Mean ± SD).

	CONTROL	DIABETES	P
LVMI [BSA] (g/m^2)	51.1±10.7	41.0±6.4	0.007
LVMI [$Ht^{1.7}$] (g/m^2)	39.5±7.5	32.8±6.2	0.02
LVMI [$Ht^{2.7}$] (g/m^2)	22.8±3.8	22.0±3.7	0.065
CONCENTRICITY	0.58±0.13	0.51±0.08	0.115
LVEF (%)	61.0±6.4	63.1±6.9	0.425
T1 ECV (%)	0.27±0.05	0.32±0.04	0.01
Resting MBF (ml/min/g)	0.75±0.17	0.86±0.24	0.177
Stress MBF (ml/min/g)	2.07±0.42	1.80±0.35	0.094

Table 7-2 Cardiac Data. (Data are expressed as Mean ± SD).

	CONTROL	DIABETES	P
LONG St	-16.0±10.8	-18.9±5.5	0.394
LONG SR	0.9±0.9	1.2±0.4	0.243
RAD St	-34.3±11.6	-32.1±17.7	0.707
RAD SR	1.3±0.7	1.5±0.5	0.412
CIRC St	-22.3±2.6	-24.9±5.2	0.109
CIRC SR	2.7±5.7	1.4±0.5	0.29
IN TAG	-19.2±2.3	-19.2±3.0	0.98

Table 7-3 Strain and strain rates. (Data are expressed as Mean ± SD).

8 Corneal Confocal Microscopy Detects Neuropathy in Subjects with Impaired Glucose Tolerance

Omar Asghar, Ioannis N Petropoulos,Uazman Alam, Maria Jeziorska, Andrew Marshall, Georgios Ponirakis, Hassan Fadavi, Andrew JM Boulton, Mitra Tavakoli and Rayaz A Malik

Contribution: Omar Asghar contributed to patient recruitment, data analysis and statistics for this study. This chapter was co-authored with Ioannis Petropoulos.

LIST OF ABBREVIATIONS

CCM: corneal confocal microscopy

Chol: total cholesterol

CNBD: corneal nerve branch density

CNFD: corneal nerve fiber density

CNFL: corneal nerve fiber length

CT: cold threshold

DSPN: distal symmetric polyneuropathy

eGFR: estimated glomerular filtration rate

HRV: heart rate variability

IENFD: intra epidermal nerve

IGT: impaired glucose tolerance

ISFN: idiopathic small fiber neuropathy

NCCA: non contact corneal aesthesiometry

NDS: neuropathy disability score

NSP: neuropathy symptom profile

PMNAmp: peroneal motor nerve amplitude

PMNCV: peroneal motor nerve conduction velocity

SSNAmp: sural sensory nerve amplitude

SSNCV: sural sensory nerve conduction velocity

VPT: vibration perception threshold

WT: warm threshold

8.1 Abstract

Objective: Impaired glucose tolerance (IGT) represents one of the earliest stages of glucose dysregulation and is associated with macrovascular disease, retinopathy and microalbuminuria, but it is unclear whether it causes neuropathy.

Research Design and Methods: 37 subjects with IGT and 20 age-matched controls underwent comprehensive assessment of neuropathy using nerve conduction studies, quantitative sensory testing, autonomic function testing, skin biopsy and corneal confocal microscopy.

Results: Subjects with IGT had a higher frequency and intensity of sensory symptoms compared to controls. There was a significant reduction in intra-epidermal nerve fiber density (IENFD) ($P=0.03$), corneal nerve fiber density (CNFD) ($P<0.001$), corneal nerve branch density (CNBD) ($P=0.002$) and fiber length (CNFL) ($P=0.05$) However, there was no difference in nerve conduction parameters and autonomic function.

Conclusions: Small fibre neuropathy is present in subjects with IGT and both skin biopsy and corneal confocal microscopy (CCM) detect this early abnormality.

8.2 Introduction

The World Health Organisation estimates that pre-diabetes affects approximately 300 million people worldwide. Pre-diabetes encompasses a metabolically heterogeneous group of clinically silent entities, namely intermediate hyperglycaemia, impaired fasting glucose and IGT and is associated with an increased risk for macrovascular disease (1). However, it remains unclear whether it is also a risk for microvascular complications as some studies report microalbuminuria (2), retinopathy (3) and neuropathy (4-5) in subjects with IGT while others have found no difference (6).

The association between IGT and peripheral neuropathy was first highlighted when subjects with idiopathic small fibre neuropathy (ISFN) were found to have an unexpectedly high prevalence of IGT (4; 7-9). These early studies were confounded by referral bias, and heterogeneous study cohorts. However, larger population-based studies such as the San Luis Valley (10) and the MONICA/KORA Augsburg (11) studies have shown that neuropathy is present in 26-28% of patients with diabetes, 11-13% in IGT and 4-8% in the control population. In contrast, Dyck et al. did not demonstrate neuropathy amongst subjects with impaired glycemia when compared with controls (6). Although of note, those with impaired glycemia included individuals with intermediate hyperglycaemia, impaired fasting glucose and only a proportion had IGT.

Establishing whether or not neuropathy occurs in subjects with IGT is important as it may provide insights into the pathogenesis of diabetic neuropathy. However, the detection of peripheral neuropathy in IGT remains challenging: the majority of studies have used a

combination of symptoms and neurologic signs, which are large-fiber weighted. Yet, an increasing body of evidence suggests a predominantly small-fiber neuropathy with minimal large-fiber involvement in IGT. Hence, a significant reduction in IENFD was demonstrated in a study of subjects with IGT receiving lifestyle intervention (12). In another study subjects with IGT had significantly impaired quantitative sudomotor axon reflex test responses (13). Similarly, sympathetic skin response amplitudes were reduced without evidence of electrophysiological abnormalities in IGT (14). In a study of patients with ISFN the presence of IGT did not worsen small fibre damage, as detected using the non-invasive technique of CCM (15). Nevertheless, CCM has been shown to detect nerve damage in diabetic patients with minimal neuropathy (16). Therefore, the objectives of this study were i) to characterise the neuropathy associated with IGT using comprehensive neuropathy assessment in subjects with IGT using neurophysiology, quantitative sensory testing and in particular IENFD and ii) to establish and validate CCM as a sensitive measure of small fibre neuropathy in subjects with IGT.

8.3 Methods

8.3.1 Study subjects

37 subjects aged 18-75 years with a diagnosis of IGT (2 hour glucose 7.8-11 mmol/l) following an oral glucose tolerance test and 20 age-matched control subjects with normal glucose tolerance were studied. Exclusion criteria were any history of congestive cardiac failure, connective tissue disease, chronic kidney (serum creatinine >250 umol/l), peripheral vascular, infectious or malignant disease, absent foot pulses, alcohol intake >21 units per week (males) or >14 units/week (females), any other cause of peripheral neuropathy, active

corneal disease or surgery and chronic contact lens use. The study was approved by the Central Manchester Research and Ethics committee, and written informed consent was obtained from all subjects prior to participation. This research adhered to the tenets of the declaration of Helsinki.

8.3.2 Clinical and Peripheral Neuropathy Assessment

All study participants underwent assessment of BMI, hemoglobin A1c (HbA1c), lipid fractions [total cholesterol (Chol), LDL, HDL and triglycerides (trig)] estimated glomerular filtration rate (eGFR). Symptoms of DSPN were assessed using the NSP and neurological deficits were evaluated using simplified neuropathy disability score (NDS) (17). Vibration perception threshold (VPT) was tested using a Neurothesiometer (Horwell, Scientific Laboratory Supplies, Wilfrod, Nottingham, UK). Cool (CT) and warm (WT) thresholds were established on the dorsolateral aspect of the left foot (S1) using the TSA-II NeuroSensory Analyser (Medoc Ltd., Ramat-Yishai, Israel) using the method of limits. Electro-diagnostic studies were undertaken using a Dantec "Keypoint" system (Dantec Dynamics Ltd, Bristol, UK) equipped with a DISA temperature regulator to keep limb temperature constantly between 32-35°C. Sural sensory nerve amplitude (SSNamp), sural sensory nerve conduction velocity (SSNCV), peroneal motor nerve amplitude (PMNamp) and peroneal motor nerve conduction velocity (PMNCV) were assessed by a consultant neurophysiologist. The peroneal motor nerve study was performed using silver-silver chloride surface electrodes at standardized sites defined by anatomical landmarks and recordings for the sural sensory nerve were taken using antidromic stimulation over a distance of 100mm. Heart rate variability (HRV) was assessed with an ANX 3.0 autonomic nervous system monitoring

device (ANSAR Medical Technologies Inc., Philadelphia, PA, USA). Sweat production, as an indication of sudomotor function, was measured using Neuropad (miro Verbandstoffe, Wiehl-Drabenderhole, Germany) (18). The Neuropad was applied to the plantar surface of the foot on the first metatarsal head and removed after 10 minutes. A colour change occurs based on a cobalt II compound changing from blue to pink. The percentage (%) colour change was estimated visually with a pink colour (100%) indicating normal sweat production and a blue colour (0%) indicating absent sweat production.

8.3.3 Corneal Confocal Microscopy

Patients underwent examination with the CCM (Heidelberg Retinal Tomograph III Rostock Cornea Module, Heidelberg Engineering GmbH, Heidelberg, Germany) as per previously established protocol (16). All scans were performed by two purpose trained optometrists. Five non-overlapping images/patient from the centre of the cornea were selected and quantified in a masked fashion. Three corneal nerve parameters were quantified: (i) CNFD - the total number of major nerves/mm2 of corneal tissue; CNBD - the number of branches emanating from all major nerve trunks/mm2 of corneal tissue and (iii) CNFL - the total length of all nerve fibers and branches (mm/mm2) within the area of corneal tissue. Corneal sensation was evaluated using a purpose-built non-contact corneal aesthesiometer (NCCA) (19).

8.3.4 Skin Biopsy and Immunohistochemistry

A 3-mm punch skin biopsy was taken from the dorsum of the foot ~2 cm above the second metatarsal head after local anesthesia (1% lidocaine). The biopsy site was closed using Steri-strips, and the specimen was immediately fixed in PBS-buffered 4% paraformaldehyde. After 18–24 h, it was rinsed in Tris-buffered saline and soaked in 33% sucrose (2–4 h) for cryoprotection. It was then embedded in optimum cutting temperature embedding compound, rapidly frozen in liquid nitrogen, and cut into 50 μm sections using a cryostat (model OTF; Bright Instruments, Huntington, UK). Four floating sections per subject were subjected to melanin bleaching (0.25% KMnO4 for 15 min followed by 5% oxalic acid for 3 min), a 4-h protein block with a Tris-buffered saline solution of 5% normal swine serum, 0.5% powdered milk, and 1% Triton X-100, and overnight incubation with 1:1,200 Biogenesis polyclonal rabbit anti-human PGP 9.5 antibody (Serotec, Oxford, U.K.). Biotinylated swine anti-rabbit secondary antibody (1:300; DakoCytomation, Ely, U.K.) was then applied for 1 h; sections were quenched with 1% H2O2 in 30% MeOH-PBS (30 min) before a 1-h incubation with 1:500 horseradish peroxidase–Streptavidin (Vector Laboratories, Peterborough, U.K.). Nerve fibers were demonstrated using 3, 3́-diaminobenzidine chromogen (Sigma-Aldrich, Manchester, U.K.). Sections were mildly counterstained with eosin to better localize the basement membrane and identify nerve fibers passing through it. Negative controls consisted of replacing the anti-PGP9.5 antibody with rabbit immunoglobulin (DakoCytomation) at a concentration matching that of the primary antibody which showed no immunostaining. IENFD, i.e., the number of fibers per millimeter of basement membrane were quantified in accord with established criteria and expressed as number per millimeter (20).

8.3.5 Statistical analysis

SPSS for Mac (Version 19.0, IBM Corporation, New York, USA) was used for descriptive and frequency statistics and OriginPro for Windows (Version 8.5.0, Origin Lab, Northampton, MA, USA) was used to plot the data. One-way ANOVA (Scheffe Post-hoc test) was used to study differences between means. All data are expressed as mean ± standard error of mean (SEM).

8.4 Results

Clinical characteristics are summarized in table 1. Subjects with IGT and controls were matched for age. The IGT group had a higher BMI (31.7 ± 1.0 vs. 27.9 ± 1.2, p=0.02) and HbA1c (6.0 ± 0.2 / 43.9 ± 1.0 vs. 5.4 ± 0.1 / 36.0 ± 0.3 mmol/mol, P<0.001) with a lower total (4.8 ± 0.2 vs. 5.5 ± 0.2 mmol/l, p=0.02) and HDL (1.2 ± 0.1 vs. 1.7 ± 0.1 mmol/l, p<0.001) cholesterol compared to controls. There was no difference between groups in systolic/diastolic blood pressure (BP), eGFR, LDL cholesterol or triglycerides.

8.4.1 Peripheral Neuropathy Assessment

NSP (4.1 ± 1.0 vs. 0.5 ± 0.2, P<0.001) and McGill pain index (2.8 ± 0.3 vs. 0.2 ± 0.1, P<0.001) scores were significantly greater in the IGT group compared to controls. NDS (2.9 ± 0.5 vs. 0.6 ± 0.2, p=0.001) and VPT (15.9 ± 2.3 vs. 6.5 ± 1.1, p=0.002) were significantly greater in the IGT group compared to controls, indicating mild neuropathy. There was no significant difference in peroneal and sural nerve conduction velocity or amplitude between subjects with IGT and control subjects. WT (40.6 ± 0.8 vs. 37.6 ± 0.6, p=0.006) was

increased and CT (24.9 ± 1.3 vs. 27.5 ± 0.6, p=0.03) was decreased, with no difference in HRV in the subjects with IGT compared to controls. The percentage response for the neuropad was significantly reduced (P<0.05) in IGT subjects (table 2).

8.4.2 Skin Biopsy, Corneal Confocal Microscopy and Corneal Sensitivity

There was a significant reduction in IENFD (6.3 ± 0.6 vs. 9.1 ± 0.7, P = 0.03) in IGT compared to control subjects. CNFD (27.6 ± 1.2 vs. 37.4 ± 1.6, P < 0.001), CNBD (55.8 ± 6.0 vs. 89.2 ± 8.4, P = 0.02) and CNFL (22.1 ± 1.2 vs. 25.7 ± 1.2, P = 0.05) (figure 1) were significantly reduced in IGT compared to control subjects. There was no difference in corneal sensation threshold between IGT and control subjects (table 3).

8.4.3 Subjects with IGT and neuropathy

Under the assumption that CNFD is normally distributed in controls and IGT (Shapiro-Wilk W Test, P > 0.05) and based on a cut-off point = 2 standard deviations from the control average (CNFD = 24.0 no./mm2), subjects with IGT were re-stratified into two groups: those without (IGT) (n=22) [CNFD > 24.0 no./mm2, (range: 24.1-45.0)] and those with IGT neuropathy (IGTN) (n=15) [CNFD ≤ 24.0 no./mm2, (range: 24.0-12.5)] small fiber neuropathy (figure 1). There was a significantly greater self-reported pain intensity (McGill Pain Index, P = 0.04) and reduction in CNBD (P = 0.02) and CNFL (P<0.001) in subjects with IGTN compared to IGT (table 4).

8.5 Discussion

The United Kingdom Prospective Diabetes Study has shown that at diagnosis of type 2 diabetes, 5-7% of patients already have neuropathy (21) and longitudinal data from the Rochester cohort (22) have shown that duration and severity of exposure to hyperglycaemia are related to the severity of neuropathy. Hence studies have explored the contribution of minor and intermittent episodes of hyperglycaemia in subjects with IGT towards the development of neuropathy. Reduced epidermal innervation (9) sudomotor dysfunction (13) and electrodiagnostic abnormalities (14) have been found in up to 25% of patients with idiopathic sensory neuropathy and IGT. Indeed pain is a common feature amongst patients with idiopathic sensory neuropathy who are subsequently diagnosed with IGT (4; 15). Transient hyperglycaemia in experimental diabetes increases spontaneous discharge from nociceptive afferent C-fibers which is associated with neuropathic pain (23). The MONICA/KORA Augsburg Surveys (11) found a threefold increase in neuropathic pain in IGT, while the San Luis Valley study (10) found that impaired vibration sensation was present in 11.2% of subjects with IGT compared to only 3.5% in controls.

Sensory deficits can occur in ~50% of patients with established diabetes (24), but the natural history of neuropathy is not clear. Previous studies have demonstrated a reduction in IENFD in subjects with IGT (4; 9; 12), which improved after lifestyle intervention, suggesting that this early abnormality may be amenable to treatment (12). Dyck and associates (6) showed no increase in the prevalence of neuropathy in subjects with impaired glycaemia. However, it is important to note that their diagnosis of neuropathy was based on composite scores of an abnormality in nerve conduction studies, which assesses only large fibre abnormalities (25-

26). In the present study we also show no significant abnormality in neurophysiology in subjects with IGT. However, we show evidence of small fibre neuropathy with a significant reduction in IENFD and using CCM we also show a significant reduction in CNFD, CNBD and CNFL. This finding is in agreement with our previous work using CCM in patients with ISFN (15). Although we report a difference in sudomotor function, we found no difference in HRV however we did not perform a comprehensive assessment of autonomic function.

CCM provides the unique opportunity to assess unmyelinated C-fibers in vivo, and an increasing body of evidence suggests it may have good diagnostic (27-28) and prognostic value (16; 29-30). Indeed, CNFL has been shown to have good diagnostic validity using a range of definitions for DSPN (31) and has also been shown to be related to three independent measures of small fibre neuropathy (32). Furthermore, in our recent study (30), simultaneous pancreas and kidney transplantation in diabetic patients was associated with corneal nerve regeneration before an improvement in any other measure of DSPN. Similarly in a randomised placebo controlled study of patients with sarcoid neuropathy, ARA 290, a small peptide that antagonizes inflammatory processes and stimulates tissue repair, was shown to significantly improve corneal nerve fibre density (32). Davidson and colleagues (33) have demonstrated corneal nerve regeneration in experimental diabetes, suggesting that subbasal nociceptive C-fibers share physiological similarities with peripheral sensory nerves. Interestingly, a recent study has shown that corneal nerve loss precedes intraepidermal nerve fibre loss in two different animal models of diabetes (34). The present study extends our previous findings using CCM as it shows that corneal nerve injury occurs not only in overt

diabetes, but also in subjects with IGT. Indeed of relevance corneal nerve fibre loss was previously related to HbA1c in healthy control subjects (35).

A diagnostic biomarker is a parameter that provides information about the presence and the progress of a disease and the effects of treatment. We hypothesised that CCM-defined parameters could serve as such biomarkers in this study. At the time of examination a subgroup of subjects with IGT had evidence of neuropathy. We therefore tested whether individuals with IGT and a significant defect in CNFD exhibited more severe symptoms or signs of neuropathy compared to individuals with IGT and a normal CNFD. As expected, CNFL and CNBD were lower in those with a lower CNFD, but there were no differences in any of the other measures of neuropathy between the subgroups. Of note, subjects with IGT and a normal CNFD had a marginally higher McGill pain index, although both subgroups scored very low on the index. This is in contrast to previous studies which have shown a reduction in IENFD (36) and both IENF length and CNFL (26) in those with painful diabetic neuropathy and is likely to be of limited clinical significance given the subjective nature of the test and inter-subject variability in pain tolerance. However, of pathophysiological relevance, Cheng et al. (37) have recently found that pain in experimental neuropathy is associated with an upregulation in peptidergic IENFD and in a study in patients with painful diabetic neuropathy they showed increased nerve regeneration and axonal swelling (38). This therefore suggests that the relationship between pain and nerve structure is complex and requires further study.

In conclusion, this study shows that small fibre neuropathy is present in subjects with IGT and both skin biopsy and corneal confocal microscopy can detect this early abnormality.

Acknowledgements

This research was facilitated by the Manchester Biomedical Research Centre and the Greater Manchester Comprehensive Local Research Network.

Funding source

This research was funded by awards from: National Institutes of Health (R105991) and Juvenile Diabetes Research Foundation International (27-2008-362).

8.6 References

1. Fuller J, Shipley M, Rose G, Jarrett RJ, Keen H: Coronary-heart-disease risk and impaired glucose tolerance The Whitehall Study. The Lancet 1980;315:1373-1376.

2. Tapp RJ, Shaw JE, Zimmet PZ, Balkau B, Chadban SJ, Tonkin AM, Welborn TA, Atkins RC: Albuminuria is evident in the early stages of diabetes onset: results from the Australian Diabetes, Obesity, and Lifestyle Study (AusDiab). American journal of kidney diseases 2004;44:792-798.

3. Harris MI, Klein R, Welborn TA, Knuiman MW: Onset of NIDDM occurs at least 4–7 yr before clinical diagnosis. Diabetes Care 1992;15:815-819.

4. Singleton JR, Smith AG, Bromberg MB: Increased prevalence of impaired glucose tolerance in patients with painful sensory neuropathy. Diabetes Care 2001;24:1448-1453.

5. Sumner CJ, Sheth S, Griffin JW, Cornblath DR, Polydefkis M: The spectrum of neuropathy in diabetes and impaired glucose tolerance. Neurology 2003;60:108-111.

6. Dyck PJ, Clark VM, Overland CJ, Davies JL, Pach JM, Klein CJ, Rizza RA, Melton LJ, 3rd, Carter RE, Klein R, Litchy WJ: Impaired glycemia and diabetic polyneuropathy: the OC IG Survey. Diabetes Care 2012;35:584-591.

7. Singleton JR, Smith AG, Bromberg MB: Painful sensory polyneuropathy associated with impaired glucose tolerance. Muscle Nerve 2001;24:1225-1228.

8. Novella SP, Inzucchi SE, Goldstein JM: The frequency of undiagnosed diabetes and impaired glucose tolerance in patients with idiopathic sensory neuropathy. Muscle Nerve 2001;24:1229-1231.

9. Smith AG, Ramachandran P, Tripp S, Singleton JR: Epidermal nerve innervation in impaired glucose tolerance and diabetes-associated neuropathy. Neurology 2001;57:1701-1704.

10. Franklin GM, Kahn LB, Baxter J, Marshall JA, Hamman RF: Sensory neuropathy in non-insulin-dependent diabetes mellitus. The San Luis Valley Diabetes Study. Am J Epidemiol 1990;131:633-643.

11. Ziegler D, Rathmann W, Dickhaus T, Meisinger C, Mielck A: Neuropathic pain in diabetes, prediabetes and normal glucose tolerance: the MONICA/KORA Augsburg Surveys S2 and S3. Pain Med 2009;10:393-400.

12. Smith AG, Russell J, Feldman EL, Goldstein J, Peltier A, Smith S, Hamwi J, Pollari D, Bixby B, Howard J, Singleton JR: Lifestyle intervention for pre-diabetic neuropathy. Diabetes Care 2006;29:1294-1299.

13. Chow DC, Sletten DM, Oyama JK, Schatz IJ, Low PA: Impaired glucose tolerance is associated with postganglionic sudomotor impairment. Clinical Autonomic Research 2007;17:231-233.

14. Isak B, Oflazoğlu B, Tanrıdag T, Yitmen I, Us O: Evaluation of peripheral and autonomic neuropathy among patients with newly diagnosed impaired glucose tolerance. Diabetes/metabolism research and reviews 2008;24:563-569.

15. Tavakoli M, Marshall A, Pitceathly R, Fadavi H, Gow D, Roberts ME, Efron N, Boulton AJ, Malik RA: Corneal confocal microscopy: a novel means to detect nerve fibre damage in idiopathic small fibre neuropathy. Exp Neurol 2010;223:245-250.

16. Petropoulos IN, Alam U, Fadavi H, Asghar O, Green P, Ponirakis G, Marshall A, Boulton AJ, Tavakoli M, Malik RA: Corneal Nerve Loss Detected With Corneal Confocal Microscopy Is Symmetrical and Related to the Severity of Diabetic Polyneuropathy. Diabetes Care 2013:In Press.

17. Young M, Boulton A, MacLeod A, Williams D, Sonksen P: A multicentre study of the prevalence of diabetic peripheral neuropathy in the United Kingdom hospital clinic population. Diabetologia 1993;36:150-154.

18. Quattrini C, Jeziorska M, Tavakoli M, Begum P, Boulton A, Malik R: The Neuropad test: a visual indicator test for human diabetic neuropathy. Diabetologia 2008;51:1046-1050.

19. Tavakoli M, Kallinikos PA, Efron N, Boulton AJ, Malik RA: Corneal sensitivity is reduced and relates to the severity of neuropathy in patients with diabetes. Diabetes Care 2007;30:1895-1897.

20. Lauria G, Bakkers M, Schmitz C, Lombardi R, Penza P, Devigili G, Smith AG, Hsieh ST, Mellgren SI, Umapathi T: Intraepidermal nerve fiber density at the distal leg: a worldwide normative reference study. Journal of the Peripheral Nervous System 2010;15:202-207.

21. Anonymous: UK Prospective Diabetes Study 6. Complications in newly diagnosed type 2 diabetic patients and their association with different clinical and biochemical risk factors. Diabetes Res 1990;13:1-11.

22. Dyck P, Kratz K, Karnes J, Litchy W, Klein R, Pach J, Wilson D, O'Brien P, Melton L: The prevalence by staged severity of various types of diabetic neuropathy, retinopathy, and nephropathy in a population-based cohort The Rochester Diabetic Neuropathy Study. Neurology 1993;43:817-817.

23. Boulton A: What causes neuropathic pain? Journal of diabetes and its complications 1992;6:58-63.

24. Thomas P: Classification, differential diagnosis, and staging of diabetic peripheral neuropathy. Diabetes 1997;46:S54-S57.

25. Loseth S, Stalberg E, Jorde R, Mellgren SI: Early diabetic neuropathy: thermal thresholds and intraepidermal nerve fibre density in patients with normal nerve conduction studies. J Neurol 2008;255:1197-1202.

26. Quattrini C, Tavakoli M, Jeziorska M, Kallinikos P, Tesfaye S, Finnigan J, Marshall A, Boulton AJM, Efron N, Malik RA: Surrogate Markers of Small Fiber Damage in Human Diabetic Neuropathy. Diabetes 2007;56:2148-2154.

27. Tavakoli M, Quattrini C, Abbott C, Kallinikos P, Marshall A, Finnigan J, Morgan P, Efron N, Boulton AJ, Malik RA: Corneal confocal microscopy a novel noninvasive test to diagnose and stratify the severity of human diabetic neuropathy. Diabetes Care 2010;33:1792-1797.

28. Ahmed A, Bril V, Orszag A, Paulson J, Yeung E, Ngo M, Orlov S, Perkins BA: Detection of Diabetic Sensorimotor Polyneuropathy by Corneal Confocal Microscopy in Type 1 Diabetes A concurrent validity study. Diabetes Care 2012;35:821-828.

29. Sivaskandarajah GA, Halpern EM, Lovblom LE, Weisman A, Orlov S, Bril V, Perkins BA: Structure-Function Relationship Between Corneal Nerves and Conventional Small-Fiber Tests in Type 1 Diabetes. Diabetes Care 2013.

30. Tavakoli M, Mitu-Pretorian M, Petropoulos IN, Fadavi H, Asghar O, Alam U, Ponirakis G, Jeziorska M, Marshall A, Efron N, Boulton AJ, Augustine T, Malik RA: Corneal Confocal Microscopy Detects Early Nerve Regeneration in Diabetic Neuropathy After Simultaneous Pancreas and Kidney Transplantation. Diabetes 2013;62:254-260.

31. Halpern EM, Lovblom LE, Orlov S, Ahmed A, Bril V, Perkins BA: The impact of common variation in the definition of diabetic sensorimotor polyneuropathy on the validity of corneal in vivo confocal microscopy in patients with type 1 diabetes: a brief report. Journal of diabetes and its complications 2013;27:240-242.

32. Sivaskandarajah GA, Halpern EM, Lovblom LE, Weisman A, Orlov S, Bril V, Perkins BA: Structure-Function Relationship Between Corneal Nerves and Conventional Small-Fiber Tests in Type 1 Diabetes. Diabetes Care 2013;36:2748-2755.

33. Davidson EP, Coppey LJ, Yorek MA: Early loss of innervation of cornea epithelium in streptozotocin-induced type 1 diabetic rats: improvement with ilepatril treatment. Investigative ophthalmology & visual science 2012;53:8067-8074.

34. Chen DK, Frizzi KE, Guernsey LS, Ladt K, Mizisin AP, Calcutt NA: Repeated monitoring of corneal nerves by confocal microscopy as an index of peripheral neuropathy in type-1 diabetic rodents and the effects of topical insulin. Journal of the Peripheral Nervous System 2013.

35. Wu T, Ahmed A, Bril V, Orszag A, Ng E, Nwe P, Perkins BA: Variables associated with corneal confocal microscopy parameters in healthy volunteers: implications for diabetic neuropathy screening. Diabetic Medicine 2012;29:e297-e303.

36. Sorensen L, Molyneaux L, Yue DK: The Relationship Among Pain, Sensory Loss, and Small Nerve Fibers in Diabetes. Diabetes Care 2006;29:883-887.

37. Cheng HT, Dauch JR, Hayes JM, Yanik BM, Feldman EL: Nerve growth factor/p38 signaling increases intraepidermal nerve fiber densities in painful neuropathy of type 2 diabetes. Neurobiol Dis 2012;45:280-287.

38. Cheng HT, Dauch JR, Porzio MT, Yanik BM, Hsieh W, Smith AG, Singleton JR, Feldman EL: Increased Axonal Regeneration and Swellings in Intraepidermal Nerve Fibers Characterize Painful Phenotypes of Diabetic Neuropathy. The Journal of Pain 2013;14:941-947.

Table 8-1 CLINICAL AND METABOLIC PARAMETERS IN CONTROL AND IGT SUBJECTS

	Controls (n=20)	**IGT (n=37)**	**P value**
Age (years)	54.0 ± 2.0	57.7 ± 1.8	NS
BMI (Kg/m2)	27.9 ± 1.2	31.7± 1.0	0.02
Fasting glucose	<6.1	6.2 ± 0.8	
2 hour glucose	<7.8	9.3 ± 1.0	
HbA1c (%) / (mmol/mol)	5.4 ± 0.1 / 36.0 ± 0.3	6.0 ± 0.2 / 43.9 ± 1.0	<0.001
eGFR (mL/min/1.73 m2)	82.4 ± 1.7	81.0 ± 2.0	NS
Chol (mmol/l)	5.5 ± 0.2	4.8 ± 0.2	0.03
HDL (mmol/l)	1.7 ± 0.1	1.2 ± 0.1	<0.001
LDL (mmol/l)	3.2 ± 0.1	2.1 ± 0.2	NS
Trig (mmol/l)	1.7 ± 0.2	2.8 ± 0.2	NS
BP sys/dia (mmHg)	132 / 78	137 / 79	NS

Data are expressed as mean ± SEM, NS: not significant

Table 8-2 PERIPHERAL NEUROPATHY ASSESSMENT IN CONTROL AND IGT SUBJECTS

	Controls	IGT	P value
NSP	0.5 ± 0.2	4.1 ± 1.0	<0.001
McGill pain index	0.2 ± 0.1	2.8 ± 0.3	<0.001
NDS	0.6 ± 0.2	2.9 ± 0.5	<0.001
VPT (V)	6.5 ± 1.1	15.9 ± 2.3	0.002
CT (oC)	27.5 ± 0.6	24.9 ± 1.3	0.03
WT (oC)	37.6 ± 0.6	40.6 ± 0.8	0.006
HRV	12.4 ± 1.5	10.5 ± 1.2	NS
Neuropad (%)	93.0 ± 5.6	71.0 ± 2.8	0.05
SSNCV (m/s)	49.9 ± 1.0	49.9 ± 0.9	NS
SSNA (µV)	16.6 ± 1.9	14.0 ± 1.4	NS
PMNCV (m/s)	47.5 ± 0.7	45.6 ± 0.7	NS
PMNA (µV)	5.3 ± 0.5	4.6 ± 0.4	NS

Data are expressed as mean ± SEM, NS: not significant

Table 8-3 INTRA-EPIDERMAL AND CORNEAL NERVE ASSESSMENT AND CORNEAL SENSATION IN CONTROL AND IGT SUBJECTS

	Controls	IGT	P value
NCCA (mbar)	0.7 ± 0.2	1.1 ± 0.2	NS
CNFD (no./mm2)	37.4 ± 1.6	27.6 v 1.2	<0.001
CNBD (no/mm2)	89.2 ± 8.4	55.8 ± 6.0	0.002
CNFL (mm/mm2)	25.7 ± 1.2	22.1 ± 1.2	0.05
IENFD (no./mm)	9.1 ± 0.7	6.3 ± 0.6	0.03

Data are expressed as mean ± SEM, NS: not significant

Table 8-4 IGT SUBJECTS WITH NEUROPATHY BASED ON CNFD

	IGT (n=22)	IGTN (n=15)	P value
NSP	4.3 ± 1.0	3.7 ± 1.2	NS
McGill Analogue	5.8 ± 0.8	3.5 ± 1.2	NS
McGill Pain Index	2.6 ± 0.4	1.4 ± 0.5	0.04
NDS	2.9 ± 0.6	3.0 ± 0.7	NS
VPT (V)	15.8 ± 2.6	16.1 ± 3.3	NS
CS (^{o}C)	24.6 ± 1.7	25.3 ± 2.0	NS
WS (^{o}C)	40.7 ± 1.3	40.5 ± 1.4	NS
HRV	9.7 ± 1.5	11.6 ± 1.7	NS
Neuropad (%)	67.1 ± 8.3	69.0 ± 8.0	NS
CNFD (no./mm2)	31.8 ± 1.0	20.7 ± 1.3	<0.001
CNBD (no./mm2)	65.6 ± 8.2	39.6 ± 6.8	0.02
CNFL (mm/mm2)	25.3 ± 1.0	16.7 ± 1.1	<0.001
NCCA (mbar)	1.1 ± 0.3	1.7 ± 0.4	NS
IENFD (no./mm)	6.9 ± 0.9	6.4 ± 0.9	NS
SSNCV (m/s)	50.5 ± 1.3	49.7 ± 1.4	NS

SSNA (µV)	15.1 ± 2.0	12.7 ± 2.0	NS
PMNCV (m/s)	4.5 ± 0.9	4.8 ± 1.5	NS
PMNA (µV)	45.7 ± 0.4	45.5 ± 0.8	NS

Data are expressed as mean ± SEM, NS: not significant

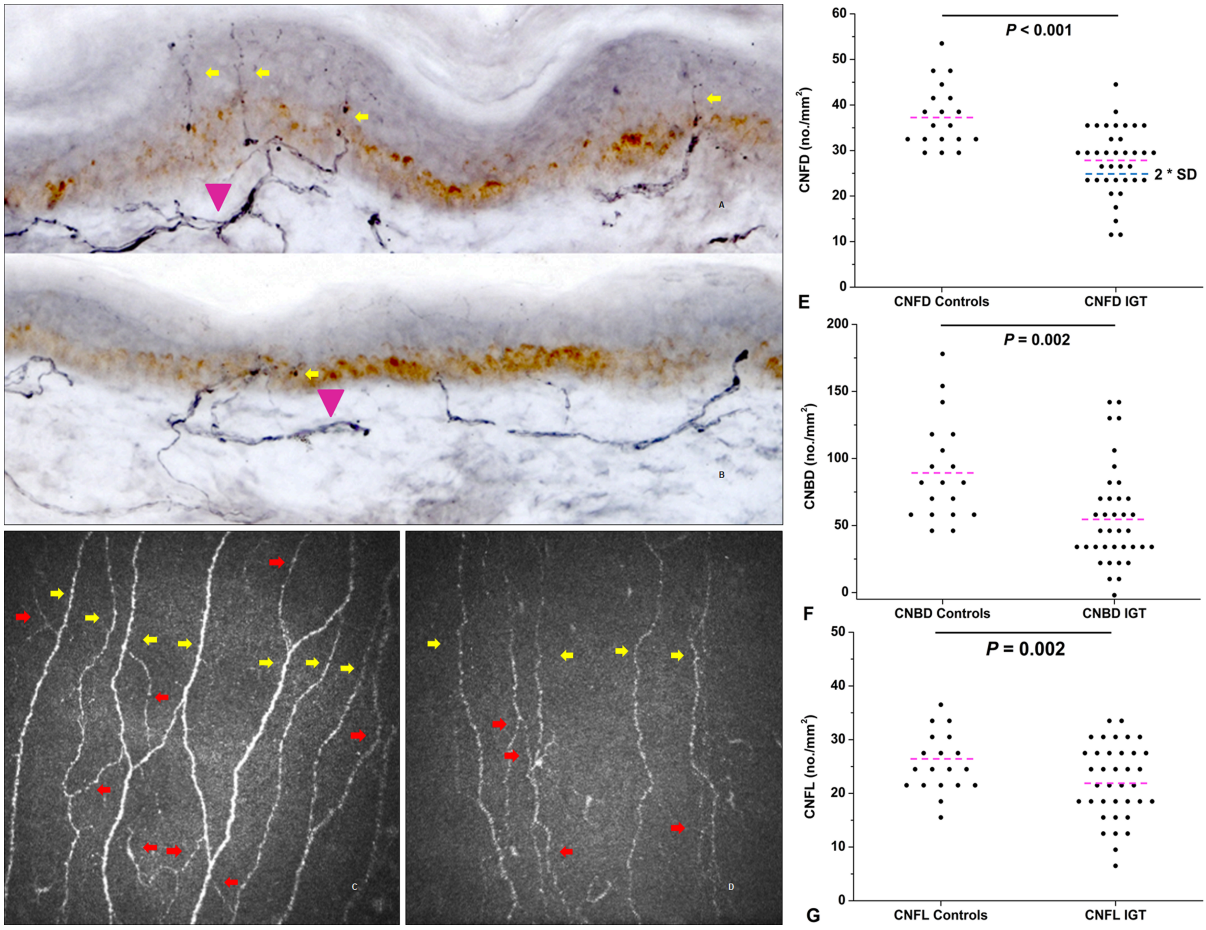

Figure 8-1 Data points represent actual corneal subbasal nerve parameters between controls (n=20) and subjects with IGT (n=37). Dashed lines represent group averages (values presented in table 8-3). A: CNFD, B: CNBD and C: CNFL. A Mann-Whitney U test was used for between group comparisons and the two-tailed P value is presented. Blue dashed line (1A) represents the diagnostic cut-off point for "risk of neuropathy" based on a mean – 2SD from controls.

Figure 8-2 Skin punch biopsies immunostained for PGP9.5 and corneal confocal microscopy images from a healthy control (A, C) and a subject with IGT (B, D). In (C) compared to (D) a significant reduction in nerve fibers (yellow arrows) and nerve branches (red arrows) is observed, which mirrors the reduction in intra-epidermal nerve fibers (yellow arrows) reaching the upper levels of epidermis in (B) compared to (A). The sub-epidermal nerve plexus is also visible (purple arrowhead).

9 Discussion

9.1 IGT and Cardiac Sympathetic Innervation

In the only published study of MIBG in subjects with IGT to date, the authors reported significantly reduced late HMR compared to healthy controls (1). The IGT cohort in this study was highly selected as the vast majority of subjects had a positive family history of DM. Furthermore, they reported regional defects in tracer uptake, predominantly affecting the apex and inferior wall in 20 of the 22 subjects with IGT.

Our findings challenge the existing literature in IGT. First, we confirm the findings of previous studies in healthy subjects demonstrating that such "defects" in the inferior wall and apex are in fact normal findings in healthy subjects (2-6). Furthermore, we show that subjects with IGT, despite an adverse CV risk profile, demonstrate normal global and detailed regional cardiac sympathetic innervation. Although regional analysis revealed reduced regional uptake in the anterior wall in some of our IGT subjects, the functional significance of this is uncertain given that there were no differences in autonomic function or WR between IGT subjects with and without such a defect. Whilst such findings may infer that this sub-set of individuals with IGT may be at greater risk of developing clinically silent cardiac dysinnervation, this will require longitudinal studies.

Studies in IGT cohorts have reported the presence of CAN (7) in some studies but not others (8,9). We found no evidence of CAN in our IGT cohort. CAN may represent a late manifestation of IGT and abnormalities in cardiac MIBG scintigraphy may not become apparent until advanced CAN (10). Further research is clearly indicated to establish when in

the natural history of subjects with IGT, CAN and sympathetic denervation develop to enable risk stratification and guide possible therapeutic intervention

A perceived weakness of our study may be the small study population, however, they were representative of uncomplicated subjects from primary care undergoing an OGTT. The strengths of the study lie in the detailed structural and functional cardiac phenotyping using gold standard imaging modalities, notably CMR. In addition, MIBG scintigraphy was carried out according recommended international standards (11).

9.2 Cardiac Structure and Function in IGT

CMR data on cardiac structure and function in IGT are limited. Previous studies in IGT cohorts have mostly used echocardiographic studies for cardiac imaging and have reported increased LVMI in subjects with IGT (11-19). In our study, subjects with IGT had comparable LVEF, LVMI and concentricity to healthy age matched controls; findings which challenge the existing literature in this group. The Multi Ethnic Study of Atherosclerosis (MESA) and the Framingham Offspring cohort study were both studies using CMR for cardiac imaging and in which LVM was associated with glycemia in subjects with impaired fasting glucose (IFG) and DM (20-25). The methodology for deriving LVM and volumes in these studies was subject to a number of limitations; the use of short axis slices alone presents difficulty in determining the true basal LV slice, end-diastole and end-systole. Furthermore, it is not clear whether their analyses included papillary muscles and trabeculae in their cavity volumes rather than within the mass. We used validated 3D modeling methods for volumetric and structural analysis in our study, which provide accurate and reproducible measurement of

LV mass and volumes (12,26). Furthermore, we used 3 different methods to calculate LVMI, to adjust for the increased BMI in our IGT group and are therefore confident that our data are robust and meaningful.

Similarly, studies of diastolic function in IGT cohorts have been limited by relatively insensitive measures of diastolic dysfunction (10,27-30). Studies using CMR are lacking. We found no differences in radial, circumferential and longitudinal strain and strain rates between subjects with IGT and healthy controls.

Coronary microvascular dysfunction is a feature of pre-diabetes and insulin resistance (12,31). Using quantitative CMR assessment of MBF, we found normal resting and stress MBF in subjects with IGT indicating that these individuals do not have evidence of coronary microvascular disease.

Although extensively studied in animal models of DM, the need for endomyocardial biopsy has limited the study of myocardial fibrosis in man (32). Fischer et al demonstrated interstitial fibrosis in myocardial biopsy, but did not differentiate subjects with IGT from those with diabetes (33). T1 mapping has been utilised to demonstrate fibrosis associated with impaired systolic and diastolic function and biomarkers of fibrosis in patients with type 1 and 2 diabetes (34-36). Quantitative assessment of myocardial extracellular volume (ECV), a surrogate of myocardial fibrosis, shows much promise and has been recently validated in man (37-39). In the only such study published to date, diabetic subjects showed ECV expansion (40). In our study we found no differences in ECV between subjects with IGT and

healthy controls, indicating that subjects with IGT do not have myocardial fibrosis and suggesting that this may be a late abnormality.

In conclusion, IGT is not associated with an adverse structural and functional cardiac phenotype with no evidence of fibrosis or microvascular disease when assessed by detailed and comprehensive multiparametric CMR. Whilst these data conflict with existing data in subjects with IGT, these studies used echocardiography, which is clearly less sensitive than CMR. Further larger and in particular longitudinal studies are required to establish when individuals with IGT develop the early pathognomonic features of diabetic cardiomyopathy.

9.3 Neuropathy in IGT

The United Kingdom Prospective Diabetes Study has shown that at diagnosis of type 2 diabetes, 5-7% of patients already have neuropathy (21) and longitudinal data from the Rochester cohort (22) have shown that duration and severity of exposure to hyperglycaemia are related to the severity of neuropathy. Hence studies have explored the contribution of minor and intermittent episodes of hyperglycaemia in subjects with IGT towards the development of neuropathy. Reduced epidermal innervation (9) sudomotor dysfunction (13) and electrodiagnostic abnormalities (14) have been found in up to 25% of patients with idiopathic sensory neuropathy and IGT. Indeed pain is a common feature amongst patients with idiopathic sensory neuropathy who are subsequently diagnosed with IGT (4; 15). Transient hyperglycaemia in experimental diabetes increases spontaneous discharge from nociceptive afferent C-fibers which is associated with neuropathic pain (23). The MONICA/KORA Augsburg Surveys (11) found a threefold increase in neuropathic pain in

IGT, while the San Luis Valley study (10) found that impaired vibration sensation was present in 11.2% of subjects with IGT compared to only 3.5% in controls.

Sensory deficits can occur in ~50% of patients with established diabetes (24), but the natural history of neuropathy is not clear. Previous studies have demonstrated a reduction in IENFD in subjects with IGT (4; 9; 12), which improved after lifestyle intervention, suggesting that this early abnormality may be amenable to treatment (12). Dyck and associates (6) showed no increase in the prevalence of neuropathy in subjects with impaired glycaemia. However, it is important to note that their diagnosis of neuropathy was based on composite scores of an abnormality in nerve conduction studies, which assesses only large fibre abnormalities (25-26). In the present study we also show no significant abnormality in neurophysiology in subjects with IGT. However, we show evidence of small fibre neuropathy with a significant reduction in IENFD and using CCM we also show a significant reduction in CNFD, CNBD and CNFL. This finding is in agreement with our previous work using CCM in patients with ISFN (15).

CCM provides the unique opportunity to assess unmyelinated C-fibers in vivo, and an increasing body of evidence suggests it may have good diagnostic (27-28) and prognostic value (16; 29-30). Indeed, CNFL has been shown to have good diagnostic validity using a range of definitions for DSPN (31) and has also been shown to be related to three independent measures of small fibre neuropathy (32). Furthermore, in our recent study (30), simultaneous pancreas and kidney transplantation in diabetic patients was associated with corneal nerve regeneration before an improvement in any other measure of DSPN. Similarly in a randomised placebo controlled study of patients with sarcoid neuropathy, ARA 290, a

small peptide that antagonizes inflammatory processes and stimulates tissue repair, was shown to significantly improve corneal nerve fibre density (32). Davidson and colleagues (33) have demonstrated corneal nerve regeneration in experimental diabetes, suggesting that subbasal nociceptive C-fibers share physiological similarities with peripheral sensory nerves. Interestingly, a recent study has shown that corneal nerve loss precedes intraepidermal nerve fibre loss in two different animal models of diabetes (34). The present study extends our previous findings using CCM as it shows that corneal nerve injury occurs not only in overt diabetes, but also in subjects with IGT. Indeed of relevance corneal nerve fibre loss was previously related to HbA1c in healthy control subjects (35).

A diagnostic biomarker is a parameter that provides information about the presence and the progress of a disease and the effects of treatment. We hypothesised that CCM-defined parameters could serve as such biomarkers in this study. At the time of examination a proportion of subjects with IGT had evidence of neuropathy. Therefore, we tested whether individuals with IGT and a significant defect in CNFD exhibited more severe symptoms or signs of neuropathy compared to individuals with IGT and a normal CNFD. As expected all three corneal nerve parameters were lower in those with a lower CNFD, but there was no difference for any other measure of neuropathy. However, interestingly subjects with IGT and a normal corneal nerve density had significantly greater self-reported pain. This is in contrast to previous studies which have shown a reduction in IENFD (36) and both IENF length and CNFL (26) in those with painful diabetic neuropathy. However, of pathophysiological relevance, Cheng et al. (37) have recently found that pain in experimental neuropathy is associated with an upregulation in peptidergic IENFD and in a study in patients

with painful diabetic neuropathy they showed increased nerve regeneration and axonal swelling (38). This therefore suggests that the relationship between pain and nerve structure is complex and requires further study.

In conclusion, our study shows that small fibre neuropathy is present in subjects with IGT and both skin biopsy and corneal confocal microscopy can detect this early abnormality.

9.3.1 Cardiac Sympathetic Innervation in Type 1 Diabetes of Extreme Duration

Medalists represent a unique group of patients with an extreme duration of Type 1 diabetes. This is the first study to investigate in detail, the presence and extent of cardiac sympathetic innervation and cardiac autonomic function in such a group of individuals.

Abnormal MIBG uptake has been demonstrated in both recently diagnosed and long duration type 1 diabetes (20,22,25). Stevens et al investigated cardiac innervation in patients with T1 diabetes with and without diabetic autonomic neuropathy (DAN), diagnosed using standard cardiovascular reflex tests (12). Using [11C]-HED PET imaging, they reported the presence of innervation defects in 40% of subjects without clinical DAN, which was characterized by distal deficits in tracer retention with preservation of the proximal myocardial segments. Whilst in subjects with severe DAN, there was evidence of proximal hyperinnervation but normal sympathetic tone, suggesting a compensatory proximal reinnervation in response to distal neuronal loss in severe DAN. Using MIBG scintigraphy we demonstrate that global MIBG uptake and washout in subjects with type 1 diabetes of extreme duration, are comparable to healthy controls. Whilst there is a more pronounced regional heterogeneity in MIBG uptake in diabetic patients, this pattern is consistent with that observed in healthy

controls. There was no difference in total and modified uptake scores on SPECT analysis, and although there was a significantly lower uptake in the inferior, basal and apical segments in the diabetic group this was similar in pattern to the control group. This regional heterogeneity in the control group is consistent with previously published data in healthy adults including the recent ADMIRE-HF study (2-6,41,42). The further reduction in regional uptake in our diabetic group may simply be explained by the effects of age, as they were older and the effects of age on MIBG have been previously reported (2,3,43,44). Irrespective of regional defects, HMR was comparable to healthy controls and HMR has been shown to be of prognostic significance in diabetic subjects (3,5,45). Despite almost half a century of persistent hyperglycemia these patients show no evidence of cardiac sympathetic denervation. Poor glycemic control is associated with a reduction in MIBG uptake (43,44,46,47), hence our findings provide further evidence of protection from complications in this unique group of patients.

CAN is a recognised complication of DM, often present at diagnosis and is an independent predictor of morbidity and mortality (17,19). However, again despite the long duration of moderate glycemic control, in our study the majority of cardiac parasympathetic autonomic function tests were normal. There was a borderline abnormal Valsalva ratio and RFa, suggestive of minimal parasympathetic dysfunction. However, LFa and the LFA/RFa ratio were normal indicating no evidence of cardiac sympathetic dysfunction in these patients with an extreme duration of diabetes.

9.4 Cardiac Structure and Function in Type 1 Diabetes of Extreme Duration

Medalists represent a unique group of patients with an extreme duration of Type 1 diabetes and a variable degree of microvascular and macrovascular complications. As such they constitute a special phenotype, which merits further study, especially given the excess cardiovascular mortality in patients with Type 1 diabetes, even in those with good glycemic control (48). Detailed cardiac studies in medalist cohorts identifying the exact phenotype are lacking. This is the first study to investigate in detail, cardiac structure, function and myocardial blood flow in a cohort of patients with an extreme duration of diabetes, including medalists (8/13).

In our study we show that extreme duration patients with Type 1 diabetes have no evidence of CHD and normal LVEF, but a lower LVMI. We have employed robust, validated and reproducible 3D modeling methods for volumetric and structural analyses by using long axis in addition to short axis slices and threshold-based contouring to identify myocardium (26). Furthermore, we have used 3 different methods to calculate LVMI to adjust for BMI. These data are not consistent with the reported association between HbA1c and CMR findings in the DCCT cohort, although LVMI was higher and LVEF was lower, only in patients with prior CVD, and there was no difference between the conventional and intensively treated patients (49). This is interesting in the context of the recent analysis showing markedly increased mortality in T1DM (8%) v controls (2.9%) and a clear relationship between poorer glycemic control and renal impairment with worse outcomes (48). In the present study, there is clearly protection from the development of left ventricular hypertrophy and a reduction in ejection fraction in these patients.

We have found no differences in longitudinal, radial and circumferential function in patients with extreme duration Type 1 diabetes. Whilst the majority of previous studies have used echocardiography to show early diastolic dysfunction in patients with Type 2 diabetes, a recent CMR study has shown diastolic function in young people with Type 2 diabetes (50) and a reduction in left ventricular longitudinal myocardial deformation has also been demonstrated in children with Type 1 diabetes (51). A lack of CMR evidence of diastolic dysfunction is in keeping with our recent echocardiographic study also showing only mild evidence of diastolic dysfunction (52) and therefore clearly warrants further study.

Studies in patients with Type 1 diabetes have demonstrated a reduction in myocardial blood flow in relation to sympathetic dysfunction (53,54). Quantitative CMR assessment of MBF is an emerging technology which shows much promise and is an attractive validated alternative to positron emission tomography (PET) in the assessment of microvascular dysfunction (55). To date, there are no published studies of CMR derived MBF in diabetic subjects. We found no differences in resting and stress MBF between patients with extreme duration Type 1 diabetes and controls, however, the stress/rest ratio, an index of coronary microvascular perfusion reserve, was significantly lower in the diabetic group. Coronary microvascular dysfunction may partly be mediated through cardiac autonomic dysfunction, however, these patients have minimal evidence of cardiac autonomic neuropathy (unpublished data).

Although extensively studied in animal models of DM, the need for endomyocardial biopsy has limited the study of myocardial fibrosis in man (32) (33). Previous studies have demonstrated myocardial fibrosis in subjects with T2DM and metabolic syndrome using integrated back scatter (56-58). In a recent study correalting histology with CMR, the latter

was shown to be a highly accurate, non-invasive assessment of regional myocardial fibrosis using LGE and diffuse interstitial myocardial fibrosis, using post-contrast T1 mapping (59). Furthermore, T1 mapping using CMR, has shown that fibrosis is associated with impaired systolic and diastolic function and biomarkers of fibrosis in patients with type 1 and 2 diabetes (34-36). Quantitative assessment of myocardial extracellular volume (ECV), a surrogate of myocardial fibrosis, shows much promise and has been recently validated in man (37-39). In the only study published to date using ECV quantification in diabetic subjects, DM was associated with ECV expansion, HF admission to hospital and death (40). We report an increase in ECV in our patients with Type 1 diabetes compared to healthy controls. However, the clinical relevance of this mild degree of myocardial fibrosis is questionable given the absence of LV mechanical dysfunction, microvascular and autonomic dysfunction.

A perceived weakness of the current study may be the small study population, however we believe the detailed structural and functional cardiac phenotyping in this unique cohort of extreme duration patients with Type 1 diabetes presents novel data. It confirms that these unique individuals are indeed protected from the long term complications of diabetes, warranting further studies to establish the basis of this protection.

9.5 References

1. Diakakis G, Parthenakis F, Patrianakos A, Koukouraki S, Stathaki M, Karkavitsas N, et al. Myocardial sympathetic innervation in patients with impaired glucose tolerance: relationship to subclinical inflammation. Cardiovascular Pathology. 2008;17(3):172–7.

2. Gill JS, Hunter GJ, Gane G, Camm AJ. Heterogeneity of the human myocardial sympathetic innervation: in vivo demonstration by iodine 123-labeled meta-iodobenzylguanidine scintigraphy. American Heart Journal. 1993 Aug 1;126(2):390–8.

3. Tsuchimochi S, Tamaki N, Tadamura E, Kawamoto M, Fujita T, Yonekura Y, et al. Age and gender differences in normal myocardial adrenergic neuronal function evaluated by iodine-123-MIBG imaging. J Nucl Med. 1995 Jun;36(6):969–74.

4. Somsen GA, Verberne HJ, Fleury E, Righetti A. Normal values and within-subject variability of cardiac I-123 MIBG scintigraphy in healthy individuals: implications for clinical studies. J Nucl Cardiol. 2004 Feb;11(2):126–33.

5. Morozumi T, Kusuoka H, Fukuchi K. Myocardial iodine-123-metaiodobenzylguanidine images and autonomic nerve activity in normal subjects. J Nucl Med.1997;38:49-52.

6. Kimura K, Ieda M, Fukuda K. Development, Maturation, and Transdifferentiation of Cardiac Sympathetic Nerves. Circulation Research. 2012 Jan 19;110(2):325–36.

7. Isak B, Oflazoglu B, Tanridag T, Yitmen I, Us O. Evaluation of peripheral and autonomic neuropathy among patients with newly diagnosed impaired glucose tolerance. Diabetes Metab Res Rev. 2008 Oct;24(7):563–9.

8. Putz Z, Nemeth N, Istenes I, Martos T, Gandhi RA, Körei AE, et al. Autonomic dysfunction and circadian blood pressure variations in people with impaired glucose tolerance. Diabet Med. 2013 Mar;30(3):358–62.

9. Putz Z, Tabak AG, Toth N, Istenes I, Nemeth N, Gandhi RA, et al. Noninvasive Evaluation of Neural Impairment in Subjects With Impaired Glucose Tolerance. Diabetes Care. 2009 Jan 1;32(1):181–3.

10. Watkins LL, Surwit RS, Grossman P, Sherwood A. Is there a glycemic threshold for impaired autonomic control? Diabetes Care. 2000 Jun;23(6):826–30.

11. Flotats A, Carrió I, Agostini D, Guludec D, Marcassa C, Schaffers M, et al. Proposal for standardization of 123I-metaiodobenzylguanidine (MIBG) cardiac sympathetic imaging by the EANM Cardiovascular Committee and the European Council of Nuclear Cardiology. Eur J Nucl Med Mol Imaging. 2010 Jun 25;37(9):1802–12.

12. Stevens MJ, Raffel DM, Allman KC, Dayanikli F, Ficaro E, Sandford T, et al. Cardiac sympathetic dysinnervation in diabetes: implications for enhanced cardiovascular risk. Circulation. 1998 Sep 8;98(10):961–8.

13. Rutter MK. Impact of Glucose Intolerance and Insulin Resistance on Cardiac Structure and Function: Sex-Related Differences in the Framingham Heart Study. Circulation. 2003 Jan 28;107(3):448–54.

14. Chen J, Folks RD, Verdes L, Manatunga DN, Jacobson AF, Garcia EV. Quantitative I-123 mIBG SPECT in differentiating abnormal and normal mIBG myocardial uptake. J Nucl Cardiol. 2011 Dec 7;19(1):92–9.

15. Henry R, Kamp O, Kostense P, Spijkerman A, Dekker J, van Eijck R, et al. Left ventricular mass increases with deteriorating glucose tolerance, especially in women: independence of increased arterial stiffness or decreased flow-mediated dilation. Diabetes Care. 2004;27(2):522.

16. Ilercil A. Relationship of impaired glucose tolerance to left ventricular structure and function: The Strong Heart Study. American Heart Journal. 2001 Jun 1;141(6):992–8.

17. Vinik AI, Ziegler D. Diabetic Cardiovascular Autonomic Neuropathy. Circulation. 2007 Jan 8;115(3):387–97.

18. Chaturvedi N. A comparison of left ventricular abnormalities associated with glucose intolerance in African Caribbeans and Europeans in the UK. Heart. 2001 Jun 1;85(6):643–8.

19. Pop-Busui R, Evans GW, Gerstein HC, Fonseca V, Fleg JL, Hoogwerf BJ, et al. Effects of cardiac autonomic dysfunction on mortality risk in the Action to Control Cardiovascular Risk in Diabetes (ACCORD) trial. Diabetes Care. 2010 Jul;33(7):1578–84.

20. Schnell O, Muhr D, Weiss M, Dresel S, Haslbeck M, Standl E. Reduced myocardial 123I-metaiodobenzylguanidine uptake in newly diagnosed IDDM patients. Diabetes. 1996 Jun;45(6):801–5.

21. Bertoni A, Goff D, D Agostino R, Liu K, Hundley W, Lima J, et al. Diabetic Cardiomyopathy and Subclinical Cardiovascular Disease. Diabetes Care. 2006;29(3):588.

22. Schnell O, Kirsch CM, Stemplinger J, Haslbeck M, Standl E. Scintigraphic evidence for cardiac sympathetic dysinnervation in long-term IDDM patients with and without ECG-based autonomic neuropathy. Diabetologia. 1995 Nov;38(11):1345–52.

23. Velagaleti RS, Gona P, Chuang ML, Salton CJ, Fox CS, Blease SJ, et al. Relations of Insulin Resistance and Glycemic Abnormalities to Cardiovascular Magnetic Resonance Measures of Cardiac Structure and Function: The Framingham Heart Study. Circulation: Cardiovascular Imaging. 2010 May 1;3(3):257–63.

24. Langer A, Freeman MR, Josse RG, Armstrong PW. Metaiodobenzylguanidine imaging in diabetes mellitus: assessment of cardiac sympathetic denervation and its relation to autonomic dysfunction and silent myocardial ischemia. JAC. 1995 Mar 1;25(3):610–8.

25. Kreiner G, Wolzt M, Fasching P, Leitha T, Edlmayer A, Korn A, et al. Myocardial m-[123I]iodobenzylguanidine scintigraphy for the assessment of adrenergic cardiac innervation in patients with IDDM. Comparison with cardiovascular reflex tests and relationship to left ventricular function. Diabetes. 1995 May;44(5):543–9.

26. Miller CA, Jordan P, Borg A, Argyle R, Clark D, Pearce K, et al. Quantification of left ventricular indices from SSFP cine imaging: Impact of real-world variability in analysis methodology and utility of geometric modeling. J Magn Reson Imaging. 2012 Nov 2;37(5):1213–22.

27. Henry R, Paulus W, Kamp O, Kostense P, Spijkerman A, Dekker J, et al. Deteriorating glucose tolerance status is associated with left ventricular dysfunction-the Hoorn Study. Neth J Med. 2008;66:110–7.

28. Okura H, Inoue H, Tomon M, Nishiyama S, Yoshikawa T, Yoshida K, et al. Impaired glucose tolerance as a determinant of early deterioration of left ventricular diastolic function in middle-aged healthy subjects. The American Journal of Cardiology. 2000;85(6):790.

29. Fujita M, Asanuma H, Kim J, Liao Y, Hirata A, Tsukamoto O, et al. Impaired glucose tolerance: a possible contributor to left ventricular hypertrophy and diastolic dysfunction. International Journal of Cardiology. 2007 May 16;118(1):76–80.

30. Shimabukuro M, Higa N, Asahi T, Yamakawa K, Oshiro Y, Higa M, et al. Impaired glucose tolerance, but not impaired fasting glucose, underlies left ventricular diastolic dysfunction. Diabetes Care. 2011 Mar;34(3):686–90.

31. Schelbert HR. Coronary Circulatory Function Abnormalities in Insulin Resistance. JAC. American College of Cardiology Foundation; 2009 Feb 3;53(5):S3–S8.

32. Asbun J, Villarreal F. The pathogenesis of myocardial fibrosis in the setting of diabetic cardiomyopathy. Journal of the American College of Cardiology. 2006;47(4):693–700.

33. Fischer VW, Fischer VW, Fischer VW, Fischer VW, Barner HB, Barner HB, et al. Pathomorphologic aspects of muscular tissue in diabetes mellitus. Human pathology [Internet]. 1984 Dec;15(12):1127–36.

34. Ng ACT, Auger D, Delgado V, van Elderen SGC, Bertini M, Siebelink HM, et al. Association Between Diffuse Myocardial Fibrosis by Cardiac Magnetic Resonance Contrast-Enhanced T1 Mapping and Subclinical Myocardial Dysfunction in Diabetic Patients: A Pilot Study. Circulation: Cardiovascular Imaging. 2012 Jan 17;5(1):51–9.

35. Jellis C, Wright J, Kennedy D, Sacre J, Jenkins C, Haluska B, et al. Association of Imaging Markers of Myocardial Fibrosis with Metabolic and Functional Disturbances in Early Diabetic Cardiomyopathy. Circulation: Cardiovascular Imaging. 2011 Sep 23.

36. Messroghli DR, Radjenovic A, Kozerke S, Higgins DM, Sivananthan MU, Ridgway JP. Modified Look-Locker inversion recovery (MOLLI) for high-resolutionT1 mapping of the heart. Magn Reson Med. 2004;52(1):141–6.

37. Flett AS, Hayward MP, Ashworth MT, Hansen MS, Taylor AM, Elliott PM, et al. Equilibrium Contrast Cardiovascular Magnetic Resonance for the Measurement of Diffuse Myocardial Fibrosis: Preliminary Validation in Humans. Circulation. 2010 Jul 12;122(2):138–44.

38. Miller CA, Naish JH, Bishop P, Coutts G, Clark D, Zhao S, et al. Comprehensive Validation of Cardiovascular Magnetic Resonance Techniques for the Assessment of Myocardial Extracellular Volume. Circulation: Cardiovascular Imaging. 2013 May 21;6(3):373–83.

39. Aus dem Siepen F, Buss SJ, Messroghli D, Andre F, Lossnitzer D, Seitz S, et al. T1 mapping in dilated cardiomyopathy with cardiac magnetic resonance: quantification of diffuse myocardial fibrosis and comparison with endomyocardial biopsy. European Heart Journal - Cardiovascular Imaging. 2014 Sep 22.

40. Wong TC, Piehler KM, Kang IA, Kadakkal A, Kellman P, Schwartzman DS, et al. Myocardial extracellular volume fraction quantified by cardiovascular magnetic resonance is increased in diabetes and associated with mortality and incident heart failure admission. European Heart Journal. 2014 Mar;35(10):657–64.

41. Kawano H, Okada R, Yano K. Histological study on the distribution of autonomic nerves in the human heart. Heart Vessels. 2003 Mar;18(1):32–9.

42. Armour JA. Functional anatomy of intrathoracic neurons innervating the atria and ventricles. HRTHM. Elsevier Inc; 2010 Jul 1;7(7):994–6.

43. Sakata K, Iida K, Mochizuki N, Ito M, Nakaya Y. Physiological changes in human cardiac sympathetic innervation and activity assessed by (123)I-metaiodobenzylguanidine (MIGB) imaging. Circ J. 2009 Feb;73(2):310–5.

44. Sakata K, Shirotani M, Yoshida H, Kurata C. Physiological fluctuation of the human left ventricle sympathetic nervous system assessed by iodine-123-MIBG. J Nucl Med. 2014 Oct 28;39(10):1667–71.

45. Nagamachi S, Fujita S, Nishii R, Futami S, Tamura S, Mizuta M, et al. Prognostic value of cardiac I-123 metaiodobenzylguanidine imaging in patients with non–insulin-dependent diabetes mellitus. J Nucl Cardiol. 2006 Jan;13(1):34–42.

46. Ziegler D, Weise F, Langen KJ, Piolot R, Boy C, Hübinger A, et al. Effect of glycaemic control on myocardial sympathetic innervation assessed by [123I]metaiodobenzylguanidine scintigraphy: a 4-year prospective study in IDDM patients. Diabetologia. 1998 Apr;41(4):443–51.

47. D'Alto M, Maurea S, Basso A, Varrella P, Polverino W, Bianchi U, et al. [The heterogeneity of myocardial sympathetic innervation in normal subjects: an assessment by iodine-123 metaiodobenzylguanidine scintigraphy]. Cardiologia. 1998 Nov;43(11):1231–6.

48. Lind M, Svensson A-M, Kosiborod M, Gudbjörnsdottir S, Pivodic A, Wedel H, et al. Glycemic Control and Excess Mortality in Type 1 Diabetes. N Engl J Med. 2014 Nov 20;371(21):1972–82.

49. Genuth SM, Backlund J-YC, Bayless M, Bluemke DA, Cleary PA, Crandall J, et al. Effects of prior intensive versus conventional therapy and history of glycemia on cardiac function in type 1 diabetes in the DCCT/EDIC. Diabetes. 2013 Oct;62(10):3561–9.

50. Khan JN, Wilmot EG, Leggate M, Singh A, Yates T, Nimmo M, et al. Subclinical diastolic dysfunction in young adults with Type 2 diabetes mellitus: a multiparametric contrast-enhanced cardiovascular magnetic resonance pilot study assessing potential mechanisms. European Heart Journal - Cardiovascular Imaging. 2014 Oct 24;15(11):1263–9.

51. Labombarda F, Leport M, Morello R, Ribault V, Kauffman D, Brouard J, et al. Longitudinal left ventricular strain impairment in type 1 diabetes children and adolescents: a 2D speckle strain imaging study. Diabetes Metab. 2014 Sep;40(4):292–8.

52. Fagan A, Asghar O, Pearce K, Stout M, Ray SG, Schmitt M, et al. Medalists With Extreme Duration of Type 1 Diabetes Exhibit Only Mild Diastolic Dysfunction and Myocardial Fibrosis. Diabetes Care. 2015 ed. 38:e1–e2.

53. Pop-Busui R, Kirkwood I, Schmid H, Marinescu V, Schroeder J, Larkin D, et al. Sympathetic dysfunction in type 1 diabetes. Journal of the American College of Cardiology. 2004 Dec;44(12):2368–74.

54. Hattori N, Rihl J, Bengel F, Nekolla S. Cardiac autonomic dysinnervation and myocardial blood flow in long-term Type 1 diabetic patients. Diabetic Medicine 2003.

55. Miller CA, Naish JH, Ainslie MP, Tonge C, Tout D, Arumugam P, et al. Voxel-wise quantification of myocardial blood flow with cardiovascular magnetic resonance: effect of variations in methodology and validation with positron emission tomography. Journal of Cardiovascular Magnetic Resonance. Journal of Cardiovascular Magnetic Resonance; 2014 Jan 24;16(1):1–15.

56. Fang Z, Yuda S, Anderson V, Short L, Case C, Marwick T. Echocardiographic detection of early diabetic myocardial disease* 1. Journal of the American College of Cardiology. 2003;41(4):611–7.

57. Kosmala W, Przewlocka-Kosmala M, Szczepanik-Osadnik H, Mysiak A, O'Moore-Sullivan T, Marwick TH. A Randomized Study of the Beneficial Effects of Aldosterone Antagonism on LV Function, Structure, and Fibrosis Markers in Metabolic Syndrome. JCMG. Elsevier Inc; 2011 Dec 1;4(12):1239–49.

58. Marwick TH, Raman SV, Carrió I, Bax JJ. Recent Developments in Heart Failure Imaging. JCMG. 2011 Jan 14;3(4):429–39.

59. Iles LM, Ellims AH, Llewellyn H, Hare JL, Kaye DM, McLean CA, et al. Histological validation of cardiac magnetic resonance analysis of regional and diffuse interstitial myocardial fibrosis. European Heart Journal - Cardiovascular Imaging. 2014 Oct 28.